

# Three-Dimensional Applications in Orthodontics

Dan Grauer

A dissertation submitted to the faculty of the University of North Carolina at Chapel Hill in partial fulfillment of the requirements for the degree of Doctor of Philosophy in the Department of Oral Biology at the School of Dentistry

Chapel Hill  
2010

Approved by:

Lucia H Cevidanes

Patrick M Flood

Donald A Tyndall

Martin A Styner

William R Proffit

© 2010  
Dan Grauer  
ALL RIGHTS RESERVED

## ABSTRACT

### DAN GRAUER: Three-Dimensional Applications in Orthodontics (Under the direction of Lucia H Cevidanes and William R Proffit)

Orthodontics as a specialty is going through a technological revolution. During the last 10 years there were more new developments in orthodontics than in the whole history of the specialty. One of the areas undergoing rapid progress is three-dimensional (3D) imaging.

3D Imaging allows for more precise evaluation of the airway. Patients displaying a Skeletal Class II had smaller airway volume while controlling for age, gender and size of face. The shape of the airway was different among individual with different antero-posterior jaw relationship. Airway volume among patients with different vertical jaw relationship displayed great variability.

A good understanding of imaging concepts is important for the contemporary clinician. Most of the three-dimensional visual information is not linked yet to a clear diagnosis and prognosis classification. Visualization, measurement, creation of two-dimensional (2D) radiographs, segmentation, registration, superimposition and other quantitative analysis require specific training and specialized software in order to manipulate 3D files.

In order to compare the newer 3D images with our current and historical databases, it is necessary to emulate 2D radiographs from 3D data. When we compared homologous landmark coordinates in digital and synthetic cephalograms,

there was no systematic error. However when both modalities are used in the same individual the error of the method could produce clinically significant differences.

A second area undergoing rapid progress is orthodontic digital models. These are qualitatively and quantitatively similar to conventional dental casts, but offer some advantages. One of these advantages is the possibility of register and superimpose them in space. The registration of digital orthodontic models to represent the patients' occlusion, as well as registration of final orthodontic models to the planned setup models was reliable.

Finally, CAD/CAM technology allows for fabricating orthodontic appliances on a setup model of the planned correction. Based on a three-dimensional comparison of the planned tooth positions with the final ones, A fully customized lingual technique was very accurate in achieving the planned tooth positions in terms of translation and rotation.

“Digital orthodontics and digital dentistry have arrived: be part of it”

To

William R. Proffit  
Frans Van der Linden  
Ruth and Julio Grauer  
Esther Grifoll

## ACKNOWLEDGMENTS

Martin A Styner  
Lucia H Cevitanes  
Donald Tyndall  
Patrick M Flood  
William R Proffit

James L Ackermann  
Inam Heulfe  
Eric T Harmon  
Mark Honerkamp  
David Hatcher

Ceib Phillips  
Yunro Chung  
Debbie Price  
Hongtu Zhu  
Camilla Tulloch

Robert Scholz  
Lindsay Kornrumpf  
Ching Ko  
Mike Marshall  
Dirk Wiechmann

## TABLE OF CONTENTS

LIST OF TABLES.....	xii
LIST OF FIGURES .....	xiii
Chapter	
I.    TECHNOLOGICAL REVOLUTION IN ORTHODONTICS .....	1
References .....	5
II.   PHARYNGEAL AIRWAY VOLUME AND SHAPE FROM CONE-BEAM COMPUTED TOMOGRAPHY: RELATIONSHIP TO FACIAL MORPHOLOGY .....	6
Abstract .....	6
Background.....	7
Material and Methods .....	9
Results.....	13
Discussion .....	15
Conclusions .....	21
References .....	22
III.  WORKING WITH DICOM CRANIOFACIAL IMAGES.....	32
Abstract .....	32
Background.....	32
DICOM Files .....	33
Visualization of CBCT Images .....	35

Measurement in CBCT images.....	36
Creation of 2D Radiographs from DICOM files .....	38
Segmentation Engines and Multimodal Images.....	39
Registration and superimposition of 3D Images .....	40
Special Applications of Quantitative Analysis .....	43
Three-Dimensional Surgical Prediction.....	45
Conclusions .....	46
References .....	47
IV. ACCURACY AND LANDMARK ERROR CALCULATION USING CONE-BEAM COMPUTED TOMOGRAPHY GENERATED CEPHALOGRAMS.....	57
Abstract .....	57
Background.....	57
Materials and Methods .....	58
Creation of a Synthetic Cephalogram .....	59
Cephalogram Tracing.....	60
Registration Method.....	60
Measurement .....	61
Plotting.....	62
Statistical Analysis .....	62
Results.....	63
Discussion .....	64
Registration Process.....	64
Sources of Variability .....	65

	Dry Skull and In Vivo Studies.....	67
	Conclusions .....	69
	References .....	70
V.	REGISTRATION OF ORTHODONTIC DIGITAL MODELS .....	78
	Abstract .....	78
	Background.....	79
	Part I: Establishing Occlusion with Independently Scanned Digital Models .....	81
	Methods .....	81
	Sample .....	81
	Software .....	82
	Statistical Analysis.....	82
	Results .....	83
	Discussion.....	83
	Part II: Registration of Setup Models to Final Models to Assess Treatment Precision.....	85
	Methods .....	86
	Sample .....	86
	Software .....	86
	Statistical Analysis.....	87
	Results .....	87
	Discussion.....	88
	Conclusion .....	90
	References .....	91

VI.	ACCURACY IN TOOTH POSITIONING WITH FULLY CUSTOMIZED LINGUAL ORTHODONTIC APPLIANCES .....	101
.....	Abstract .....	101
.....	Background.....	102
.....	Materials and Methods .....	106
	Sample.....	106
	Scanning of dental casts and- establishment of occlusion .....	107
	Removal of the gingival tissue and- surface-to-surface registration .....	107
	Segmentation of teeth and Measurement- of tooth discrepancy in position.....	108
	Statistical analysis.....	109
	Results.....	110
	Clinical outcomes.....	110
	Discrepancies between planned and actual tooth positioning: translational discrepancies.....	111
	Discrepancies between planned and actual tooth positioning: rotational discrepancies .....	112
	Relation between covariates and outcome variable.....	112
	Discussion .....	115
	Sample characteristics .....	115
	Influences on translational accuracy .....	116

Influences on rotational accuracy.....	118
Other Considerations .....	120
Conclusion.....	123
References .....	125
VII. CONCLUSION .....	144
APPENDIX A: DETAILED STATISTICAL METHOD FOR CHAPTER 4 .....	149
APPENDIX B: DETAILED STATISTICAL METHOD FOR CHAPTER 6 .....	151

## LIST OF TABLES

Table		
2.1	Sample distribution .....	24
2.2	Adjusted and unadjusted means.....	24
2.3	Regression models .....	25
4.1	Landmarks and average difference vectors .....	72
4.2	Difference between modalities.....	73
5.1	Maximum difference in replicate positioning .....	94
5.2	Statistical model analysis part I.....	94
5.3	Estimated standard deviation.....	94
5.4	Statistical model analysis part II.....	95
6.1	Descriptive statistics for continuous variables.....	130
6.2	Descriptive statistics for categorical variables.....	131
6.3	Mean of absolute discrepancies for maxilla .....	132
6.4	Mean of absolute discrepancies for mandible .....	132
6.5	Type III mixed effects model .....	133
B.1	Between and within subject variables .....	151
B.2	Interpretations for the parameter in the model .....	153
B.3	Parameter estimates for translational discrepancies .....	155
B.4	Parameter estimates for rotational discrepancies .....	156

## LIST OF FIGURES

### Figure

2.1	Facial morphology reflecting underlying skeleton .....	26
2.2	Size of the face prism .....	27
2.3	Segmentation of the airway .....	28
2.4	Bisecting plane of the airway .....	29
2.5	Different airway shapes among facial patterns .....	30
2.6	Registration or airway segmentations.....	31
3.1	DICOM record.....	50
3.2	Visualization modes.....	51
3.3	Creation of synthetic cephalograms.....	52
3.4	Registration and superimposition of CBCT images .....	53
3.5	Airway analysis module .....	54
3.6	Implant simulation module .....	55
3.7	Matching pictures on 3D data .....	55
3.8	Three-dimensional surgical simulation.....	56
4.1	Conventional versus synthetic cephalogram .....	74
4.2	Procrustes registration of landmarks .....	75
4.3	Difference vectors grouped by landmark .....	76
4.4	Difference lengths by landmark .....	77
5.1	Interpremolar width change .....	96
5.2	Registration of occlusal position .....	97

5.3	Color-map comparison of surface distances.....	98
5.4	Registration of setup and final dental arches .....	99
5.5	Local coordinate systems .....	100
6.1	Incognito lingual technique .....	134
6.2	Final and setup models differences .....	135
6.3	Local coordinate systems with known displacements.....	136
6.4	Example of dental Class II patient: photographs.....	137
6.5	Example of dental Class II patient digital models.....	138
6.6	Registered and superimposed models .....	139
6.7	Boxplot diagrams each discrepancy .....	140
6.8	Rugae-based registration of sequential models.....	143

## CHAPTER 1

### TECHNOLOGICAL REVOLUTION IN ORTHODONTICS

Orthodontics as a specialty is going through a technological revolution. During the last 10 years there were more new developments in orthodontics than in the whole history of our specialty; this progress is parallel to the world's technological evolution. Technological changes include almost all aspects of orthodontic practice, research and education; from internet search databases to the public availability of information, from better diagnosis tools to appliances completely designed and produced by computers, from interactive teaching sessions to distance learning applications.

One of the areas undergoing rapid progress is three-dimensional (3D) imaging. These changes have a direct effect on diagnosis, treatment planning, knowledge generation, treatment implementation, design and fabrication of appliances, communication, marketing, interdisciplinary interaction and education in orthodontics. A search performed with the key words "Three-Dimensional" in the American Journal of Orthodontics and Dentofacial Orthopedics, showed that there were 25 related articles published in the entire year 2000, and there were 145 related articles published between January and October 2010.

New technology and new research create more questions and unknowns. Three-dimensional images are impressive in their detail and their ability to show

spatial relationships in three-dimensions. However, today we do not have a clear link between the morphological findings and our orthodontic diagnosis and prognosis systems, which are based on two-dimensional concepts and two-dimensional databases. Because of that indications and contraindications of the use of 3D images are not clear yet. Representatives of the American Association of Orthodontists and the American Association of Maxillofacial Radiology are working on a joint position paper on the appropriate selection of diagnostic images for orthodontics<sup>1</sup>. The paper in chapter 2 assessed the volume and shape of the airway (nasal and oropharynx) in three dimensions, in an attempt to link these airway characteristics to our current diagnosis scheme in terms of facial morphology.

Technology is usually ahead of the evidence to support it. This happens because in a first stage more money is invested in the development of new products rather than in validation studies. In a second stage more money is again invested in marketing rather than in validation studies. In orthodontics this translates into a practice guided by a sales pitch<sup>2</sup>. Chapter 3 is an overview of current imaging concepts with special emphasis on the evidence available to support claims and philosophies. For each concept a literature review was conducted and the basics are described. Further research directions are also outlined.

The advent of 3D technology creates the need for normative data. For ethical and legal reasons the use of radiation in untreated individuals (i.e. those who will not benefit individually) in order to generate growth databases is not longer available. Because of that, it is not likely that we will generate normative data in three dimensions. It makes sense then to compare the data generated with these new

modalities with historical growth databases<sup>3</sup>. Three-dimensional images allow for extraction of simulated two-dimensional images. In chapter 4 the position of landmarks in conventional two-dimensional cephalograms is compared with the position of landmarks on Cone-Beam CT generated cephalograms. A method for calculation of error while measuring distances between landmarks in sequential cephalograms belonging to different modalities is also presented.

Three-dimensional imaging in orthodontics also includes surface-type images generated with scanners or 3D cameras. Research in this area is conducted at universities and at the development laboratories of various companies. Working with scanned surfaces requires specific software packages for visualization, measurement, orientation, registration, Boolean operations and CAD/CAM procedures. Validation studies of these procedures are difficult to publish given that they involve a technical background. Chapter 5 is a validation study on two procedures. First the reliability of reproducing the occlusion of the dental casts in the virtual world was assessed. Upper and lower dental casts were scanned independently and in order to reproduce their occlusion in 3D a scan of the dental models in occlusion is used as registration surface. Second, the reproducibility of registering surface-to-surface the digital models corresponding to the planned correction on the digital models obtained at the end of treatment was determined.

The cutting-edge in customization of delivery of orthodontic treatment is CAD/CAM procedures to fabricate orthodontic appliances. 3D imaging and technology play a key role in this area. The main three patient-customized treatment planning and manufacturing techniques are Insignia, SureSmile and Incognito<sup>4-7</sup>. In

order to validate the use of goal-oriented techniques of this type a method of comparing tooth positions in three-dimensions is needed. This method would be applied on a sample of consecutively treated patients where we could compare the results obtained with the initial planned correction. In Chapter 6 we joined forces with Dr. Wiechmann's team in Bad Essen, Germany to collect a sample of all patients treated between 2008 and 2009. We were also helped by the engineers from Geodigm Corporation. A method of assessing discrepancies in tooth position between the planned and achieved position is presented; and statistical models were created to explain variability in tooth position by demographic, clinical and treatment difficulty variables.

We hope that these five articles will encourage the reader to be critical with new developments. Clinicians and researchers should avoid the acceptance of claims that are not supported by evidence. At the conclusion of each chapter we highlight future research directions. It is a very exciting time in orthodontics and in dentistry. Digital dentistry and digital orthodontics are around the corner.

“Three-dimensional technology has arrived: be part of it”.

## REFERENCES

1. Turpin DL. Clinical guidelines and the use of cone-beam computed tomography. *Am J Orthod Dentofacial Orthop* 2010;138:1-2.
2. O'Brien K, Sandler J. In the land of no evidence, is the salesman king? *Am J Orthod Dentofacial Orthop* 2010;138:247-249.
3. Hunter WS, Baumrind S, Moyers RE. An inventory of United States and Canadian growth record sets: preliminary report. *Am J Orthod Dentofacial Orthop* 1993;103:545-555.
4. Scholz RP, Sachdeva RC. Interview with an innovator: SureSmile Chief Clinical Officer Rohit C. L. Sachdeva. *Am J Orthod Dentofacial Orthop* 2010;138:231-238.
5. Scholz RP, Sarver DM. Interview with an Insignia doctor: David M. Sarver. *Am J Orthod Dentofacial Orthop* 2009;136:853-856.
6. Wiechmann D. A new bracket system for lingual orthodontic treatment. Part 1: Theoretical background and development. *J Orofac Orthop* 2002;63:234-245.
7. Wiechmann D. A new bracket system for lingual orthodontic treatment. Part 2: First clinical experiences and further development. *J Orofac Orthop* 2003;64:372-388.

## CHAPTER 2

### PHARYNGEAL AIRWAY VOLUME AND SHAPE FROM CONE-BEAM COMPUTED TOMOGRAPHY: RELATIONSHIP TO FACIAL MORPHOLOGY

#### ABSTRACT

Introduction: The aim of this study was to assess the differences in airway shape and volume among subjects with various facial patterns. Methods: Cone-beam computed tomography records of 62 non-growing patients were used to evaluate the pharyngeal airway volume (superior and inferior compartments) and shape. This was done by using 3-dimensional virtual surface models to calculate airway volumes instead of estimates based on linear measurements. Subgroups of the sample were determined by anteroposterior jaw relationships and vertical proportions. Results: There was a statistically significant relationship between the volume of the inferior component of the airway and the anteroposterior jaw relationship ( $P = 0.02$ ), and between airway volume and both size of the face and sex ( $P = 0.02$ ,  $P = 0.01$ ). No differences in airway volumes related to vertical facial proportions were found. Skeletal Class II patients often had forward inclination of the airway ( $P < 0.001$ ), whereas skeletal Class III patients had a more vertically oriented airway ( $P = 0.002$ ). Conclusions: Airway volume and shape vary among patients with different anteroposterior jaw relationships; airway shape but not volume differs with various vertical jaw relationships. The methods developed in this study make it

possible to determine the relationship of 3-dimensional pharyngeal airway surface models to facial morphology, while controlling for variability in facial size.

## BACKGROUND

Several lines of evidence from cephalometric studies support a link between presumed respiratory mode and facial morphology. These include the classic studies of mandibular orientation and growth in patients before and after adenoidectomy by Linder-Aronson<sup>1</sup> and Linder-Aronson et al<sup>2</sup> and a case report that documents downward-backward rotation in patients with total nasal obstruction.<sup>3</sup> More recently, Zettergren-Wijk et al<sup>4</sup> showed a certain degree of normalization of growth after adenoidectomy in a group of obstructive sleep apnea patients. Guray and Karaman,<sup>5</sup> studying a similar group, could not replicate the results of Linder-Aronson and concluded that adenoidectomy might change only the breathing mode, without a significant effect on malocclusion and facial type. Fields et al,<sup>6</sup> using special instrumentation to totally account for the amount of oral vs. nasal airflow in normal and long-faced children, showed that the relationship between oral vs. nasal breathing and growth in the long-faced pattern is not clear-cut. Long-faced children were overrepresented in the group of these subjects with a high percentage of oral breathing, but predominantly oral breathing was found in some children with normal facial morphology, and some long-faced children had a low percentage of oral breathing. The normal and long-faced subjects had similar tidal volumes and minimum nasal cross-sectional areas.

Postural relationships of the head, jaws, and tongue are established in the first moments after birth as the airway is opened and stabilized, and are altered as necessary thereafter to maintain the airway.<sup>7</sup> It seems reasonable that the link between respiratory mode and the development of malocclusion could be soft-tissue pressures against the dentition that might affect tooth eruption, dental arch form, and possibly the direction of mandibular and maxillary growth. Solow and Kreiborg<sup>8</sup> and Solow and Sandham<sup>9</sup> formally expressed this view in their “soft-tissue stretching hypothesis.” A change in jaw posture that led to downward-backward rotation of the mandible, or a change in head posture such as head extension, could lead to stretching of the lips, cheeks, and musculature. The result would be upright incisors and narrower dental arches, which often (but not always) are observed in patients with a long-faced and open-bite growth pattern. Solow’s hypothesis implies that oral and pharyngeal soft tissues also would be affected by a change in head, jaw, or tongue posture.

The value of lateral cephalometric radiographs to evaluate the upper airway is limited because they provide 2-dimensional (2D) images of complex 3-dimensional (3D) anatomic structures.<sup>10</sup> Three-dimensional analyses of the airway volumes and shape are required to understand oral and pharyngeal adaptations to varying respiratory conditions and proprioceptive stimuli. Aboudara et al<sup>11</sup> showed that records from cone-beam computed tomography (CBCT) obtained for clinical problems such as impacted teeth or temporomandibular disorders now are an acceptable way to evaluate pharyngeal soft-tissue relationships and airway volume. The goal of this study was to examine the hypothesis that pharynx volumes and

shapes differ among the various facial morphologies, controlling for differences of facial size.

## MATERIAL AND METHODS

From the records of an oral radiology clinic in Sacramento, California, 62 patients (ages, 17-46 years) who had CBCT scans of the head along with facial photographs and a lateral cephalometric radiograph were selected for this study (Fig 2.1). None had previous orthognathic surgery, a syndrome diagnosis, or detectable pathology along the upper airway through inspection of the images. Age and sex characteristics of the subjects, subdivided as outlined below, are shown in Table 2.1 Age was not statistically significantly different between the sexes ( $P = 0.12$ ).

The CBCT images were obtained with an iCAT scanner (Imaging Sciences International, Hatfield, Pa) with a single 360 degree rotation, producing 306 basis images. All images had a medium or full field of view that allowed visualization of both the cranial base and the face. Primary and secondary reconstructions of the data were performed with the iCAT software, leading to images with an isotropic voxel size of  $0.3 \text{ mm}^3$ . Before they were entered into the database for this study, the CBCT images were anonymized by an algorithm that removed patient identifiers from the files.

Anteroposterior (AP) skeletal type (Class I, Class II, or Class III) was established initially from visual inspection of the facial photographs and the lateral cephalometric radiograph, and confirmed via measurement of overjet, mandibular

length, and ANB angle on synthetic lateral and posteroanterior (PA) cephalograms created with Dolphin 3D beta (version 2.3, Dolphin Imaging, Chatsworth, Calif).

The discrimination process for the vertical groups was based on a bony facial index, calculated as the ratio between the bony bizygomatic width divided by the nasion-menton distance projected onto an orthogonal coordinate system. The facial index values were split into tertiles to establish the vertical groups. Age, sex, and distribution of the subjects by AP and vertical groups are shown in Table 2.1.

For both the lateral and PA synthetic cephalograms, the head was oriented with line 6 degrees down from sella-nasion as the horizontal axis (approximately the true horizontal in most people). Whenever this orientation method created an unrealistic head posture, the synthetic cephalogram was reoriented according to the soft-tissue appearance on the CBCT data. This occurred in 4 of the 62 subjects.

The size of the face was established from the PA and lateral synthetic cephalograms, as a rectangular prism encompassing the facial bones. This prism was constructed as shown in Figure 2.2. As expected, the average size of the face was greater in the men than in the women ( $P < 0.01$ ).

To build 3D models of the airways for the 62 subjects, the anonymous CBCT data were loaded into InsightSNAP software (version 1.4.0, Cognitica, Philadelphia, Pa) that had been adapted at the University of North Carolina by the Neuro-Image Analysis Laboratories to allow semiautomatic segmentation of the airway. The semiautomatic nature of the segmentation process refers to the 3D growth of the level-set geodesic snakes. Although it is mainly automatic, there are 2 interactive steps to the segmentation: selection of an initial threshold and placement of initial

seed regions.<sup>12</sup> The segmentation process is then defined as the construction of 3D virtual surface models (called segmentations) by regional growth of the initial seed regions to match best the volumetric data. This segmentation method has been described, validated, and tested for accuracy, and is superior to the conventional slice-by-slice, manual tracing method.<sup>12</sup> The limits for segmentation and an example of a virtual surface model of the pharyngeal airway are shown in Figure 2.3.

Once segmented, the pharyngeal airways were refined to obtain the true shape of the airway by eliminating projections that did not belong to the airway and then were subdivided into superior and inferior compartments by a plane perpendicular to the sagittal plane that included the posterior nasal spine and the lower medial border of the first cervical vertebra (Fig 2.4). Airway volumes were measured in cubic millimeters with the InsightSNAP measuring tool. The reliability of the volumetric measurements was assessed on 5 randomly selected subjects stratified on AP grouping criteria. Segmentations were created 3 times for each subject, and their volumes were measured. The mean coefficient of variation (COV  $5 \text{ SD}/\text{mean volume}$ ), measured by averaging the COV for each of the 5 subjects, was 1.9%. This rather low COV value was most likely due to the semiautomatic nature of the segmentation procedure, since comparable purely manual segmentations normally have larger COVs.<sup>12</sup> This COV is more than an order of magnitude smaller than the volumetric variability in the groups, and thus the segmentation can be judged as reliable and unlikely to introduce significant errors.

Statistical analysis: Linear regression models were used to assess the relationship between face morphology and airway volume, controlling for age, sex,

size of the face, and interaction between size of face and sex. The variable age was centered at its average. The reference group for the AP pattern was the Class I group, and the middle group of the vertical pattern variable was used as the vertical reference group.

Bivariate relationships between variables were assessed with the Spearman correlation. A partial F test showed that, among all possible interactions of explanatory variables, only that between size of face and sex was potentially related to airway volume. This interaction was included in the regression model along with the covariate and primary main effects.

The shape of the airway was analyzed qualitatively by visual inspection and frequency count. The orientation of the airway passages viewed from the sagittal plane was defined as vertical, average, or forward, based on the inclination of the vertical axis of the airway to the horizontal orientation of the head (SN rotated down 6 degrees). The relative width of the overall airway passage and whether there was an indentation into the airway space that coincided with the dorsum of the tongue were also recorded. The frequencies of the various airway orientations and the indentations into the airway space were compared between groups with the Spearman rank correlations.

## RESULTS

The average volume of the pharyngeal airway was 20.3 cm<sup>3</sup> (SD, 7.3 cm<sup>3</sup>), with mean volumes of 8.8 cm<sup>3</sup> (SD, 2.9 cm<sup>3</sup>) for the superior component and 11.5

cm<sup>3</sup> (SD, 4.9 cm<sup>3</sup>) for the inferior component. Preliminary bivariate analysis showed no statistically significant relationship between volume of the airway and age or sex. The average size of the face was statistically significantly larger in the men than in the women ( $P < 0.01$ ). The size of the face was also significantly associated with total, inferior, and superior airway volumes, with Spearman correlation values of 0.399 ( $P < 0.01$ ), 0.368 ( $P < 0.01$ ), and 0.303 ( $P = 0.02$ ), respectively. Among the covariate variables, size of the face was significantly correlated with sex (Spearman correlation,  $-0.668$ ,  $P < 0.01$ ).

Data for measured and adjusted volumes are shown in Table 2.2. The adjusted volumes are derived from regression analyses, taking into account age, sex, face size, and interaction between face size and sex. The adjustments in most groups were small, despite the statistical significance of these variables.

There was a statistically significant difference ( $P = 0.02$ ) in the volume of the inferior component of the airway between the AP groups, after controlling for the effects of age, sex, size of face, and interaction between size of face and sex (Table 2.3). From the contrast tests, the mean value for the Class II subjects was significantly different from Class I ( $F = 7.97$ ;  $P < 0.01$ ) and Class III ( $F = 4.12$ ;  $P = 0.05$ ), but there was no difference between Class I and Class III ( $F = 0.50$ ;  $P = 0.48$ ). There was no significant difference ( $P = 0.26$ ) in the volume of the superior component of the airway.

There were no significant differences in the inferior, superior, and total airway volumes among the long, normal, and short groups, after controlling for the effects of age, sex, size of face, and interaction between size of face and sex (Table 2.3).

There was a statistically significant relationship ( $P = 0.01$ ) between sex and upper airway volume.

Quantitative analysis of airway shapes is not available yet for intergroup comparison. This type of shape description is an ongoing research project at the University of North Carolina. From visual inspection, the following qualitative observations were noted.

1. The segmentation contours were highly variable in all 3 AP groups.
2. Subjects with a Class III skeletal pattern had a more vertical orientation of the airway in the sagittal plane compared with the other groups, whereas a Class II skeletal pattern was associated with a more forward orientation of the airway ( $P < 0.001$ ) (Fig 2.5, A and C).
3. The postero-superior area of the tongue dorsum was visualized at the anterior wall of the airway segmentation as a blunt indentation (Fig 2.5, B and C). Skeletal Class II patients had a greater frequency of tongue indentations ( $P = 0.045$ ). The apparent projections of the tongue into the airway at various points along the anterior wall of the pharynx show how a 2D view of the tongue-pharynx relationship could be misleading.
4. The plane used to bisect the segmentations from posterior nasal spine to the lower medial anterior border of the first cervical vertebra had a more horizontal orientation in the skeletal Class III group and was more oblique, down toward the posterior aspect in the skeletal Class II group (Fig 2.4).

5. The airway passages of the skeletal Class II group were narrower when viewed from the coronal plane than in the other 2 groups (Fig 2.5, C), even though the difference was not statistically significant.

Variability was greater among the vertical groups, and differences in shape were more difficult to characterize. An extremely narrow airway, both anteroposteriorly and coronally, was observed more often in patients in the long-faced group when compared with patients with normal faces (38% vs 20%). Most long-faced patients also had a skeletal AP malocclusion (48% Class II, 38% Class III), and often a strong tongue indentation was noted at the anterior wall of the airway (Fig 2.5, B and C).

## DISCUSSION

The construction of virtual 3D surface models of the airway by using in-house tools differs from the 3D visualization tools allowed by commercial software that display the 3D data as projections based on thresholding filters. In this study, we used a volumetric characterization of the pharynx. No linear or angular measurements were used. To our knowledge, this is the first report of airway volumes based on this advanced technique.

This study controlled for the following factors.

1. Airway differences related to growth status. The subjects ranged from 17 to 46 years of age (average, 24.7 years), so they had already undergone their

adolescent growth spurt; thus, it is no surprise that airway volume did not correlate with age. To date, there are no 3D longitudinal data on airway changes during growth. From 2D cephalometric data, King,<sup>13</sup> Bench,<sup>14</sup> and, later, Tourne<sup>15</sup> described the growth of the bony nasopharynx as mainly vertical, with a slight AP increase early in life and minimal change after the growth spurt. It is unlikely that growth contributed to the differences that we noted in airway orientation and shape.

2. Differences in face size. In this study, the size of the face was established as a rectangular prism encompassing the facial bones. Because the lines used to determine the lengths of the edges of the prism were not perpendicular, their projection was transposed into an orthogonal system that created the edges of the prism (Fig 2.2). Thus, the size of the face was independent of head orientation and face morphology, and, by simple trigonometry, the 2D planes could be projected onto an orthogonal coordinate system. Pharyngeal airway volumes (total, superior, and inferior) were significantly if weakly correlated with face size:  $r = 0.40$  ( $P < 0.01$ ),  $0.37$  ( $P < 0.01$ ), and  $0.30$  ( $P = 0.02$ ), respectively. Subjects with larger faces would be expected to have larger airway volumes. The means and standard deviations for face size in the groups were almost identical.

3. Male and female composition of the groups. Face size is significantly larger in men than in women, and, because airway volume is correlated to face size, a sex difference would be expected. Martin et al<sup>16</sup> reported that 2D nasopharyngeal soft-tissue patterns were different in men and women. In an

earlier longitudinal study, Linder-Aronson and Leighton<sup>17</sup> also found sexual dimorphism during growth of the posterior wall of the pharynx. Sexual dimorphism between airways was not addressed in our study, but our data confirms that airway volumes are significantly larger in men. Because we controlled for face size, sex, and interaction between sex and face size, the male-female composition of our groups should not have affected the differences by facial morphology groups that we found.

There were other potential influences on airway dimensions and shape. We found a significant difference in the inferior compartment of the airway volume between skeletal Class II and Class I and Class III patients (skeletal Class II inferior compartment airway volume was smaller,  $P = 0.02$ ), but there were no significant differences in airway volume among the long, normal, and short face-height groups. Airway orientation and shape differed between the Class II and Class III groups, with no difference between the vertical groups. Several factors might have contributed to these outcomes.

With 62 subjects divided into 3 groups for analysis, the sample size in each group was about 20. It is possible that, with larger numbers in each group, other differences would have been statistically significant. Further studies with larger groups are needed. On the other hand, with groups of this size, the differences that were statistically significant are large enough to be clinically significant.

Each subject was in both an AP and a vertical group, with the vertical grouping created by simply dividing the sample into 3 equal groups by face height.

There was a weak relationship between the patients' vertical and AP characteristics. Many patients with longer faces also were classified as skeletal Class II or Class III, whereas those with shorter faces tended to be classified as skeletal Class I. Bias from this source, however, seems more likely to lead to differences in airway volumes between the vertical groups than to conceal differences.

Patient positioning and respiration phase during data acquisition are other possible factors. Cephalometric studies in the laboratory have shown that, with a change in body position from upright to supine, changes in volume and contours occur in the upper airway in patients with obstructive sleep apnea and control subjects.<sup>18</sup> For our study, the iCAT scanner was chosen because the patient sits upright during CBCT acquisition. In the other most widely used CBCT scanner, NewTom 3 G (Aperio Services, Sarasota, Fla), patients are scanned in a supine position. In our view, the upright position is closer to the normal position outside sleeping hours and a better starting point for a study of this type. It will be interesting, however, to see whether the differences in airway shape between the 2 positions show different upper and lower airway volumes, and also to determine whether the differences in airway shape that we observed in the Class I, Class II, and Class III subjects, would be seen in supine CBCT scans.

One other aspect of positioning in the iCAT machine that might lead to differences in supine vs upright scans is the influence of the patient's chin position on head orientation during CBCT acquisition. With the first generation of iCAT CBCT scanners, the radiology technician positioned the subject with a strap around the forehead and a platform for the chin. A more prominent chin could lead to changes

in the extension of the head, and a less prominent chin could have the opposite effect. The latest iCAT CBCT machines do not have a chin platform, and the head is stabilized with a strap around the forehead. During NewTom 3 G scan acquisition, patients are supine with their heads on a noncustomized pillow for support. This type of positioning is not reproducible for studies in which head orientation must be controlled.

No attempt was made during CBCT acquisition for our subjects to control for respiratory movements (inspiration, resting, exhalation). Lowe et al<sup>19</sup> reported changes in airway dimensions related to the respiration phase. The acquisition times for our iCAT scanner were 20 to 38 seconds; this is too long to ask the patient not to breathe during the scan. Newer scanners have reduced the acquisition time to about 10 seconds, and that allows control of the respiration phase. In this study, volume changes during respiration are part of the systematic error, and future investigations can determine whether there is a correlation between the physiology of respiration and the 3D facial morphology. In our study, no data for body weight and patients' height were available. It could have been interesting to include these parameters in our regression models, and, in future prospective studies, these data will be collected.

Airway patency is considered to be strongly related to the equilibrium between extraluminal tissue pressure and intraluminal pressure. Transmural pressure is the difference between intraluminal and extraluminal pressures. When transmural pressure is positive, the airway remains patent; it occludes when transmural pressure is negative.<sup>20</sup> The continuous positive airway pressure machine

preserves the patency of the airway by maintaining greater intraluminal pressure than extraluminal pressure. A second factor influencing airway patency is mucosal tension; when airways are subjected to tension, their collapsibility decreases.<sup>21</sup> Future research is needed to assess the relationship between the tension of the external soft tissues to the tension of the internal soft tissues to establish a physiologic connection between these equilibrium mechanisms.

Airflow demands trigger reflex changes in the posture of the head, mandible, and tongue. The AP position of the tongue seen in 2D images is closely related to oropharyngeal depth. Compared with control children, those with enlarged tonsils have an extended posture of the head and an anteroinferior posture of the tongue<sup>22</sup> (shown in cephalometric radiographs by the position of the hyoid bone), and patients who underwent mandibular setback have a more inferior position of the hyoid bone.<sup>23</sup> An association between extended head posture and facial retrognathism was reported.<sup>24</sup> Stratemann<sup>25</sup> recently reported that specific sites of upper airway constriction are associated with specific patterns of skeletal adaptations of the craniofacial complex. This was based on CBCT data from patients with nonextreme facial types, and the precise sites and adaptations are still to be characterized.

## CONCLUSIONS

Three-dimensional images of the airway allow improved evaluation of sites of airway obstruction, and further studies are needed to clarify the physiologic response to pharyngeal stenosis. Computer software that allows determination of volumes from surface contours is more accurate for these research studies. In

addition, it already is possible to use the cranial base surface to superimpose 3D models for different times in the same patient, so that changes in airway volume and orientation relative to this stable reference can be studied before and after surgery (Fig 2.6, A).<sup>26</sup> New registration methods for growing patients and interpatient comparisons have been used in preliminary studies involving surgical and orthopedic changes. In the future, these could be applied to airway studies (Fig 2.6, B), and we can expect a much better understanding of adaptive changes in the airway shape and volume. Head posture, mandibular rotation, hyoid position, and patency of the airway are interrelated, and further 3D studies of the airway should clarify the relationships.

## REFERENCES

1. Linder-Aronson S. Adenoids. Their effect on mode of breathing and nasal airflow and their relationship to characteristics of the facial skeleton and the dentition. A biometric rhino-manometric and cephalometro-radiographic study on children with and without adenoids. *Acta Otolaryngol Suppl* 1970;265:1-132.
2. Linder-Aronson S, Woodside DG, Lundstrom A. Mandibular growth direction following adenoidectomy. *Am J Orthod* 1986; 89:273-84.
3. McNamara JA. Influence of respiratory pattern on craniofacial growth. *Angle Orthod* 1981;51:269-300.
4. Zettergren-Wijk L, Forsberg CM, Linder-Aronson S. Changes in dentofacial morphology after adeno-tonsillectomy in young children with obstructive sleep apnea—a 5-year follow-up study. *Eur J Orthod* 2006;28:319-26.
5. Guray E, Karaman AI. Effects of adenoidectomy on dentofacial structures: a 6-year longitudinal study. *World J Orthod* 2002;3: 73-81.
6. Fields HW, Warren DW, Black K, Phillips CL. Relationship between vertical dentofacial morphology and respiration in adolescents. *Am J Orthod Dentofacial Orthop* 1991;99:147-54.
7. Shelton RL Jr, Bosma JF. Maintenance of the pharyngeal airway. *J Appl Physiol* 1962;17:209-14.
8. Solow B, Kreiborg S. Soft-tissue stretching: a possible control factor in craniofacial morphogenesis. *Scand J Dent Res* 1977; 85:505-7.
9. Solow B, Sandham A. Cranio-cervical posture: a factor in the development and function of the dentofacial structures. *Eur J Orthod* 2002;24:447-56.
10. Preston CB. The upper airway and cranial morphology. In: Graber TM, Vanarsdall R, Vig KWL, editors. *Orthodontics: principles and techniques*. 4th ed. St Louis: C.V. Mosby; 2005. p. 117-43.
11. Aboudara CA, Hatcher D, Nielsen IL, Miller A. A three-dimensional evaluation of the upper airway in adolescents. *Orthod Craniofac Res* 2003;6(Suppl 1):173-5.
12. Yushkevich PA, Piven J, Hazlett HC, Smith RG, Ho S, Gee JJ, et al. User-guided 3-D active contour segmentation of anatomical structures: significantly improved efficiency and reliability. *Neuroimage* 2006;31:1116-28.
13. King EW. A roentgenographic study of pharyngeal growth. *Angle Orthod* 1952;22:23-37.

14. Bench RW. Growth of the cervical vertebrae as related to tongue, face and denture behavior. *Am J Orthod* 1963;49:183-214.
15. Tourne´ LP. Growth of the pharynx and its physiologic implications. *Am J Orthod Dentofacial Orthop* 1991;99:129-39.
16. Martin O, Muelas L, Vinas MJ. Nasopharyngeal cephalometric study of ideal occlusions. *Am J Orthod Dentofacial Orthop* 2006;130:436.e1-9.
17. Linder-Aronson S, Leighton BC. A longitudinal study of the development of the posterior nasopharyngeal wall between 3 and 16 years of age. *Eur J Orthod* 1983;5:47-58.
18. Pae EK, Lowe AA, Sasaki K, Price C, Tsuchiya M, Fleetham JA. A cephalometric and electromyographic study of upper airway structures in the upright and supine positions. *Am J Orthod Dentofacial Orthop* 1994;106:52-9.
19. Lowe AA, Gionhaku N, Takeuchi K, Fleetham JA. Three-dimensional CT reconstructions of tongue and airway in adult subjects with obstructive sleep apnea. *Am J Orthod Dentofacial Orthop* 1986;90:364-74.
20. Schwartz AR. Extraluminal tissue pressure: what does it mean? *J Appl Physiol* 2006;100:5-6.
21. Rowley JA, Permutt S, Willey S, Smith PL, Schwartz AR. Effect of tracheal and tongue displacement on upper airway airflow dynamics. *J Appl Physiol* 1996;80:2171-8.
22. Behlfelt K, Linder-Aronson S, Neander P. Posture of the head, the hyoid bone, and the tongue in children with and without enlarged tonsils. *Eur J Orthod* 1990;12:458-67.
23. Takagi Y, Gamble JW, Proffit WR, Christiansen RL. Postural change of the hyoid bone following osteotomy of the mandible. *Oral Surg Oral Med Oral Pathol* 1967;23:688-92.
24. Tallgren A, Solow B. Hyoid bone position, facial morphology and head posture in adults. *Eur J Orthod* 1987;9:1-8.
25. Stratemann SA. Three-dimensional craniofacial imaging: airway and skeletal morphology [thesis abstract]. *Am J Orthod Dentofacial Orthop* 2006;130:807.
26. Cevidanes LH, Styner MA, Proffit WR. Image analysis and superimposition of 3-dimensional cone-beam computed tomography models. *Am J Orthod Dentofacial Orthop* 2006;129: 611-8.

TABLE 2.1

Table 2.1 Sample distribution in terms of age, gender and size of face according to the two grouping criteria: vertical and antero-posterior

	Vertical Groups			Antero-posterior Groups		
	Short (n= 21)	Average (n= 20)	Long (n=21 )	I (n= 21)	II (n= 22)	III (n=19 )
<b>Age</b>						
Mean (SD)	24.54 (7.36)	26.00 (7.88)	23.55 (7.42)	25.16 (7.63)	24.83 (7.61)	23.97 (7.57)
<b>Gender</b>						
Female	12 (32%)	13 (35%)	12 (32%)	14 (38%)	14 (38%)	9 (24%)
Male	9 (33%)	7 (28%)	9 (36%)	7 (28%)	8 (32%)	10 (40%)

TABLE 2.2

Table 2.2 Unadjusted and Adjusted means of volumetric measurements for the each effect of Vertical and Antero-posterior grouping criteria

	Total Airway Volume		Lower Portion Airway Volume			Upper Portion Airway Volume		
	Unadjusted Means (mm <sup>3</sup> )	Adjusted Means (mm <sup>3</sup> )*	Unadjusted Means (mm <sup>3</sup> )	Adjusted Means (mm <sup>3</sup> )*	95% Confidence Interval Adjusted Means*	Unadjusted Means (mm <sup>3</sup> )	Adjusted Means (mm <sup>3</sup> )*	95% Confidence Interval Adjusted Means*
<b>Vertical Groups</b>								
<b>Short</b>	18641	18714	10724	10784	8835 - 12733	7917	7930	6769 - 9090
<b>Average</b>	22485	22955	12823	13228	11213 - 15243	9662	9727	8527 - 10927
<b>Long</b>	20025	19504	11100	10654	8669 - 12639	8925	8850	7668 - 10031
<b>Antero-posterior Groups</b>								
<b>I</b>	22430	22660	13008	13163	11271 - 15056	9422	9497	8307 - 10687
<b>II</b>	18049	18170	9289	9399	7540 - 11259	8760	8771	7602 - 9940
<b>III</b>	20712	20318	12486	12187	10192 - 14182	8226	8131	6878 - 9386

\* Adjusted for age, gender, size of face, and the interaction between size of face and gender.

TABLE 2.3

Table 2.3 Regression models controlling for age, gender, size of face and the interaction between gender and size of face for upper and lower airway volumes by antero-posterior and vertical groups.

<b>Analysis Airway Volume for vertical groups</b>				
	<b>Lower Portion Airway</b>		<b>Upper Portion Airway</b>	
<b>Source</b>	<b>F Value</b>	<b>Pr &gt; F</b>	<b>F Value</b>	<b>Pr &gt; F</b>
<b>Age</b>	2.96	0.09	0.26	0.62
<b>Gender</b>	1.52	0.22	5.1	.01*
<b>Size of Face</b>	4.72	.01*	7.39	<.01*
<b>Vertical proportion</b>	2.08	0.13	2.35	0.11

\* significant at the level .05

<b>Analysis Airway Volume for Antero-posterior groups</b>				
	<b>Lower Portion Airway</b>		<b>Upper Portion Airway</b>	
<b>Source</b>	<b>F Value</b>	<b>Pr &gt; F</b>	<b>F Value</b>	<b>Pr &gt; F</b>
<b>Age</b>	2.55	0.12	0.17	0.68
<b>Gender</b>	2.73	0.07	5.07	.01*
<b>Size of Face</b>	4.57	.02*	7.16	<.01*
<b>Antero-posterior groups</b>	4.27	.02*	1.25	0.29

\* significant at the level .05

FIGURE 2.1



Fig 2.1 Facial morphology reflects the underlying skeletal configuration and internal soft tissues. The sample was divided into 3 groups according to 2 criteria: A, the AP relationship of the jaws, and B, the vertical pattern of the face.

FIGURE 2.2

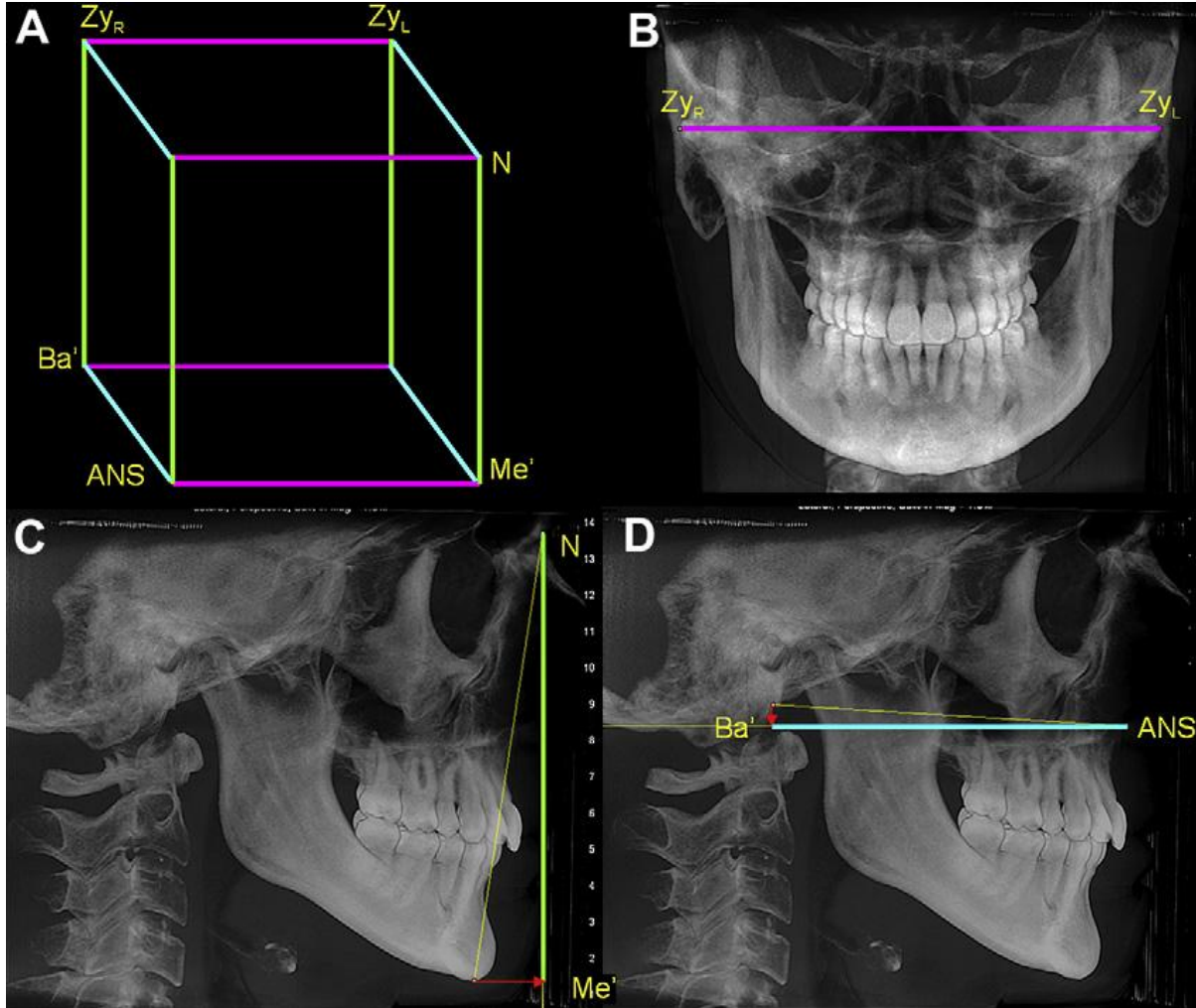


Fig 2.2 The size of face was established by creating a prism (A) with edges as (B) the bizygomatic width, which is parallel to the true horizontal and does not need to be projected, (C) the Na-Me distance projected on the y-axis and (D) the Ba-ANS distance projected on the z-axis.

FIGURE 2.3

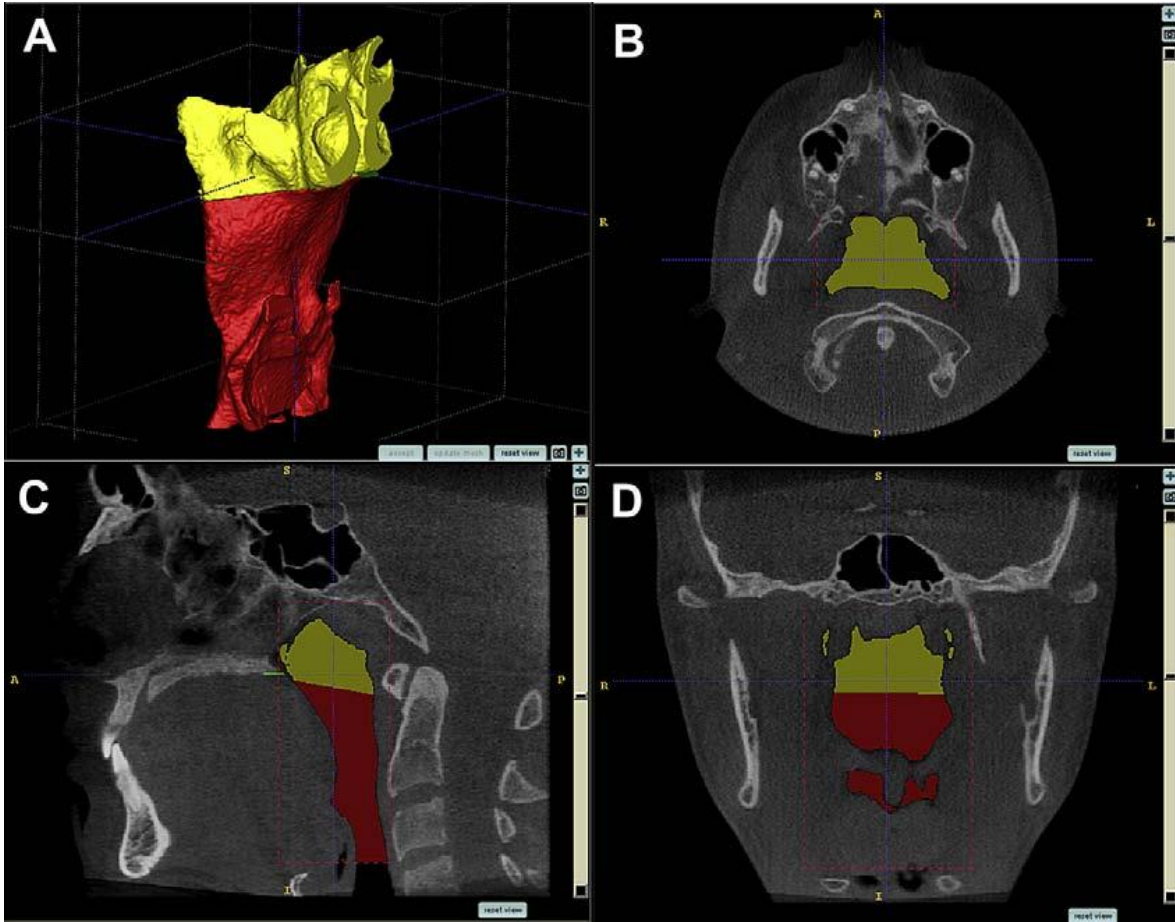


Fig 2.3 Segmentation by user-initialized 3D surface evolution (A). Limits for airway analysis are: (B, C) anterior, a vertical plane through posterior nasal spine perpendicular to the sagittal plane at the lowest border of the vomer; posterior, the posterior wall of the pharynx; lateral, the lateral walls of the pharynx, including the full extensions of the lateral projections; lower, a plane tangent to the most caudal medial projection of the third cervical vertebra perpendicular to the sagittal plane; (C, D) upper, the highest point of the nasopharynx, coinciding with the posterior choanae and consistent with the anterior limit.

FIGURE 2.4

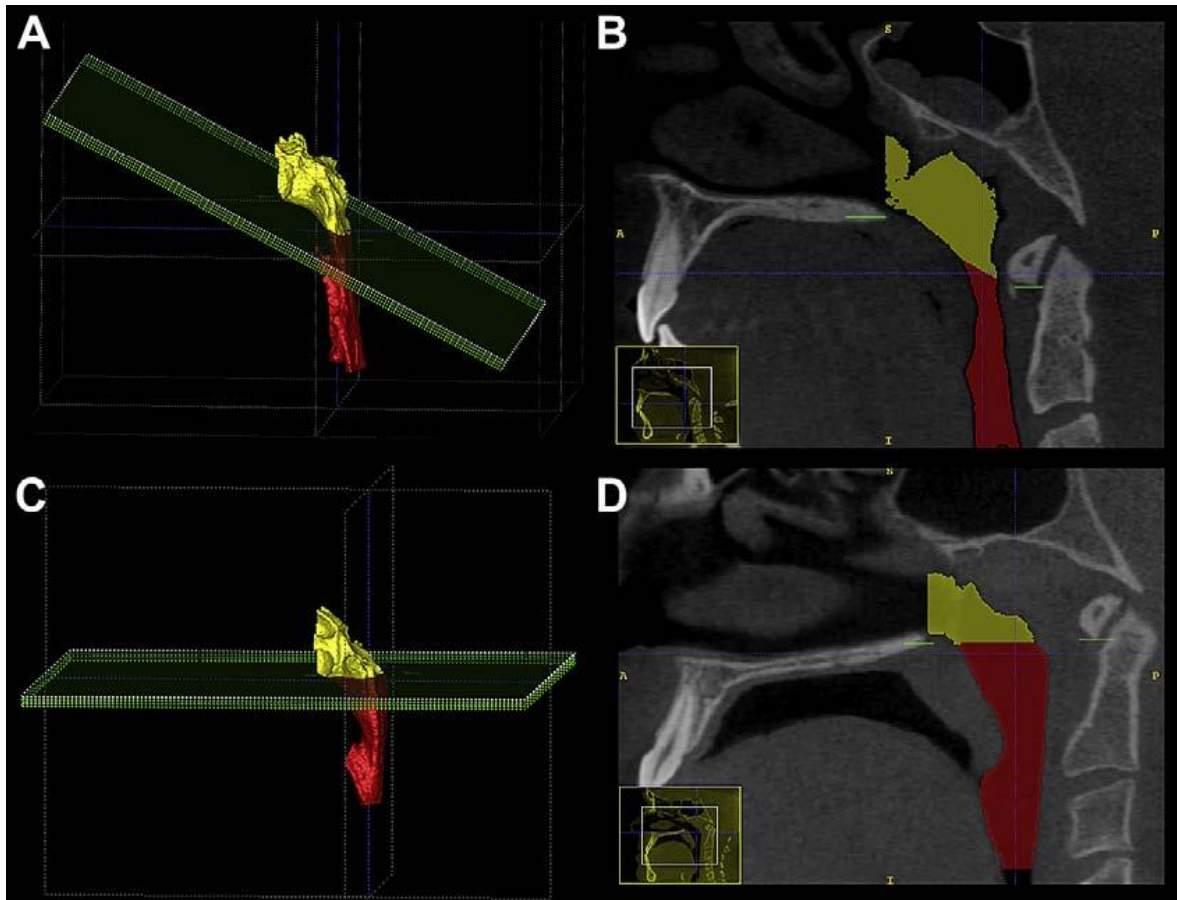


Fig 2.4 The orientation of the bisecting plane for the superior and inferior airway compartments was different between A and B, skeletal Class II, and C and D, skeletal Class III; the latter was more horizontal, and the former was more oblique, reflecting an anatomic difference between these groups.

FIGURE 2.5

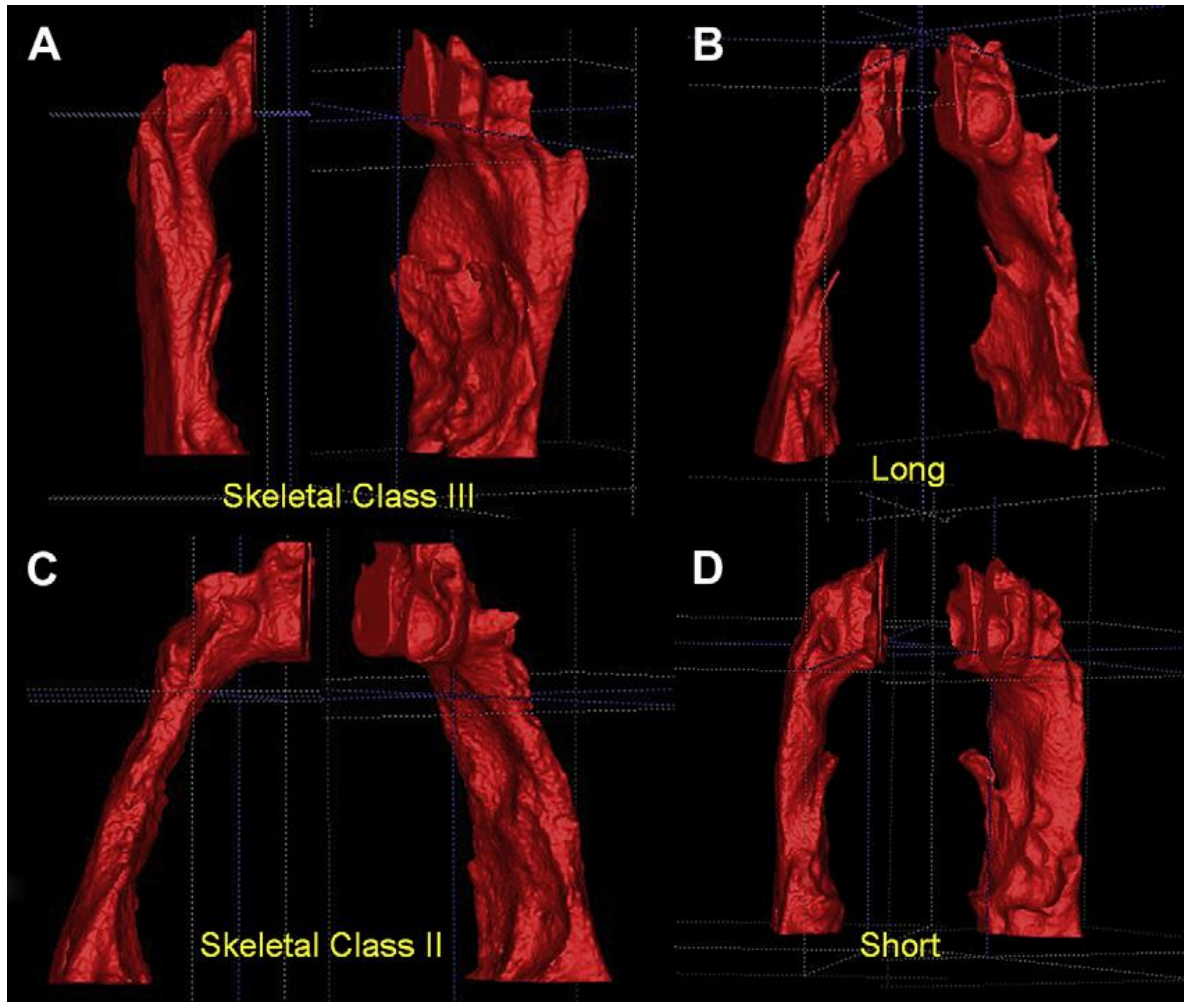


Fig 2.5. Different airway shapes of skeletal Class II and Class III subjects, depicting a more vertical orientation of the airway in Class III subjects. A and C, This finding was statistically significant,  $P < 0.001$ . B and D, The differences between subjects in the vertical groups are less apparent, with no statistically differences found.

FIGURE 2.6

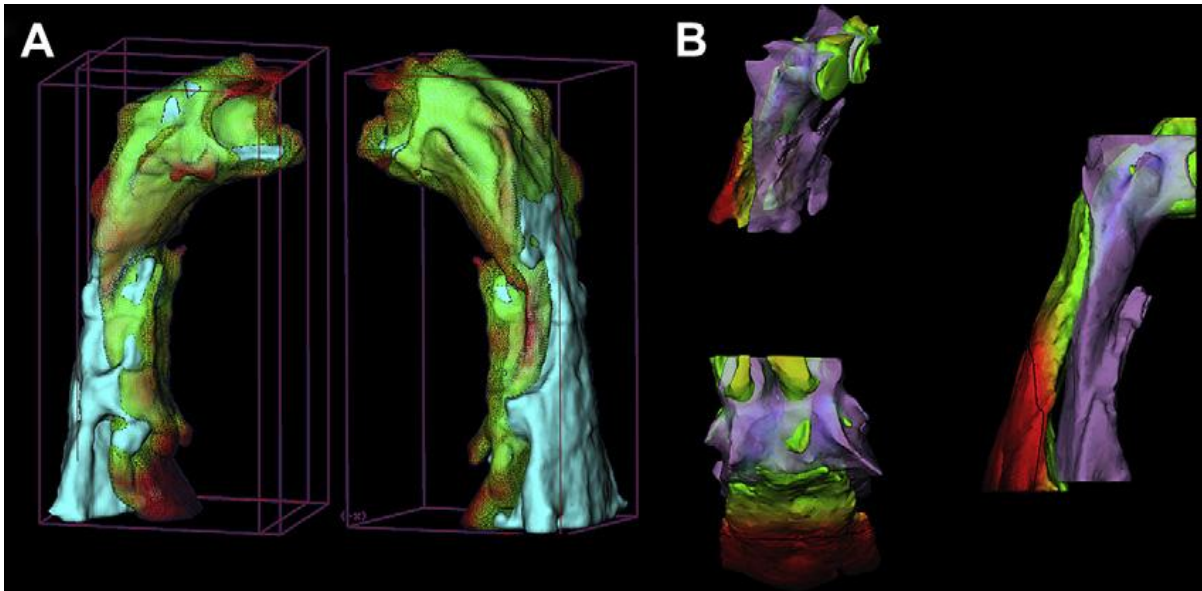


Fig 2.6 Registration techniques for 3D data adapted for airway study use: A, pre-and postmandibular advancement 3D models of the airway registered on the cranial base (semiautomatic registration); B, interpatient manual airway registration shows a skeletal Class II subject and a skeletal Class I subject.

## CHAPTER 3

### WORKING WITH DICOM CRANIOFACIAL IMAGES

#### ABSTRACT

The increasing use of cone-beam computed tomography (CBCT) requires changes in our diagnosis and treatment planning methods as well as additional training. The standard for digital computed tomography images is called *digital imaging and communications in medicine* (DICOM). In this article we discuss the following concepts: visualization of CBCT images in orthodontics, measurement in CBCT images, creation of 2-dimensional radiographs from DICOM files, segmentation engines and multimodal images, registration and superimposition of 3-dimensional (3D) images, special applications for quantitative analysis, and 3D surgical prediction. CBCT manufacturers and software companies are continually working to improve their products to help clinicians diagnose and plan treatment using 3D craniofacial images.

#### BACKGROUND

The numbers of clinicians using 3-dimensional (3D) records during diagnosis and treatment planning stages are increasing steadily. Cone-beam computed tomography (CBCT) scanners are becoming more efficient with reduced acquisition

time, and software packages developed to process, manage, and analyze 3D images are also undergoing a rapid growth phase. The management of CBCT images differs from that of conventional 2-dimensional (2D) images. Most orthodontists were trained in the 2D era, and the transition to 3D images requires a learning stage. With today's hardware and software improvements, the learning curve is not as steep, but some basic concepts should be taken into account with this new technology.

The purpose of this article is to give the clinician some core concepts for 3D diagnosis and treatment planning. The current commercial software applications for clinical management of craniofacial CBCT images are presented and compared with the current standards. The concepts presented here are applicable regardless of the constantly changing software applications.

## DICOM FILES

In the early 1980s, the American College of Radiology and the National Electrical Manufacturers Association joined forces to standardize the coding of images obtained through computed tomography and magnetic resonance imaging. After successive improvements, in 1993, the term digital imaging and communications in medicine (DICOM) was adopted.<sup>1</sup> A DICOM record consists of (1) a DICOMDIR file, which includes patient information, specific information about image acquisition, and a list of images that correspond to axial slices forming the 3D image; and (2) a number of sequentially coded images that correspond to the axial

slices. (When those axial slices are combined in the correct order they form the 3D image) (Fig 3.1).

Once a CBCT scan has been acquired, some basic handling and measurements on the data set can be performed with the software provided by the manufacturers. CBCT manufacturers also offer the option through their software to convert their proprietary formats into an exportable DICOM file; this is a first step in managing 3D CBCT information. When ordering a CBCT acquisition through an imaging laboratory, this is normally performed at the laboratory, and the patient or the clinician is given a compact disk containing the DICOM file. If the clinician owns a CBCT scanner, its software allows for exporting images in DICOM format. Further research is needed to validate the process of converting images from a proprietary format into DICOM format.

The tools for visualization, landmarking, measurement, registration, superimposition, and computation of 3D images are different from those used in their counterpart 2D images.<sup>2</sup> The information obtained through 3D visualization in orthodontics has not been completely linked to a diagnostic or prognostic meaning. For instance, when we observe a differently shaped mandibular condyle, it does not necessarily mean pathology. Further research should establish the links between observed morphology, pathology, pathogenesis, and response to treatment.

The legal implications of acquiring a CBCT image are also important. More information than the conventional diagnostic records is obtained through a full 3D image of the head and neck, leading to responsibility and accountability issues regarding the diagnosis of pathology outside the region of interest. Whether the

orthodontist or a radiologist should be accountable for any pathology beyond the region of interest is a current controversy beyond the scope of this article.<sup>3</sup>

## VISUALIZATION OF CBCT IMAGES

Among the increasing number of software packages dedicated to managing and analyzing DICOM images, we focus on 3 with special emphasis in orthodontics. In alphabetical order they are 3dMDvultus software (3dMD, Atlanta, Ga), Dolphin Imaging (Dolphin Imaging, Chatsworth, Calif), and InVivoDental (Anatomage, San Jose, Calif). There are other software packages and applications (even freeware) available to manage DICOM files.

A 3D image is composed of a stack of 2D images or slices. In a similar fashion that a 2D image is composed of pixels, a 3D image is composed of voxels. Each voxel has a gray-level value based on indirect calculation of the amount of radiation absorbed or captured by the charge-coupled device and calculated through a filtered-back projection algorithm. Visualization is based on a threshold filter. This filter assigns a binary value, either transparent or visible, to each voxel based on its gray-level value. The user defines the critical value that splits the voxels into visible and invisible. The result is a rendered image on the screen composed of all visible voxels.

The operator can visualize the data set by looking at the stack of slices or the rendered 3D image. Computers can reformat the 3D image, allowing the operator to scroll through these 2D images in any direction (Fig 3.1, C). The most common ones are sagittal, coronal, and axial. All 3 orthodontic programs allow scrolling through the

stack of images. A cursor represented by 2 crossing lines indicates the precise localization in virtual space. The data set can also be rotated, panned, or zoomed to allow visualization of the region of interest; at any angle, scale, or position, a rendered image can be created. Multiple threshold filters can be applied to the same image to distinguish between tissues of different density—eg, soft and hard tissues. Transparency can also be applied to allow visualization of hard tissues through the soft tissues (Fig 3.2). Clipping tools are also available. These allow for isolation and visualization of specific regions—eg, the mandibular condyles. Dolphin Imaging allows for 2 threshold filters: for hard tissues and soft tissues. Transparency can be applied to visualize soft-tissue thickness at various points. InVivoDental allows the user to modify the threshold values through preloaded filters. Additionally, segmentations can be created. The 3dMDvultus software also has threshold filters, in addition to the ability to create segmentations to isolate and define regions of interest (described later).

It is crucial to understand that the rendered image is the result of a user-entered threshold value. The visual perception of the operator defines what is bone and what is soft tissue, and many factors can affect this: contrast of the image, noise in the image, individual visual perception and prior knowledge of anatomy among others. For a qualitative assessment, these rendered images are appropriate, but, for a quantitative assessment, they present many challenges that are discussed in the next section.

## MEASUREMENT IN CBCT IMAGES

In 2D radiographs, distances and angles are measured between landmarks. These landmarks are defined by the superimposition of the projection of different structures. This is a property of transmission radiographs. Landmarks can be defined as an inflection point in a curved line, the geometric center of a structure, superimposition of projection of different structures, the tip of a structure, or the crossing point of 2 planes. Most landmarks cannot be visualized or are difficult to locate on a curved surface in a 3D image. There are no clear operational definitions for specific cephalometric landmarks in the 3 planes of space.<sup>4</sup> A second challenge is that the rendered image depends on many factors, including contrast of the image, movement during acquisition, presence of metal that creates noise, overall signal-to-noise ratio of the image, and the threshold filters applied by the operator. Because of all these factors, it makes sense that the landmarks should be located in the stack of slices rather than in the 3D rendered volume.<sup>5</sup>

Many studies have assessed the accuracy and reliability of measurements on CBCT images. Those studies can be classified based on 2 criteria. The first is whether they use radiopaque markers or structures of known geometry. This classification yields 2 groups: when landmark location does not need anatomic operational definitions, and when anatomic definitions are important, and another interexaminer or intraexaminer factor (landmark location) is introduced. The second classification, applicable to both groups, is based on where the landmarks were located. According to this second criterion, 3 groups are established: (1) landmarks located in the stack of slices, (2) landmarks located on a segmented surface (more later), and (3) landmarks located on the rendered image.

Studies from group 1 report good accuracy regardless of where the measurements were made. For most measurements, there were no statistically significant differences compared with the gold standard (measurements with a caliper or structures of known geometry). Some measurements had statistically significant differences, but those were small and not clinically significant.<sup>6-11</sup> Studies from group 2 report subclinical accuracy when landmarks were located on segmentations or in the stack of slices,<sup>12,13</sup> but not when they were located on the rendered image.<sup>14</sup> When all studies are considered regardless of their classification, reliability in measurements and landmark identification in CBCT images was reported to be good to very good.<sup>5,10,14,15</sup>

Based on the available evidence, we can conclude that it is more accurate to locate landmarks in the stack of slices or on a segmented surface; this is possible in all 3 software packages. Landmarks located in the rendered volume must be carefully evaluated.

## CREATION OF 2D RADIOGRAPHS FROM DICOM FILES

Longitudinal growth databases are no longer allowed for ethical reasons, and there are no normative data in 3 dimensions. However, available 2D growth databases can be used to compare with current clinical data.<sup>16</sup> To be able to compare the new modalities with our current databases, algorithms have been created to extract information from the CBCT image and simulate a conventional cephalogram, panoramic projection, tomographic image of the temporomandibular joint, and posteroanterior cephalogram. Cephalogram registration and superimposition are the

most common and efficient ways to quantitatively assess growth and treatment changes. All 3 software packages allow for the extraction of synthetic radiographic projections. The procedure starts by orienting the patient's head image in virtual space similarly to what the technician does in a cephalostat (Fig 3.3). The advantage of this virtual orientation is the possibility of using a semitransparent image to match bilateral structures and obtain the correct head rotation.

Measurements performed on CBCT synthetic cephalograms have proven to be on average similar to those on conventional cephalograms.<sup>17-20</sup> Some statistically significant differences were found between some measurements, but no clinically significant differences were found. When both modalities—conventional and CBCT synthetic cephalograms—are combined in the same longitudinal study, the researcher must account for an increase in landmark error calculation.<sup>21</sup>

For the creation of CBCT synthetic cephalograms, Dolphin Imaging allows the user to choose an orthogonal or a perspective projection type, and, with the latter, the projection center can be repositioned to match the transporionic axis. Once created, many visualization filters can be applied to the synthetic cephalogram. The 3 companies are now working to improve the options offered by the cephalogram-creation module. The creation of CBCT synthetic panoramic radiographs starts by delineating the focal trough, its upper and lower limits, and its thickness.

## SEGMENTATION ENGINES AND MULTIMODAL IMAGES

The segmentation process in medical imaging could be defined as the construction of 3D virtual surface models (called segmentations) to best match the

volumetric data. There are many different segmentation processes, and this topic is beyond the scope of this article. For more information, the reader is referred to the study of Yushkevich et al.<sup>22</sup> The reader must distinguish between a virtual surface and a rendered image. The importance of having a segmentation engine in the software package is twofold. First, it allows the user to export anatomic models in a nonproprietary format; this information can be used in research and will always be accessible regardless of constantly changing software applications. The second advantage is the option of loading anatomic models—segmentations—in a nonproprietary format into the imaging software interface; that allows combining different modalities with the CBCT images. An example is combining digital models obtained through laser or optical scanners with the CBCT data and soft-tissue meshes obtained through 3D cameras. These multimodal images are the foundation of digital dentistry, rapid prototyping, and computer-aided design and computer-aided manufacturing applications.

Currently, InVivoDental offers a segmentation engine that allows the user to export anatomic models. Dolphin Imaging allows importing 3D soft-tissue meshes to be combined with the CBCT data. The 3dMDvultus software has a segmentation engine, which performs segmentations by thresholding and smoothing filters (Fig 3.2, C). The 3dMDvultus software also allows for both exporting and importing segmentations.

## REGISTRATION AND SUPERIMPOSITION OF 3D IMAGES

Traditionally, the best and almost only way to quantitatively assess changes in orthodontics was cephalogram superimpositions. Stable structures described by Bjork,<sup>23</sup> Bjork and Skieller,<sup>24-26</sup> and others<sup>27</sup> are used as registration and orientation landmarks. Changes can be described relative to those reference structures.<sup>28</sup> Registration can be defined as the process of combining 2 or more images from different time points, each with its own coordinate system, into a common coordinate system. Today, it is possible to register CBCT records acquired at different time points and analyze changes due to treatment, growth, aging, and relapse in 3 dimensions.

The 3 software packages can register and superimpose CBCT images from different time points in the same virtual space. The procedure differs slightly between Dolphin Imaging and InVivoDental and 3dMDvultus software. In the first 2 programs, the process includes 5 steps.

- 1 The user loads the 2 CBCT images from different time points.
- 2 The user inputs homologous landmarks found in both images. Those landmarks will be the registration references and must be anatomically stable between time points.
- 3 Once the landmarks are input, the program computes the best fit between the 2 sets of landmarks in each CBCT image. A transformation matrix is obtained (rotation and translation). The program then relocates 1 CBCT image relative to the other based on this transformation matrix, and the result is that both images share the same coordinate system.

- 4 Because of the difficulty of locating stable landmarks in curved surfaces, especially along the cranial base, both programs allow for manually refining the registration process until most cranial base structures match.
- 5 Once the images are registered, the user can evaluate changes in the rendered volume with semitransparencies or at the stack of slices. Changes can be described relative to the registration landmarks (Fig 3.4, A, B, C, G, and H).

The 3dMDvultus software operates in a slightly different manner; the process also consists of 5 steps.

- 1 The images are loaded into the software interface, and segmentations are created.
- 2 The user unlocks the rotation and translation parameters of 1 segmentation.
- 3 The user performs an initial manual registration to approximate the surfaces as much as possible.
- 4 Anatomically stable surfaces must be selected by the user. In this case, the registration is surface-based, rather than landmark-based. The program performs a surface-to-surface registration to refine the initial manual registration.
- 5 Once the segmentations are registered, the user can visualize them by means of semitransparencies and assess changes in the

segmentations, the rendered volume, or the stack of slices. Change can be described relative to the registration surfaces (Fig 3.4, D through F).

We believe the latter registration process offers a more precise registration, because it is based on surfaces composed of thousands of landmarks instead of a few landmarks selected by the user; however, it still depends on the precision of the 3D surface models. Researchers at the University of North Carolina have developed a registration process that does not depend on the precision of the 3D surface models. This process compares voxel by voxel between gray-level CBCT images. The region to be compared is defined by the user. A transformation matrix (translation and rotation) is computed and applied to a CBCT image.<sup>2,29</sup>

## SPECIAL APPLICATIONS OF QUANTITATIVE ANALYSIS

Today, it is easier to analyze the shape and contours of airway passages in 3 dimensions. All 3 programs have tools to measure airway volume. This will open the door to research on airway volume changes with growth, treatment, and pathology. InVivoDental allows for segmenting the airway passages and measuring their volumes. Dolphin Imaging has a tool for segmenting the airway and allows for careful visual examination of airway contours and shapes. Airway volume can also be calculated (Fig 3.5). The 3dMDvultus software computes airway volume and allows visualization of the cross-section images along the airway. This software detects the smallest cross-sectional area or airway stenosis. A virtual endoscopy is also a feature of this program.

An implant simulation module is offered by InVivo-Dental software. The program allows the user to visualize and measure the alveolar bone and sections of the dental arch. The operator can then simulate the placement of a dental implant or an orthodontic temporary skeletal anchorage device (Fig 3.6, A). The size and manufacturer of the implant are chosen by the operator. The implant and its relationship to the bone and neighboring roots can be assessed and measured in both the 3D volume view and the arch section slices (Fig 3.6, B and C). The position of the implant can be controlled in 3 dimensions. On the left lower corner, a color map representing bone density around the implant is shown.

Dolphin Imaging allows combining the CBCT data with either a 3D or a 2D photograph. The registration is performed by landmark selection. The user locates homologous landmarks in both the CBCT volume and the photograph. The program then matches those landmarks, registering the 2 records (Fig 3.7).

InVivoDental also has this feature. Users or company technicians combine the CBCT volume with the photograph. Segmentations of the dental arches from the CBCT can also be incorporated into this anatomic model.

The 3dMDvultus software uses a surface-to-surface registration process to combine CBCT volume with the 3D photograph. The soft tissue must be segmented based on the CBCT volume. The photograph is then loaded, approximated, and registered.

All methods are an approximation of actual anatomic truth. Because the CBCT image and the photograph are not taken at the same time, the soft tissue extracted from the CBCT data is not exactly the same as the soft tissue obtained

through 3D photography. Many variables could be involved: differences in head position, muscular tone, movement during CBCT acquisition, and circadian rhythms. In the future, we hope that CBCT acquisition will be faster to prevent patient motion during acquisition (respiratory movements, deglutition, involuntary movements), and that the CBCT and photograph can be taken at the same time and in natural head position.

### THREE-DIMENSIONAL SURGICAL PREDICTION

The 3dMDvultus software released a 3D surgical prediction module. This process encompasses 6 steps.

- 1 The CBCT volume is loaded, and hard-and soft-tissue segmentations are created (Fig 3.8, A).
- 2 A 3D photograph could be combined with the CBCT segmentations (optional).
- 3 Virtual cuts are made to simulate the actual surgical cuts (Fig 3.8, B).
- 4 The bone segments are repositioned (translated and rotated) to the desired position (Fig 3.8, C).
- 5 The program applies soft-tissue algorithms to calculate the soft-tissue changes
- 6 The user visualizes and measures the changes (Fig 3.8, D and E).

These soft-tissue algorithms are based on series of patients before and after surgery. Because of the great variability in soft-tissue response to surgical changes and the huge amount of data points predicted on the skin surface, a large sample is

needed to obtain valid algorithms. It is also important to be consistent during sample collection; timing of records acquisition, surgical procedure, patient's age, sex, ethnicity, and head position are variables that should be controlled for.

## CONCLUSIONS

The soft-tissue paradigm has paved the road toward 3D diagnosis, treatment planning, and computer-aided design and computer-aided manufacturing orthodontics. Because of the advances in both CBCT scanners and software designed to manage CBCT data, it is possible to take advantage of CBCT information in a clinical setting. Clinicians should be careful in 2 areas: first, most visual information gathered with these systems has not been yet linked to a clear diagnosis classification. Further research is needed in the interpretation of orthodontic information from CBCT data. Second, some available tools have not been validated yet, and studies to assess accuracy and precision are mandatory before these applications become standard. Companies are investing huge amounts of time and money to improve their programs, and we as clinicians should use them and give the companies feedback; their success affects our patients and our success.

This is an extraordinary and interesting time in orthodontics and dentistry; digital dentistry is around the corner. In a few years, all specialties will have common goals and be able to interact, predict results, and improve their outcomes by taking advantage of the virtual patient. We hope that this introductory article will clarify some 3D image analysis concepts and encourage the reader to use this fascinating technology.

## REFERENCES

1. DICOM digital imaging and communications in medicine. Rosslyn, Va: National Electrical Manufacturers Association (NEMA); 2008.
2. Cevidanes LH, Styner MA, Proffit WR. Image analysis and superimposition of 3-dimensional cone-beam computed tomography models. *Am J Orthod Dentofacial Orthop* 2006;129:611-8.
3. Jerrold L. Liability regarding computerized axial tomography scans. *Am J Orthod Dentofacial Orthop* 2007;132:122-4.
4. Bookstein FL. Landmark methods for forms without landmarks: morphometrics of group differences in outline shape. *Med Image Anal* 1997;1:225-43.
5. Oliveira AE, Cevidanes LH, Phillips C, Motta A, Burke B, Tyndall D. Observer reliability of three-dimensional cephalometric landmark identification on cone-beam computerized tomography. *Oral Surg Oral Med Oral Pathol Oral Radiol Endod* 2000;107:256-65.
6. Ballrick JW, Palomo JM, Ruch E, Amberman BD, Hans MG. Image distortion and spatial resolution of a commercially available cone-beam computed tomography machine. *Am J Orthod Dentofacial Orthop* 2008;134:573-82.
7. Lascala CA, Panella J, Marques MM. Analysis of the accuracy of linear measurements obtained by cone beam computed tomography (CBCT-NewTom). *Dentomaxillofac Radiol* 2004;33:291-4.
8. Marmulla R, Wortche R, Muhling J, Hassfeld S. Geometric accuracy of the NewTom 9000 cone beam CT. *Dentomaxillofac Radiol* 2005;34:28-31.
9. Mischkowski RA, Pulsfort R, Ritter L, Neugebauer J, Brochhagen HG, Keeve E, et al. Geometric accuracy of a newly developed cone-beam device for maxillofacial imaging. *Oral Surg Oral Med Oral Pathol Oral Radiol Endod* 2007;104:551-9.
10. Pinsky HM, Dyda S, Pinsky RW, Misch KA, Sarment DP. Accuracy of three-dimensional measurements using cone-beam CT. *Dentomaxillofac Radiol* 2006;35:410-6.
11. Stratemann SA, Huang JC, Maki K, Miller AJ, Hatcher DC. Comparison of cone beam computed tomography imaging with physical measures. *Dentomaxillofac Radiol* 2008;37:80-93.
12. Hassan B, van der Stelt P, Sanderink G. Accuracy of three-dimensional measurements obtained from cone beam computed tomography surface-rendered

images for cephalometric analysis: influence of patient scanning position. *Eur J Orthod* 2009;31:129-34.

13. Ludlow JB, Laster WS, See M, Bailey LJ, Hershey HG. Accuracy of measurements of mandibular anatomy in cone beam computed tomography images. *Oral Surg Oral Med Oral Pathol Oral Radiol Endod* 2007;103:534-42.

14. Periago DR, Scarfe WC, Moshiri M, Scheetz JP, Silveira AM, Farman AG. Linear accuracy and reliability of cone beam CT derived 3-dimensional images constructed using an orthodontic volumetric rendering program. *Angle Orthod* 2008;78:387-95.

15. Moerenhout BA, Gelaude F, Swennen GR, Casselman JW, Van Der Sloten J, Mommaerts MY. Accuracy and repeatability of cone-beam computed tomography (CBCT) measurements used in the determination of facial indices in the laboratory setup. *J Craniomaxillofac Surg* 2009;37:18-23.

16. Hunter WS, Baumrind S, Moyers RE. An inventory of United States and Canadian growth record sets: preliminary report. *Am J Orthod Dentofacial Orthop* 1993;103:545-55.

17. Cattaneo PM, Bloch CB, Calmar D, Hjortshoj M, Melsen B. Comparison between conventional and cone-beam computed tomography-generated cephalograms. *Am J Orthod Dentofacial Orthop* 2008;134:798-802.

18. Kumar V, Ludlow JB, Mol A, Cevidanes L. Comparison of conventional and cone beam CT synthesized cephalograms. *Dentomaxillofac Radiol* 2007;36:263-9.

19. Moshiri M, Scarfe WC, Hilgers ML, Scheetz JP, Silveira AM, Farman AG. Accuracy of linear measurements from imaging plate and lateral cephalometric images derived from cone-beam computed tomography. *Am J Orthod Dentofacial Orthop* 2007;132:550-60.

20. Van Vlijmen OJ, Berge SJ, Swennen GR, Bronkhorst EM, Katsaros C, Kuijpers-Jagtman AM. Comparison of cephalometric radiographs obtained from cone-beam computed tomography scans and conventional radiographs. *J Oral Maxillofac Surg* 2009;67:92-7.

21. Grauer D, Cevidanes LH, Styner MA, Heulfe I, Harmon ET, Zhu H, Proffit WR. Accuracy and landmark error calculation using CBCT generated cephalograms. *Angle Orthod* 2009 (in press).

22. Yushkevich PA, Piven J, Hazlett HC, Smith RG, Ho S, Gee JC, et al. User-guided 3D active contour segmentation of anatomical structures: significantly improved efficiency and reliability. *Neuroimage* 2006;31:1116-28.

23. Bjork A. Sutural growth of the upper face studied by the implant method. *Acta Odontol Scand* 1966;24:109-27.
24. Bjork A, Skieller V. Facial development and tooth eruption. An implant study at the age of puberty. *Am J Orthod* 1972;62: 339-83.
25. Bjork A, Skieller V. Growth of the maxilla in three dimensions as revealed radiographically by the implant method. *Br J Orthod* 1977;4:53-64.
26. Bjork A, Skieller V. Normal and abnormal growth of the mandible. A synthesis of longitudinal cephalometric implant studies over a period of 25 years. *Eur J Orthod* 1983;5:1-46.
27. Doppel DM, Damon WM, Joondeph DR, Little RM. An investigation of maxillary superimposition techniques using metallic implants. *Am J Orthod Dentofacial Orthop* 1994;105:161-8.
28. Johnston LE Jr. Balancing the books on orthodontic treatment: an integrated analysis of change. *Br J Orthod* 1996; 23:93-102.
29. Cevidanes LH, Bailey LJ, Tucker GR Jr, Styner MA, Mol A, Phillips CL, et al. Superimposition of 3D cone-beam CT models of orthognathic surgery patients. *Dentomaxillofac Radiol* 2005; 34:369-75.

FIGURE 3.1

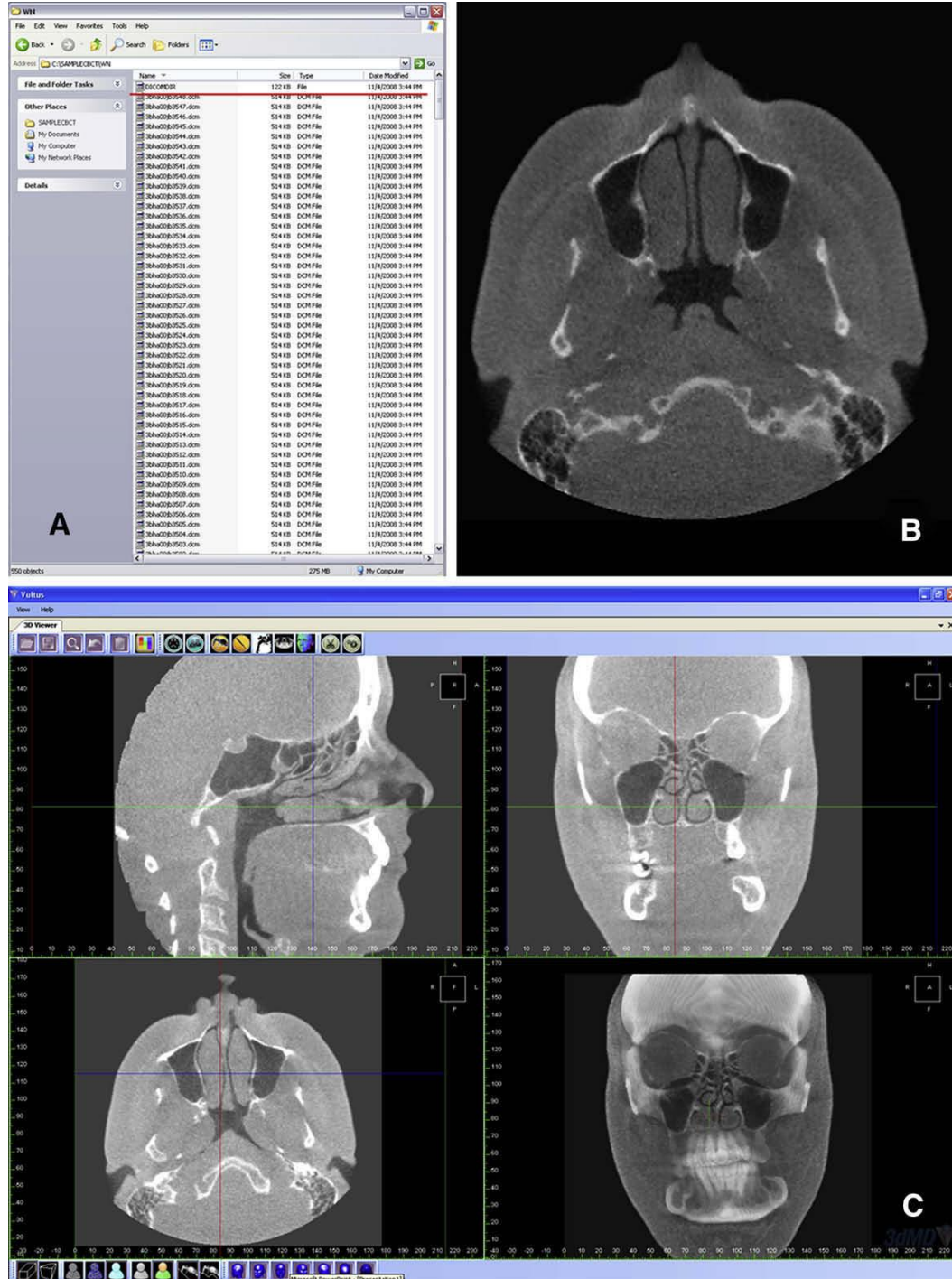


Fig 3.1. Example of a DICOM record: A, DICOMDIR file (*red underline*) and sequential axial slices; B, an axial slice; C, reformatted stack of slices allows the user to scroll in any direction (sagittal, coronal, axial). Three-dimensional view of the CBCT volume is also available (3dMDvultus Software).

FIGURE 3.2

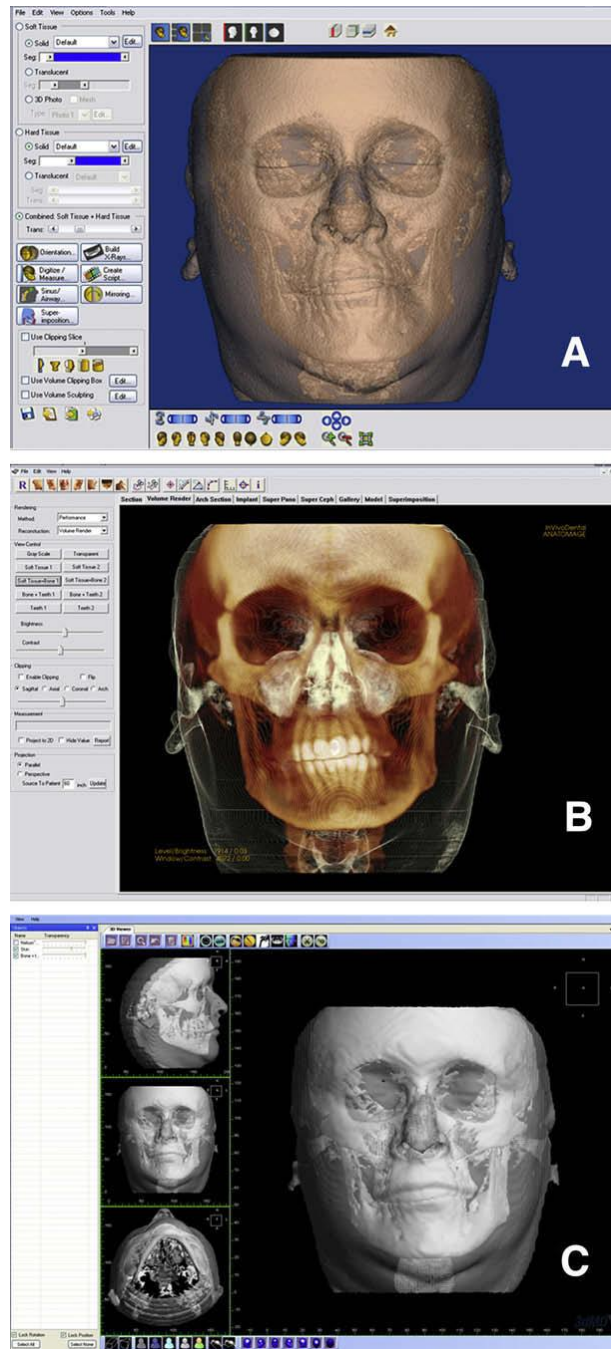


Fig 3.2. Different visualization modes and interfaces of 3 programs: A, Dolphin Imaging interface, with thresholding filters applied to visualize both hard and soft tissues, and a semitransparency applied to the soft tissue to visualize the hard tissue underneath; B, InVivoDental volume interface, with modified thresholding filters applied by a preset visualization “Soft tissue 1 Bone 1”; C, 3dMDvultus software interface, with hard-and soft-tissue surface models created (segmentations) and a semi-transparency applied to the soft-tissue segmentation.

FIGURE 3.3

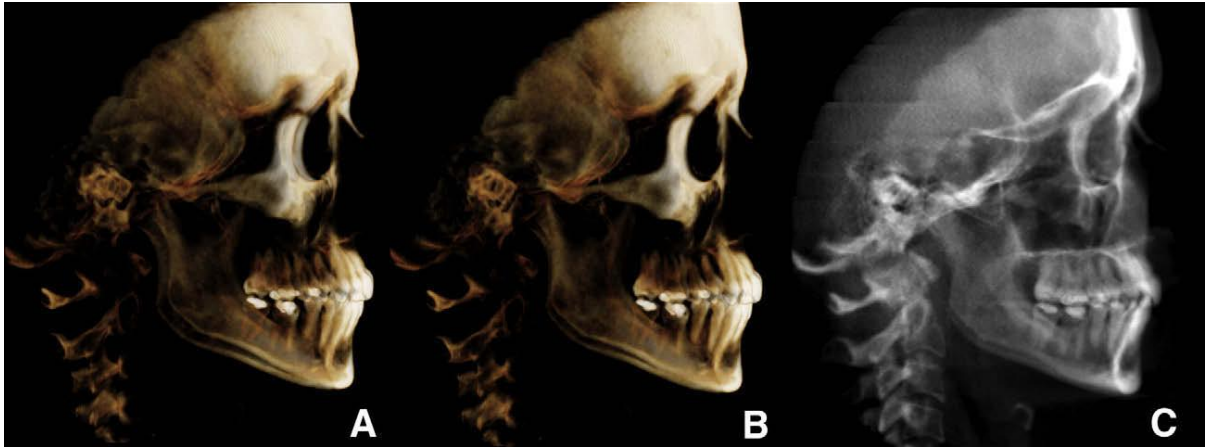


Fig 3.3. Creation of synthetic cephalograms: A, unoriented volume; B, oriented to obtain the correct head rotation (note the difference between the orbits and zygomatic bone); C, once oriented, the cephalogram was generated or has been generated (InVivoDental).

FIGURE 3.4

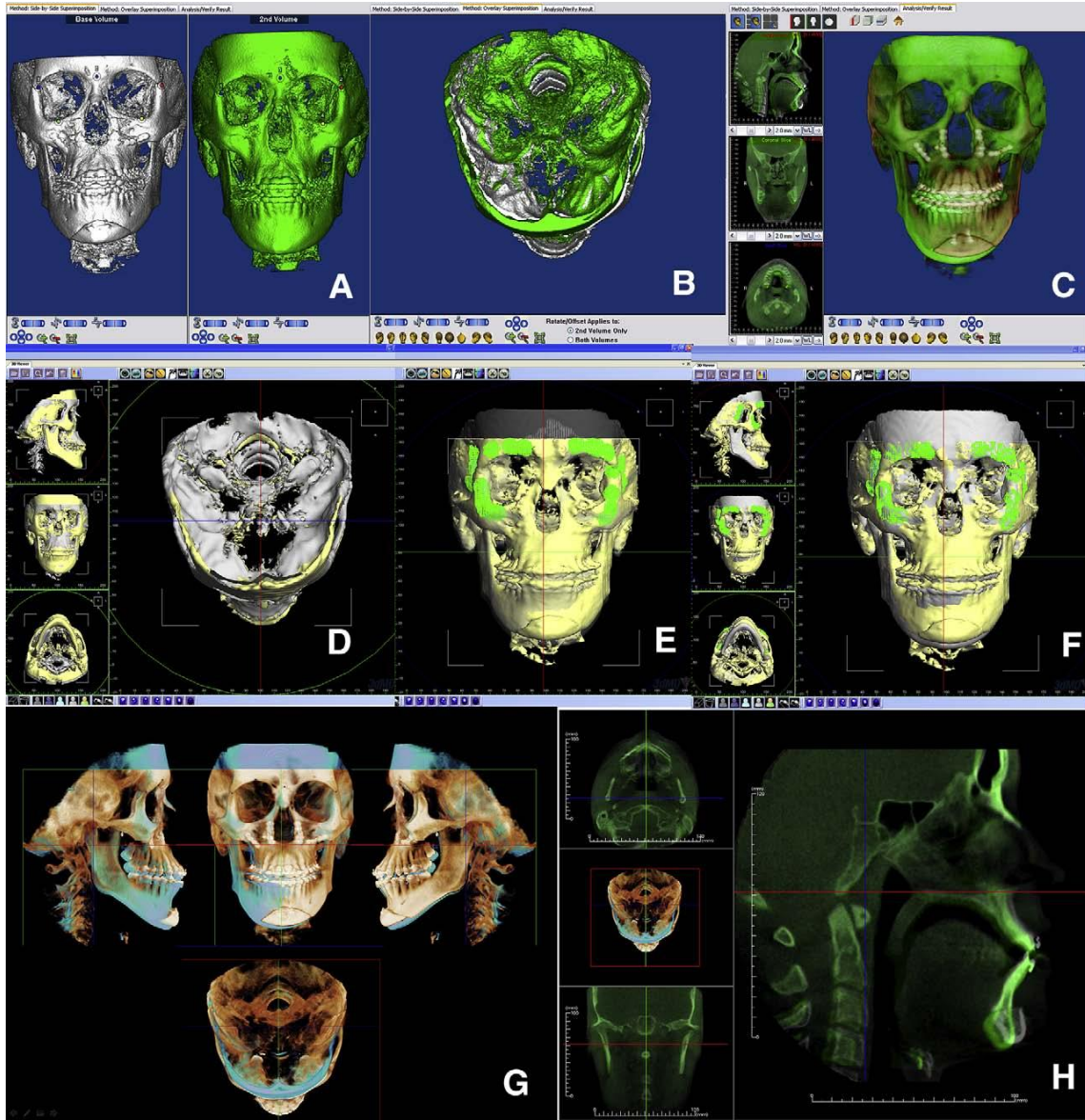


Fig 3.4. Registration and superimposition of sequential CBCT images: A, Dolphin Imaging uses a landmark-based registration process that allows the user to manually refine the relative position of the CBCT images until, B, stable structures are matching. C, Once registered, semitransparency visualization allows the user to measure and assess changes. D, The 3dMDvultus software uses a surface-based registration process in which the first 2 images are manually positioned; E, anatomically stable surfaces are selected, and the program refines the registration by matching those surfaces; once registered, changes can be determined. F, Surgical outcome assessment—in this case, maxillary advancement, autorotation of the mandible and genioplasty—can be measured and visualized in the volumetric rendered image and the stack of slices. G and H, Different InVivoDental visualizations of the registered volumes.

FIGURE 3.5

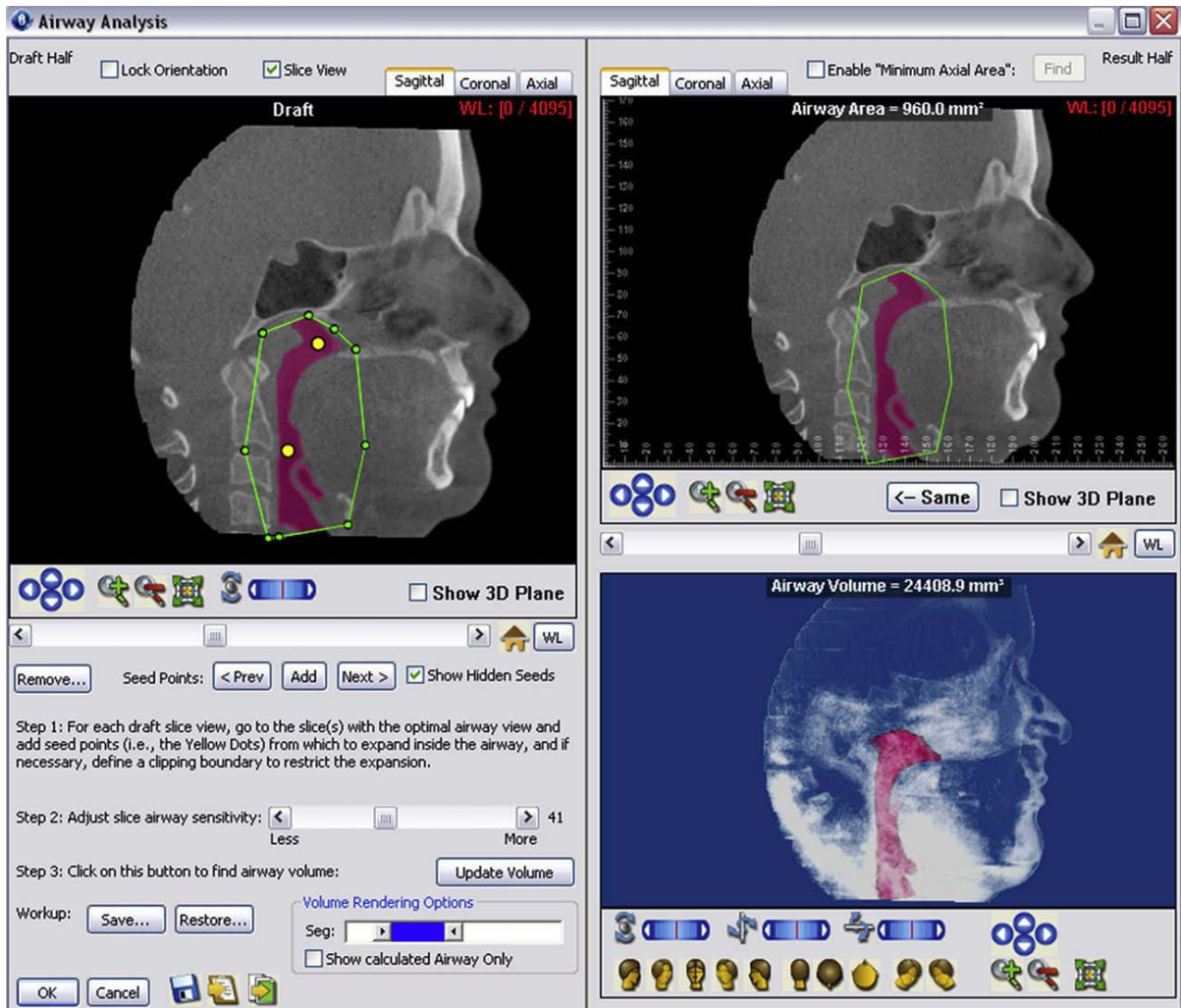


Fig 3.5. Airway analysis module by Dolphin Imaging: at the *upper right corner*, the airway passages are segmented by initialization spheres. Both area and volume can be calculated. The airway segmentation can be rotated, panned, and zoomed in space.

FIGURE 3.6

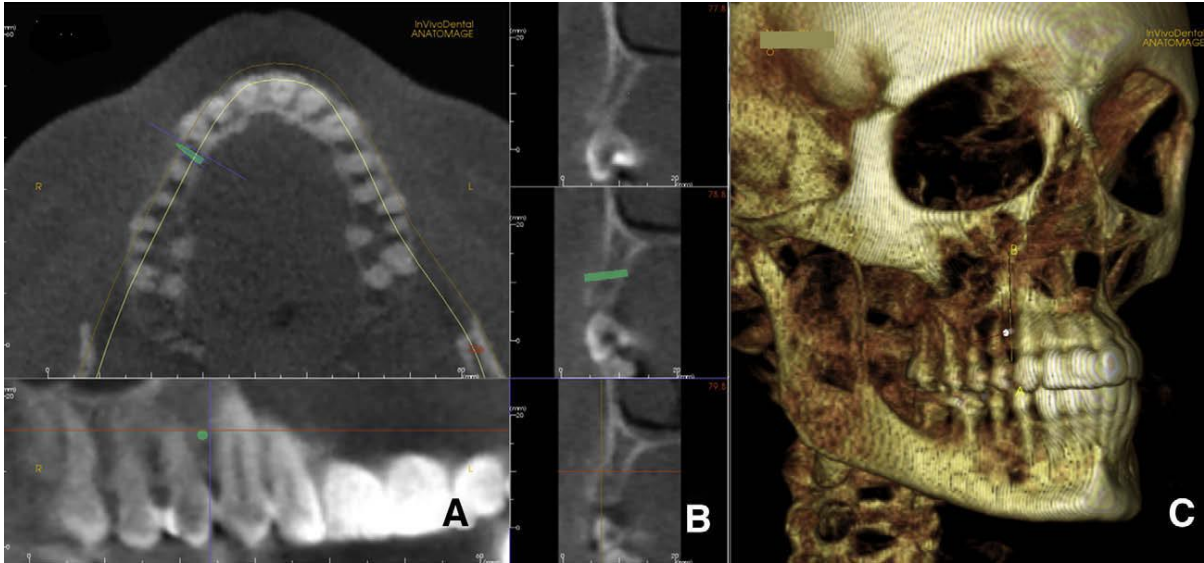


Fig 3.6. Implant simulation and arch section module in InVivoDental: A, a microimplant is virtually placed between the roots of the maxillary right canine and first premolar; B, cortical bone thickness can be measured as well as total bone; C, InVivoDental also allows 3D visualization to assess anatomic relationships. The position on the implant can be modified with 6 degrees of freedom.

FIGURE 3.7

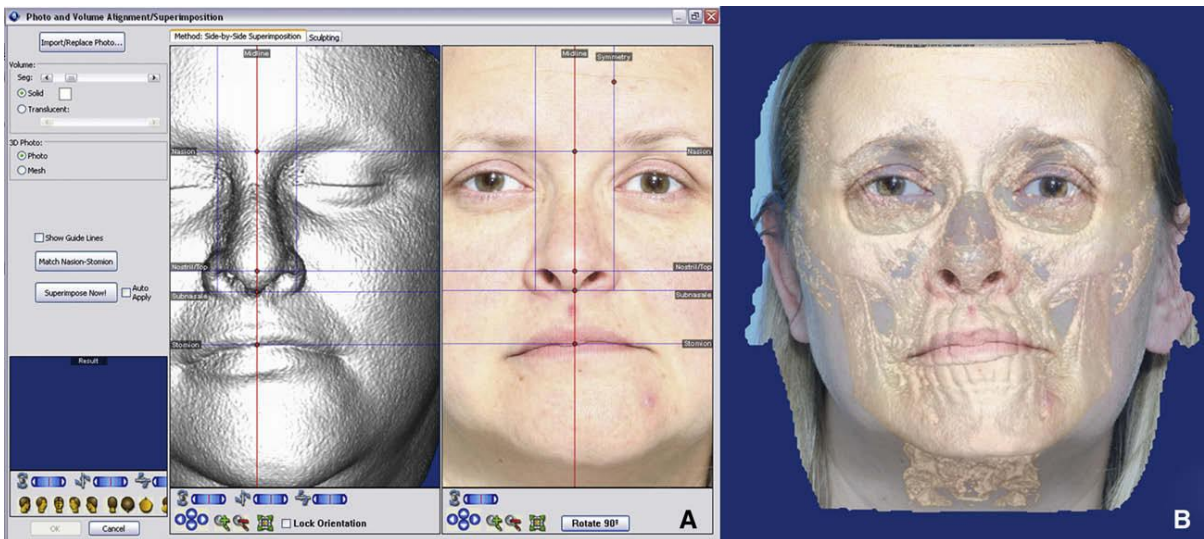


Fig 3.7. Matching a 2D picture on the 3D soft-tissue volume: A, homologous landmarks are located in the volume and the 2D picture; B, Dolphin Imaging registers both images to create a multimodal image. Note the eye difference between the 2 modalities. There might be other, less-obvious areas of discrepancy between photographic and CBCT data.

FIGURE 3.8

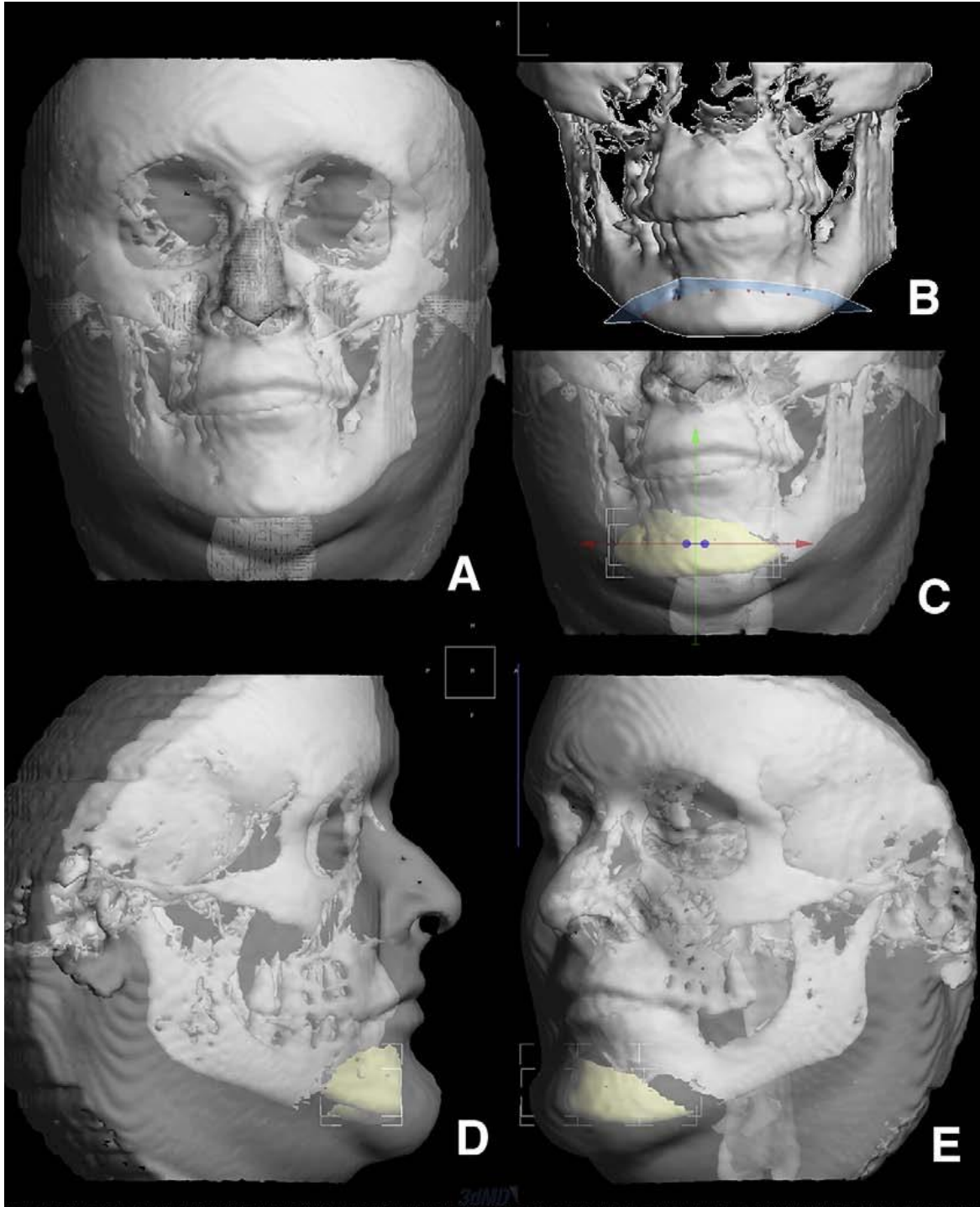


Fig 3.8. Three-dimensional surgical simulation by the 3dMDvultus software: A, surface models were created for both hard and soft tissues; B, virtual surgical osteotomies are performed—here, a lower border osteotomy (genioplasty); C, the chin segment is slid to the left to correct the asymmetry and also moved forward for illustration purposes; D and E, changes predicted in the soft tissues.

## CHAPTER 4

### ACCURACY AND LANDMARK ERROR CALCULATION USING CONE-BEAM COMPUTED TOMOGRAPHY GENERATED CEPHALOGRAMS

#### ABSTRACT

Objective: To evaluate systematic differences in landmark position between cone-beam computed tomography (CBCT)–generated cephalograms and conventional digital cephalograms and to estimate how much variability should be taken into account when both modalities are used within the same longitudinal study. Materials and Methods: Landmarks on homologous cone-beam computed tomography– generated cephalograms and conventional digital cephalograms of 46 patients were digitized, registered, and compared via the Hotelling  $T^2$  test. Results: There were no systematic differences between modalities in the position of most landmarks. Three landmarks showed statistically significant differences but did not reach clinical significance. A method for error calculation while combining both modalities in the same individual is presented. Conclusion: In a longitudinal follow-up for assessment of treatment outcomes and growth of one individual, the error due to the combination of the two modalities might be larger than previously estimated.

#### BACKGROUND

The advent of cone-beam computed tomography (CBCT) for craniofacial imaging provides volumetric information that allows development of virtual three-dimensional (3-D) models that can be quite valuable in locating impacted teeth, visualizing the temporomandibular joints, and diagnosing asymmetries in complex craniofacial patients.<sup>1</sup> Although new applications such as 3-D cephalometrics are developing rapidly, cephalograms are still necessary for comparison to existing databases,<sup>2</sup> and while 3-D registration and superimposition of CBCT data is being developed,<sup>3</sup> sequential cephalograms provide an easy clinical method for assessing growth and treatment changes. In order to be able to compare the new modalities with our current databases, algorithms have been created to extract information from the CBCT image and to simulate a conventional lateral cephalogram, P-A cephalogram, and panoramic projection. Previous in vitro and in vivo studies comparing both conventional cephalograms and CBCT-extracted cephalograms reported some statistically significant differences that did not reach clinical significance.<sup>4-7</sup>

The aims of this in vivo study were (1) to evaluate any systematic differences in landmark position between CBCT-generated cephalograms and conventional digital cephalograms, using an optimization method to superimpose sets of landmarks, and (2) to estimate how much variability should be taken into account when combining conventional and synthetic cephalograms within the same longitudinal study.

## MATERIALS AND METHODS

Records of consecutive patients who had radiographic examination at a radiology clinic between January 2005 and August 2006 were screened. Those for whom both a digital cephalogram (Planmeca, Helsinki, Finland) and a CBCT of the head (iCAT, Imaging Sciences International, Hatfield, Pa) had been obtained were selected. Initial inclusion criteria for this study were a medium-or full-field of view that allowed visualization of both the cranial base and the face and a patient age between 17 and 46 years. Records of 46 patients were available and included in the sample.

#### Creation of a Synthetic Cephalogram

CBCT images were converted into DICOM files and were rendered anonymous by an algorithm included in the iCAT software. Images were loaded into Dolphin 3D (version 2.3 beta) (Dolphin Imaging, Chatsworth, Calif). Threshold filters were set for optimal visualization of the soft and hard tissues.

Images were reoriented to align the cranium relative to the tridimensional coordinate system of Dolphin 3D (version 2.3 beta). Orbits were oriented parallel to the horizontal plane in the frontal view. In the sagittal view the cranium was rotated along the long axis so that the key ridges and orbits were aligned. A cranial view was used to confirm the correct head rotation by aligning the intracranial medial structures with the default coordinate system. Once the virtual 3-D models were aligned, synthetic cephalograms were created. The magnification factor was set to 7.5%, the typical magnification for midline structures with a 60-inch distance from radiation source to the midline with conventional cephalometrics, to simulate the

magnification in conventional digital cephalograms. The images were enhanced for better visualization by fine tuning of the contrast and brightness options and were saved as JPEG files (Figure 4.1).

### Cephalogram Tracing

Both conventional and synthetic cephalograms were loaded into Dolphin (version 9.1; Dolphin Imaging) and traced by a single operator. When landmarks were difficult to locate the operator was instructed to change the contrast, gamma, and brightness setting of the image until structures could be visualized. Whenever bilateral structures were not aligned, or when the difference in magnification was obvious between left and right structures, the operator chose the midpoint between the two structures. Cephalograms were verified for anatomic contour and landmark identification by a second operator. Fifteen cephalograms were selected from the sample and were retraced three times, with at least 24 hours in between tracing sessions. Intraclass correlation coefficients were above 0.9 for all landmarks both for x and y coordinates.

### Registration Method

The two sets of landmarks belonging to each patient were registered in order to combine landmarks from both modalities into the same coordinate system. The following landmarks were used in the registration process: nasion, orbitale, ethmoid reg, sella ant, sella, articulare, pns, ans, a pt, menton, gnathion, pogonion, b pt, gonion, and porion.

In order to register the landmarks identified on the synthetic cephalogram to the ones belonging to the conventional digital cephalogram, rigid Procrustes registration was employed. Landmark coordinates were exported from Dolphin (version 9.1) into MathLab Software (The MathWorks Inc, Boston, Mass). First, the centers of gravity across all measurements were computed in each set of patient landmarks, both for the conventional and synthetic cephalograms. The centers of gravity of the conventional cephalogram landmarks and the synthetic cephalogram landmarks were superimposed. This process minimizes the translation differences between homologous landmarks while considering all the landmarks in the set. Secondly, an objective function that equals the sum of square distances between the landmark pairs was created. By minimizing this objective function, the best fit relative to the rotation of the two sets of landmarks was obtained.

## Measurement

Average difference vector. The residual distances for each patient between homologous landmarks belonging to the two cephalogram modalities were calculated as vectors and will be referred to as “difference vectors” (Figure 4.2). The average difference at each landmark between synthetic and conventional cephalograms was calculated by averaging difference vectors from all patients. This difference will be referred to as the “average difference vector” (Table 4.1).

Average difference length. The absolute length of the individual difference vector is referred to as the “difference length.” Based on these length values, we

then computed the “average difference length” via standard geometric averaging see (Table 4.1).

### Plotting

In order to visualize the difference vectors around each landmark, these vectors were transposed onto an arbitrarily selected landmark set (Figure 4.3). In order to visualize the envelope of landmark location probability, we plotted the average difference length (and two standard deviations) around each one of the landmarks (Figure 4.4).

### Statistical Analysis

Statistical analyses were performed using SAS (version 9.1; SAS Institute Inc, Cary, NC). The hypothesis of interest was that there was no systematic difference between the two modalities at each landmark. We calculated the Hotelling  $T^2$  statistic for the difference vectors between each pair of homologous landmarks in order to formally assess any systematic difference between the two modalities. To account for multiple comparisons across all landmarks, the false-discovery rate method was used.<sup>8</sup>

In order to calculate the bias and variability of the measurement errors obtained from the use of the two modalities at each landmark (see statistical details), we used a two-step process. First, we calculated the difference vectors for all subjects and then computed the sample covariance matrix of these difference vectors. Second, we used the Gaussian random vector with a mean of zero and the

half of the estimated covariance matrix to characterize measurement errors from both modalities.

To estimate the bias and variability of the distance between any two landmarks obtained from the use of the two modalities, we calculated the difference between the measured location difference vectors obtained from the two modalities and estimated their sample covariance matrix. Then, we can use the Gaussian random vector with a mean of zero and the half of the estimated covariance matrix to characterize measurement errors of location difference vectors between any two landmarks from both modalities.

## RESULTS

The average differences in location between homologous landmarks in both modalities are shown in Table 4.1 and Figure 4.2 as the average difference vector and average difference length. In order to compare difference vectors between patients, all sets of difference vectors around each landmark were transposed to an arbitrary center of coordinates and plotted (Figure 4.3). Most landmarks displayed a circular array of difference vectors. The average difference length and two standard deviations were also transposed to an arbitrary center of coordinates and plotted (Figure 4.4), which illustrates landmark location probability.

The distribution of the difference vectors was centered around zero for most landmarks, and there was no systematic difference between the two modalities.

After adjustment for multiple comparisons via the false-discovery rate method (Table 4.2), only three landmarks (ANS, MxI and B) showed a statistically significant

difference, and even for these landmarks the magnitude of the differences did not reach clinical significance (0.5 mm).

## DISCUSSION

### Registration Process

The Procrustes registration process is necessary to avoid an uneven distribution of error (differences) across landmarks. In order to compute the differences between modalities, homologous sets of landmarks have to be combined in the same coordinate system. Most studies simply compare absolute linear or angular measurements between modalities. These methods do not allow for establishment of directionality or discrimination between envelopes of landmark location probability.<sup>4-7,9</sup> Combining homologous sets of landmarks through an arbitrary coordinate center introduces bias.

The most frequent arbitrary coordinate center is centered in sella, with a horizontal plane described by a line 6 degrees inferiorly rotated from sella-nasion plane. However, small differences in the locations of the landmarks that compose the coordinate system will have a great impact on the relative locations of landmarks located at a distance from the center of coordinates. The use of this arbitrary coordinate system to describe the relative coordinates of landmarks across modalities could lead to errors. Studies using the sella as the arbitrary coordinate center find their greater differences at mandibular structures or related measurements that are located far away from the coordinate system center.<sup>10</sup> In our

method, the registration of homologous sets of landmarks and establishment of envelopes of landmark location probability did not depend on a single landmark but rather on a set of landmarks distributed uniformly across the head and face anatomy.

### Sources of Variability

Main sources of variability that could affect our results are variability due to landmark identification and variability due to head orientation and alignment of x-ray emitter.

Landmark identification. The variability due to landmark identification displays characteristic patterns described by Baumrind and Frantz.<sup>11</sup> The systematic error in landmark identification affects both modalities, and it is likely that the net effect on the difference between modalities is negligible. In terms of landmark identification, general findings in this study are in agreement with in vitro studies by Kumar et al<sup>6</sup> and Moshiri et al.<sup>9</sup> These studies measured dry skulls, and it is important to note that landmark identification is slightly more complex when soft tissue is present. The general aspect of a CBCT synthetic cephalogram is different from that of a conventional digital cephalogram (Figure 4.1). Landmark identification was easier in the synthetic cephalograms. Some landmarks that often lack the adequate contrast for an easy identification in conventional digital cephalograms were easily recognized because of the higher difference in contrast in the synthetic cephalograms.

Head orientation and alignment of x-ray emitter. Some of the differences found between homologous landmarks could be related to different head orientation. Malkoc et al<sup>12</sup> have found that linear and angular measurements on lateral cephalograms change from 16.1% to 44.7% with 14 degrees of head rotation. Positioning of the patient inside the Planmeca cephalostat depends on the technician's skill, and that introduces another factor for which we cannot control.

The patient's anatomy also affects head positioning in the cephalostat. When the ears are used as a reference, we assume that the patient is relatively symmetric and that his/her ears are at the same level. In asymmetric patients this could create a head positioning error. Once the image is acquired, no corrections can be made to the roll and yaw of the head. Conversely, when a synthetic cephalogram is created the operator can easily manipulate the DICOM three-dimensionally to orient the head until bilateral structures are matching. The operator is able to see through the skull and match the position of para-medial structures. The position of the anatomical structures inside the field of view of the CBCT, in terms of rotation and translation, does not influence the accuracy of the measurements.<sup>13</sup> In this study, while creating the synthetic cephalograms, no effort was made to replicate the position of the patient's head obtained in the conventional cephalograms.

Another source of projection errors is the misalignment of the x-ray emitter focal spot, which affects the conventional cephalogram machines. Even though we are certain that our x-ray unit was calibrated periodically, the fact that the cephalograms were obtained over a period of 18 months implies that the alignment of the x-ray source may have not been constant throughout the whole period. In an

ex vivo study, Lee et al<sup>14</sup> reported that this type of misalignment could cause systematic error in the interpretation of facial asymmetry in PA cephalograms. That could be the case for conventional digital cephalograms too.

### Dry Skull and In Vivo Studies

The accuracy and precision of measurements with CBCT have been assessed by several studies.<sup>13,15,16</sup> Ludlow et al<sup>17</sup> concluded that measuring in both reconstructed panoramic projection and in the 3-D volume through the stack of slices provides accurate measurements of mandibular anatomy. Lascala et al<sup>18</sup> reported a slight underestimation in linear measurements compared with direct measurements with a caliper used on skulls.

Our results are in agreement with ex vivo studies that have compared the accuracy and reliability of CBCT-generated cephalograms using skulls. Kumar et al<sup>6</sup> concluded that with dry skulls CBCT is comparable to conventional cephalometry in terms of precision and accuracy. In a recent article Moshiri et al<sup>9</sup> reported that CBCT-extracted cephalograms were, on average, more accurate than conventional digital lateral cephalograms when compared using direct measurement on skulls as a gold standard. In both studies, linear measurements of the mandible differed between the conventional and the CBCT synthetic cephalograms.

The findings from in vivo studies that assess differences in modalities are more directly comparable to our results. Recent in vivo studies have compared measurements between conventional cephalograms and CBCT-generated cephalograms and have concluded that even though some differences were found,

they were not statistically or clinically significant.<sup>4,5,7</sup> These studies compared absolute measurements between modalities independently of landmarks' absolute coordinates. Given that there is no systematic error in landmark location between modalities, it is expected that the average differences in measurements reported between modalities would be centered around zero. When applied to an individual, the error in landmark location between modalities (or difference vector) could be much greater than the population average. When the two modalities are utilized in a longitudinal study of the same individual and when linear or angular measurements are computed, the reported error should include the envelope of landmark location probability at both landmarks (and at three landmarks if it is an angular measurement).

With the method presented here, by calculating the envelope of landmark location probability around each landmark we can estimate the mean increase in error while measuring linear distances (Table 4.2). For instance, according to our method, if both modalities were used to calculate the distance between condylion and gnathion in an individual, the error could be as high as or higher than 2.36 mm (one out of 10 cases would display an error greater than 2.36 mm). This has an obvious impact when one is measuring small changes in mandibular length between time points. With our method, the error in measurement for any combination of two landmarks can be computed, and angular measurements can be analyzed similarly. In longitudinal follow-up for assessment of treatment outcomes and growth of one individual, the error due to combination of the two modalities might be larger than previously estimated.

In agreement with previous reports, the average difference in our study is below clinical significance. In longitudinal studies, when both modalities are used in the same individual, we should consider that the error of the method could produce clinically significant differences. This is especially the case when the variables measured display small incremental differences with growth. CBCT-generated cephalograms could be used as a diagnostic tool, but when assessing treatment outcomes at different times for one individual, the variability between modalities makes it advisable to obtain sequential records with the same modality.

## CONCLUSIONS

There is no systematic error when we compare average homologous landmark coordinates in conventional digital cephalograms and CBCT-generated cephalograms.

In longitudinal studies, when both modalities are used in the same individual, the error of the method could produce clinically significant differences.

## REFERENCES

1. Ludlow JB, Davies-Ludlow LE, Brooks SL. Dosimetry of two extraoral direct digital imaging devices: NewTom cone beam CT and Orthophos Plus DS panoramic unit. *Dentomaxillofac Radiol.* 2003;32:229–234.
2. Hunter WS, Baumrind S, Moyers RE. An inventory of United States and Canadian growth record sets: preliminary report. *Am J Orthod Dentofacial Orthop.* 1993;103:545–555.
3. Cevidanes LH, Styner MA, Proffit WR. Image analysis and superimposition of 3-dimensional cone-beam computed tomography models. *Am J Orthod Dentofacial Orthop.* 2006;129:611–618.
4. Cattaneo PM, Bloch CB, Calmar D, Hjortshoj M, Melsen B. Comparison between conventional and cone-beam computed tomography-generated cephalograms. *Am J Orthod Dentofacial Orthop.* 2008;134:798–802.
5. Kumar V, Ludlow J, Soares Cevidanes LH, Mol A. In vivo comparison of conventional and cone beam CT synthesized cephalograms. *Angle Orthod.* 2008;78:873–879.
6. Kumar V, Ludlow JB, Mol A, Cevidanes L. Comparison of conventional and cone beam CT synthesized cephalograms. *Dentomaxillofac Radiol.* 2007;36:263–269.
7. Van Vlijmen OJ, Berge SJ, Swennen GR, Bronkhorst EM, Katsaros C, Kuijpers-Jagtman AM. Comparison of cephalometric radiographs obtained from cone-beam computed tomography scans and conventional radiographs. *J Oral Maxillofac Surg.* 2009;67:92–97.
8. Benjamini Y, Hochberg Y. Controlling the false discovery rate: a practical and powerful approach to multiple testing. *J R Statist Soc Ser.* 1995;57:289–300.
9. Moshiri M, Scarfe WC, Hilgers ML, Scheetz JP, Silveira AM, Farman AG. Accuracy of linear measurements from imaging plate and lateral cephalometric images derived from cone-beam computed tomography. *Am J Orthod Dentofacial Orthop.* 2007;132:550–560.
10. Ludlow JB, Gubler M, Cevidanes L, Mol A. Precision of cephalometric landmark identification: CBCT vs conventional cephalometric views. *Am J Orthod Dentofacial Orthop.* In press.
11. Baumrind S, Frantz RC. The reliability of head film measurements. 1. Landmark identification. *Am J Orthod.* 1971;60:111–127.

12. Malkoc S, Sari Z, Usumez S, Koyuturk AE. The effect of head rotation on cephalometric radiographs. *Eur J Orthod.* 2005;27:315–321.
13. Kobayashi K, Shimoda S, Nakagawa Y, Yamamoto A. Accuracy in measurement of distance using limited cone-beam computerized tomography. *Int J Oral Maxillofac Implants.* 2004;19:228–231.
14. Lee KH, Hwang HS, Curry S, Boyd RL, Norris K, Baumrind S. Effect of cephalometer misalignment on calculations of facial asymmetry. *Am J Orthod Dentofacial Orthop.* 2007; 132:15–27.
15. Marmulla R, Wortche R, Muhling J, Hassfeld S. Geometric accuracy of the NewTom 9000 cone beam CT. *Dentomaxillofac Radiol.* 2005;34:28–31.
16. Mischkowski RA, Pulsfort R, Ritter L, et al. Geometric accuracy of a newly developed cone-beam device for maxillofacial imaging. *Oral Surg Oral Med Oral Pathol Oral Radiol Endod.* 2007;104:551–559.
17. Ludlow JB, Laster WS, See M, Bailey LJ, Hershey HG. Accuracy of measurements of mandibular anatomy in cone beam computed tomography images. *Oral Surg Oral Med Oral Pathol Oral Radiol Endod.* 2007;103:534–542.
18. Lascala CA, Panella J, Marques MM. Analysis of the accuracy of linear measurements obtained by cone beam computed tomography (CBCT-NewTom). *Dentomaxillofac Radiol.* 2004;33:291–294.

TABLE 4.1

Table 4.1. Landmarks, Average Difference Vectors (X and Y Components and Module), Significance, False-Discovery Rate Method Correction, and Average Difference Lengths. Statistical Significance Was Established at 0.01 (Measurements are in mm)

Landmark	Average X	Average Y	(ADV) Magnitude	P Value	P Value (FDR)	Average Difference Length (ADL)	SD <sub>s</sub> (ADL)
Nasion	0.10	0.23	0.25	.595	.617	0.70	1.94
Orbitale	-0.07	0.38	0.39	.017	.067	1.26	1.88
Pterygo-maxillary fissure	0.01	-0.16	0.16	.638	.638	1.29	2.22
Ethmoid registration	0.11	-0.37	0.38	.122	.289	0.67	2.24
Sella anterior	-0.07	0.11	0.13	.415	.553	0.61	2.11
Sella	-0.09	0.01	0.09	.567	.611	0.51	2.03
Basion	-0.42	-0.49	0.64	.004	.031	1.18	2.50
Articulare	-0.19	-0.14	0.24	.124	.289	0.81	1.87
Condylion	0.18	-0.36	0.40	.212	.361	1.23	2.18
Posterior nasal spine	-0.25	-0.11	0.27	.048	.139	0.55	2.24
Anterior nasal spine	-0.48	-0.11	0.49	.001	.007	0.82	2.10
A pt	0.12	-0.03	0.12	.175	.350	0.65	1.79
Upper incisor incisal tip	0.34	-0.14	0.37	.000	.003	0.58	2.17
Upper incisor root apex	-0.05	-0.17	0.18	.172	.350	0.69	1.91
Upper first molar mesial contact	-0.13	-0.09	0.16	.459	.584	0.90	1.88
Upper first molar mesial cusp	0.05	-0.10	0.11	.539	.603	0.90	2.04
Upper first molar distal contact	-0.03	-0.17	0.17	.499	.603	0.79	2.36
Menton	-0.06	0.18	0.19	.219	.361	0.69	1.80
Gnathion	0.18	0.17	0.24	.266	.414	0.58	2.26
Pogonion	0.24	0.30	0.38	.007	.037	0.62	2.39
B pt	0.22	-0.45	0.50	.001	.007	0.99	1.61
Lower incisor incisal tip	0.19	-0.16	0.25	.015	.067	0.55	1.96
Lower incisor root apex	0.13	-0.08	0.15	.368	.516	0.72	1.85
Lower first molar mesial contact	0.20	-0.26	0.33	.046	.139	0.91	2.04
Lower first molar mesial cusp	0.23	-0.02	0.23	.333	.491	1.00	1.99
Lower first molar distal contact	0.14	-0.26	0.29	.050	.139	0.93	1.90
Gonion	-0.02	-0.20	0.21	.534	.603	0.94	2.32
Porion	0.28	0.02	0.28	.208	.361	1.04	2.10

SD indicates standard deviation, FDR indicates False-Discovery Rate method

TABLE 4.2

Table 4.2. Difference Between Modalities for Four Linear Measurements. Mean Difference, Standard Deviation (SD), and Percentiles (Measurements are in mm)

Lengtha	Mean Difference	SD	Percentile					
			10%	25%	40%	60%	75%	90%
ANS-me	0.90	0.49	0.32	0.53	0.71	0.96	1.21	1.56
N-Me	1.25	0.80	0.38	0.65	0.90	1.31	1.70	2.38
Co-Gn	1.37	0.73	0.53	0.83	1.09	1.48	1.80	2.36
Co-ANS	1.32	0.70	0.50	0.79	1.06	1.42	1.71	2.25

FIGURE 4.1

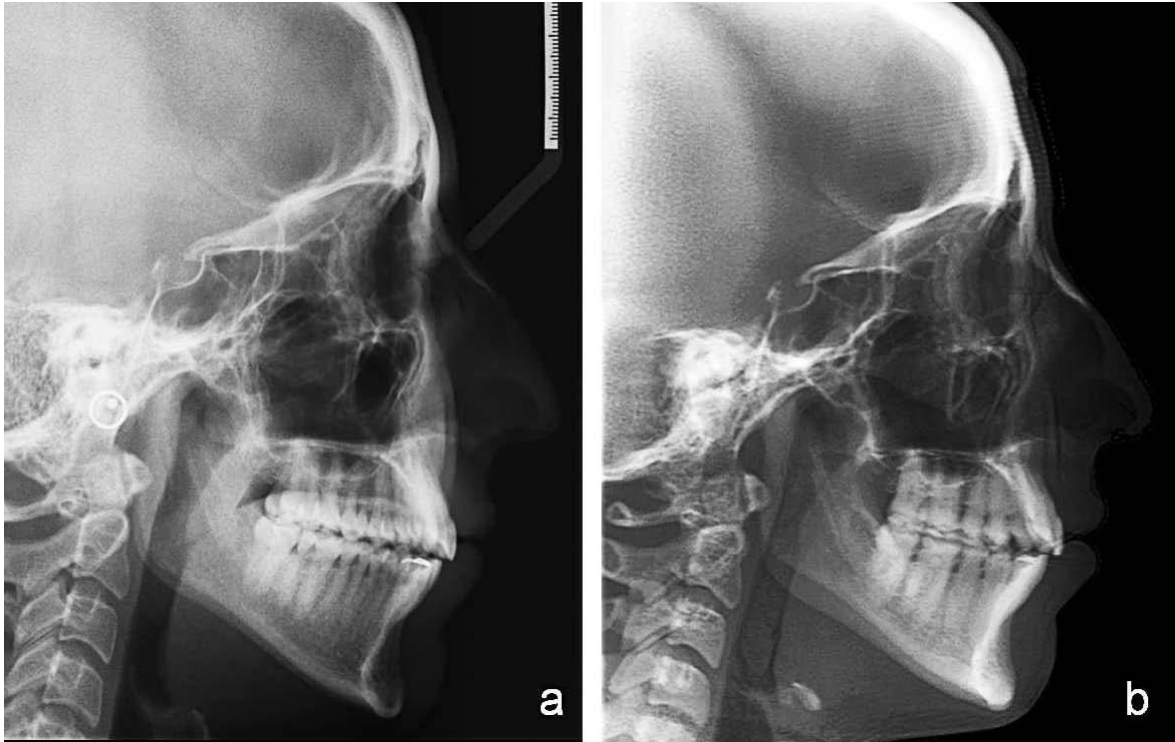


Figure 4.1. Different aspect of a conventional digital cephalogram (a) and a CBCT-generated cephalogram. (b) Note the difference in contrast and structure superimposition. For the digital cephalogram (JPEG file, 1360 3 2045; 8-bit; Proline, Planmeca, Helsinki, Finland); for the CBCT-generated cephalogram (16 x 22 cm large field of view, primary/axial image type, 1500/5000 window center/width, 400/400 rows/columns; iCAT, Imaging Sciences International).

FIGURE 4.2

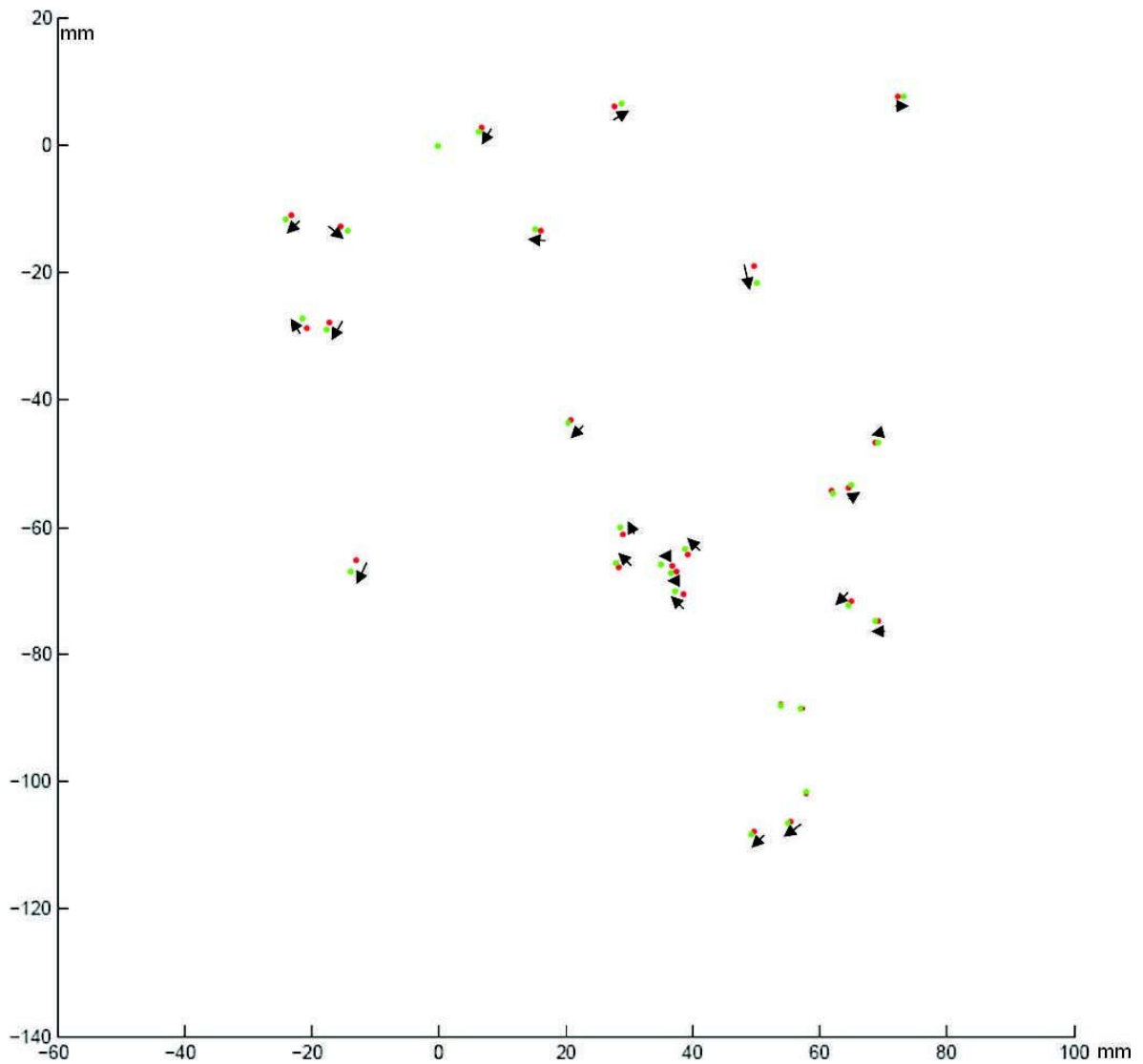


Figure 4.2. Landmarks located in the CBCT-generated cephalogram (red) have been registered via Procrustes method to the landmarks located on the conventional digital cephalogram (green). Difference vectors are depicted.

FIGURE 4.3

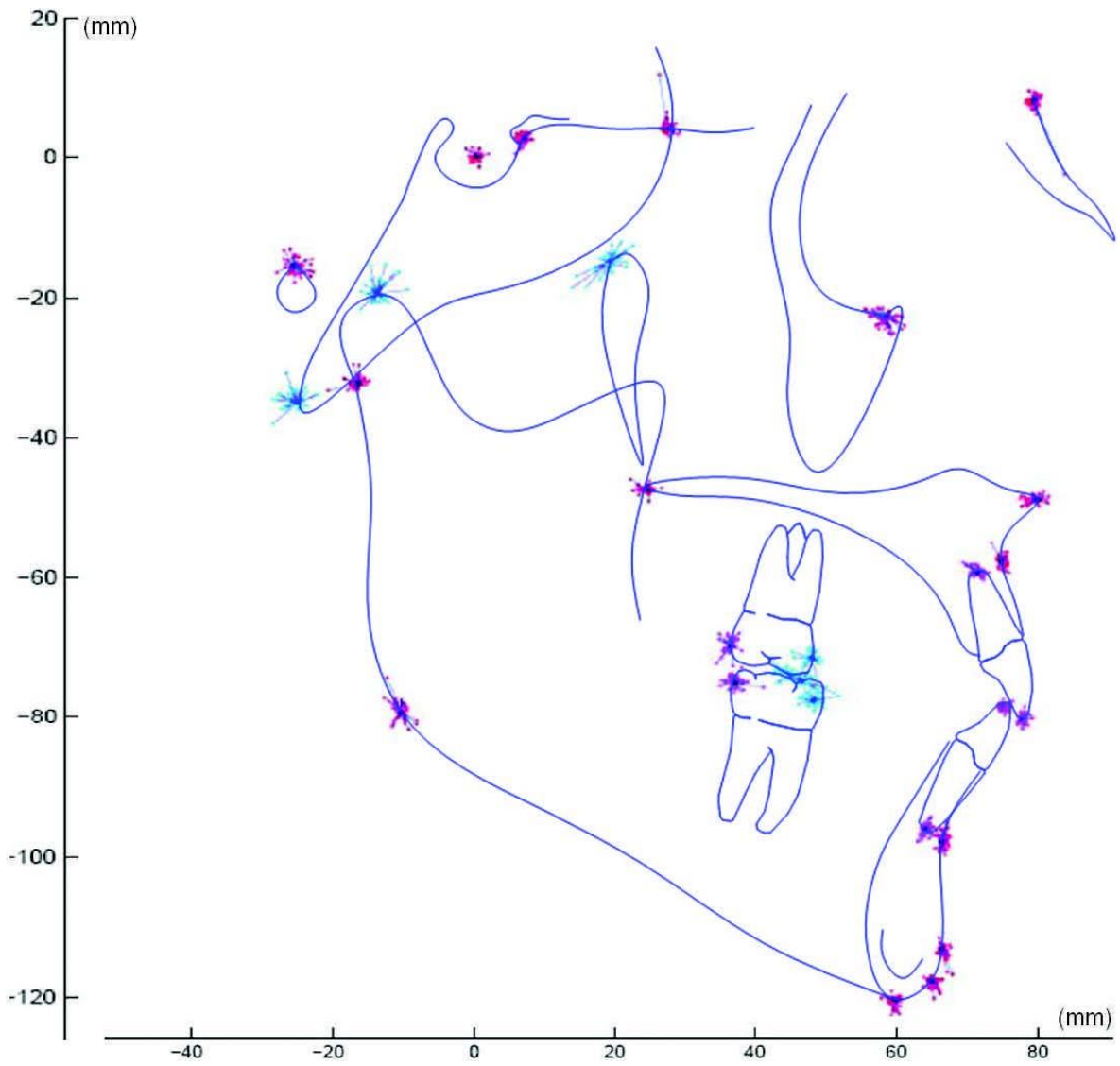


Figure 4.3. Difference vectors are grouped by landmark on a cephalogram tracing. The envelope of error—or difference between modalities—can be visualized. (Red and purple landmarks were used in the registration process; blue landmarks were only plotted.)

FIGURE 4.4

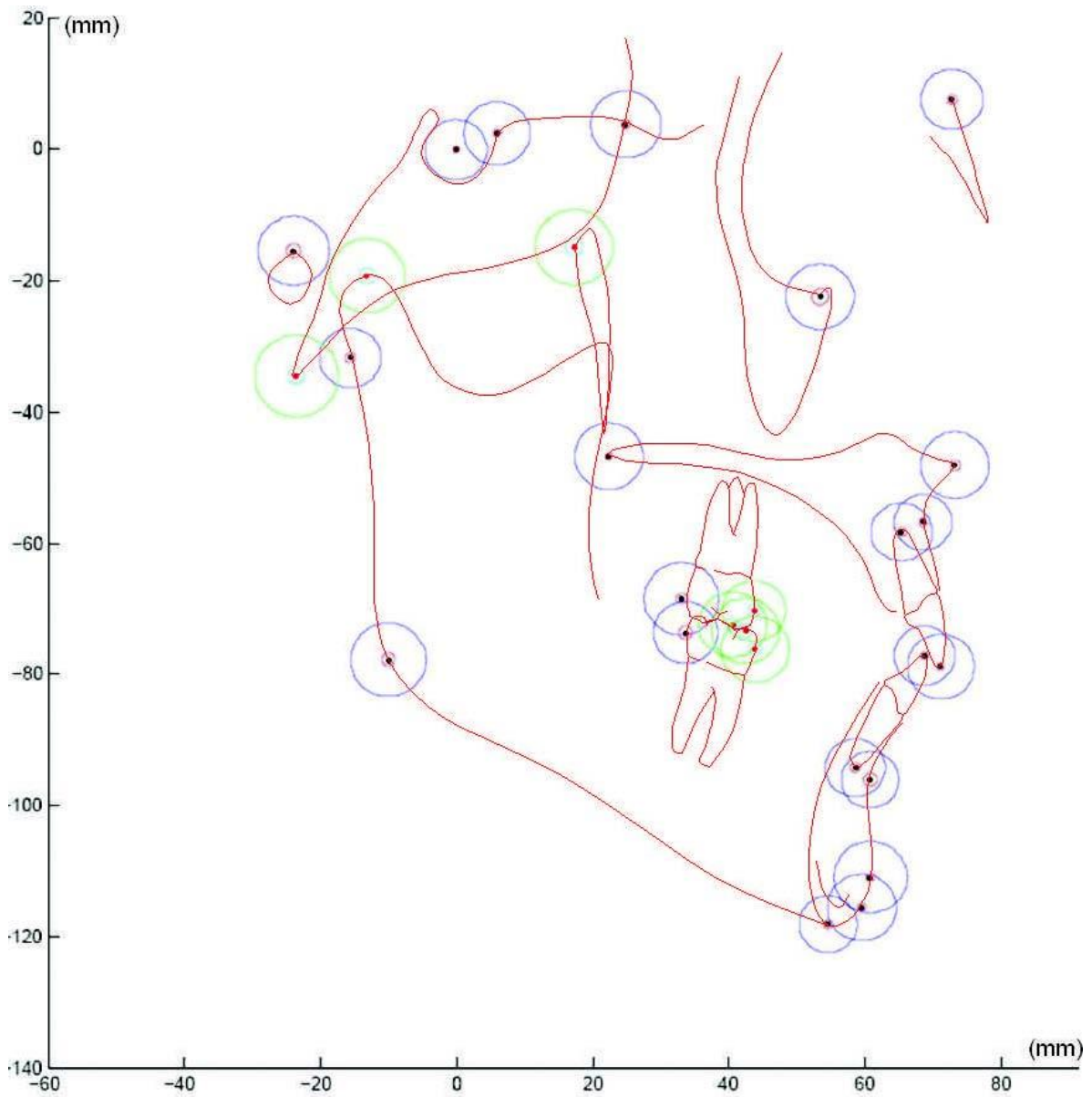


Figure 4.4. Difference lengths depicted as average plus three standard deviations are plotted on a cephalogram tracing. (Purple landmarks were used in the registration process; green landmarks were only plotted.)

## CHAPTER 5

### REGISTRATION OF ORTHODONTIC DIGITAL MODELS

#### ABSTRACT

Current methods to assess outcomes and change in orthodontics are comparison of photographs, cephalometric measurements and superimpositions, and comparisons/measurements on dental casts. Digital models are a relatively new records modality in orthodontics. They offer numerous advantages in terms of storage space, spatial registration and superimposition. The purpose of this paper is 1) to determine the reproducibility of establishing occlusion of independently scanned digital models; and 2) to determine the reproducibility of registering digital models obtained after treatment on their homologous digital model setups produced before treatment. Reliability of both procedures was assessed with two random samples of five patients' models. In both experiments three replicate positioning of the models per patient were created and variability in position was evaluated by the maximum surface difference between replicates, and the standard deviation of the surface distances between replicates respectively. Based on the data obtained we concluded that it is reliable to register independently scanned models to a scanned surface of the models in occlusion. Surface to surface registration of final orthodontic digital models to planned setup models is also reproducible.

## BACKGROUND

Excellence in orthodontics depends on careful assessment of treatment outcomes. In order to evaluate and quantify changes, records and measurements are obtained at different time points and compared.

Current methods to assess outcomes and change in orthodontics are comparison of photographs, cephalometric measurements and superimpositions, and comparisons/measurements on dental casts. Photographs offer a qualitative assessment in orthodontics and are a valuable communication tool. However, due to the likelihood of different camera angulation during photograph acquisition, it is not practical to obtain quantitative information for precise assessment of change<sup>1</sup>. Cephalometric superimpositions are the current gold standard for assessment of change in orthodontics, and it has been shown that they provide great precision and accuracy<sup>2,3</sup>. Cephalometric measurements can also be compared to normative data<sup>4</sup>. Their main disadvantage is that cephalometric radiographs are a two-dimensional representation of three-dimensional structures, and due to the overlapping of the left and right sides of the dental arches it is particularly difficult to obtain a precise assessment of tooth movement.

Dental casts are the most frequently used three dimensional record in orthodontics and are, after the clinical evaluation, the most valuable orthodontic record<sup>5</sup>. However, their physical nature prevents them from being superimposed in space, and hence only linear two-dimensional measurements can be obtained. Moreover, they cannot be registered within the same coordinate system. Because we do not know the spatial relationship between models acquired at different time

points, measurements of change are not directional. For example, we know that a change occurred between point 1 and point 2 but we do not know whether that change was due to movement of point 1, point 2 or both, and we cannot quantify the percentage of change at each point (Figure 5.1).

The American Board of Orthodontics developed an Objective Grading System in order to assess treatment outcomes in orthodontics<sup>6</sup>. This method has proven to be reliable and is now a standard method for orthodontic outcomes assessment. The OGS is based in linear measurements on dental casts and includes the disadvantages previously mentioned. A digital version of the OGS is currently under development but has not been validated yet<sup>7,8</sup>.

Digital models are a relatively new records modality in orthodontics. They offer numerous advantages in terms of storage space, spatial registration and superimposition. Digital models are not qualitatively different from conventional dental casts in terms of diagnosis and treatment planning<sup>9,10</sup>. Quantitatively some differences have been found when comparing measurements between digital and dental casts, but these differences were not clinically significant<sup>11-20</sup>. Digital models of the same patient obtained at different times can be registered in the same coordinate system, and that allows for assessing change among time points. The challenge is to find stable references across time to be used as registration structures<sup>21</sup>. The rugae region of the palate has been suggested as stable region<sup>22-29</sup>. It seems that once these difficulties are overcome, digital models will offer a quantifiable, directional, accurate and reliable way of assessing change.

The purpose of this paper is 1) to determine the reproducibility of establishing

occlusion of independently scanned digital models; and 2) to determine the reproducibility of registering digital models obtained after treatment on their homologous digital model setups produced before treatment.

#### Part I: establishing occlusion with independently scanned digital models

One method of creating digital models from dental casts involves independently scanning each dental cast upper and lower, and then scanning the facial surfaces of both models in occlusion. This last scan is used as mutual information to reposition the independently scanned upper and lower models in a spatial relationship that reproduces the patient's occlusion.

## METHODS

### Sample

In order to register the dental arches in space to represent the patients' occlusion a sample consisting of pretreatment models of five patients was randomly selected from a population of 94 consecutively treated patients. The originating sample is composed by consecutive cases treated with Incognito lingual technique and debonded between January 2008 and January 2009. Inclusion and exclusion criteria for the originating sample of treated patients are described elsewhere<sup>30</sup>. In order to create the scanned surfaces, poly-vinyl siloxane impressions were made with Bisico impression material (Bielefelder Dentsilicone GmbH & Co. KG, Bielefeld, Germany) and poured with Type IV extra hard white stone. Models were

scanned with an ATOS optical scanner (GOM mbH, Braunschweig, Germany) at a spatial resolution of 20 microns. For each patient three scans or surfaces were created: one surface of the upper arch, one surface of the lower arch and one surface of the models in occlusion. The latter one included only the facial aspect of the models in occlusion. Figure 5.2 (A).

### Software

The upper arch surface was registered to the corresponding buccal upper arch surface on the occlusion models using Occlusomatch software (TopService, 3M, Bad Essen Germany). Parameters for the registration were set to select 2500 points on each surface and with a search radius of 1 mm (reduced to 0.25 mm, factor of 0.50 mm). Iterations were automatically performed until a 0.06 mm average surface distance was obtained. The success threshold was set at 0.06 mm Figure 5.2 (B). This two-step process was repeated three times per patient for each dental arch, rendering three positions for the upper dental arch and three positions for the lower dental arch. Dental arches were compared pair-wise and average surface distances were computed between homologous dental arches in Geomagic Studio10.0 software (Geomagic U.S., Research Triangle Park, NC, USA). The variable of interest was the maximum surface distance between homologous dental arches as a proxy for the maximum discrepancy due to the registration process (Figure 5.3).

### Statistical analysis

In order to assess whether the discrepancy in positioning varies by dental arch, the largest discrepancy in replicate positioning was analyzed using a repeated measures analysis, allowing for different compound symmetry covariance structures for each dental arch.

## RESULTS

The estimated maximum difference in replicate positioning is shown in Table 5.1. Three positions per dental arch were compared pair-wise across patients. The summary of the statistical model analysis is displayed in Table 5.2.

This data suggests that there is no statistically significant difference between the upper and lower arches in the average discrepancy in replicate positioning and no statistically significant differences between replicate positioning across the entire sample. Positioning the digital models in occlusion by using the scanned surface of the buccal surface of the models in occlusion is reproducible.

## DISCUSSION

Even though it is likely that validation studies like this one have been conducted, we could not find any publication of a similar approach.

A second method to position the digital models in occlusion involves using a three dimensional surface scan of a wax bite – an interocclusal record – to obtain a

reference to which the digital models could be registered in space. This method is based in registering the upper model to the upper surface of the wax bite, and the lower model to the lower surface of the wax bite. The structures involved in this surface to surface registration are the upper and lower cusps and incisal edges in the digital models and their homologous indentations produced in the wax material while the patient bit on it. This second method requires surface-to-surface registration of complimentary surfaces (for example dental cusps and indentations on the wax bite) rather than homologous surfaces (for example facial surfaces of dental model in occlusion and not in occlusion); and it is likely to involve a greater error of the method due to approximation operations during the complementary surfaces registration.

A third method of establishing occlusion of the digital models would involve scanning the models mounted in an articulator. By using fiducial structures attached to the articulator the relative position of the upper model to the lower model could be calculated. This is a potentially very accurate method but its main caveat is the constant calibration of the scanner needed to be sure that the articulator position is registered to the global coordinate system of the scanner.

Currently using the scanned surface of the models in occlusion to register digital models (but with different registration parameters) is widely used by clinicians thanks to the introduction of in-office model scanners. The 3Shape model scanner (3Shape, Copenhagen, Denmark), is a relatively economical device that allows the user to scan models independently and in occlusion. Through the proprietary OrthoAnalyzer software the user can establish the occlusion of the models and

perform measurements, digital setup and export the models as non-proprietary files (STL). It is very important that when the models are locked in occlusion this position remains the same throughout the entire scanning process. There are different devices to maintain the models in a fixed position while the scanner platform is moving to allow scanning of all surfaces of the models. Extreme care should be taken because a minimal movement of the models in occlusion during scanning will render a non-valid occlusion registration.

We have chosen the absolute value of the maximum discrepancy between surfaces (homologous dental arches were compared pair-wise in three replicate positioning) as our variable of interest. This variable is representative of the maximum error between registration instances and it may overestimate the error. However given the small variability obtained, we considered it safer to overestimate rather than to underestimate. This small magnitude estimates for the upper and lower dental arch are not considered clinically significant.

Part II: registration of setup models to final models to assess treatment precision.

Digital models offer a clear advantage over dental casts in assessing longitudinal changes given that they can be registered and superimposed in space<sup>21,28</sup>. Among other methods of treatment results assessment in orthodontics, outcomes in orthodontics can be also assessed by comparing the obtained outcome with the planned setup. Spatial registration of the setup model on the final digital models is achieved by an iterative closest point algorithm or “best fit” of surfaces. In

order to evaluate the reliability of the ICP registration of setup models to their homologous final outcome model the following study was accomplished.

## METHODS

### Sample

In order to assess the reliability of registration of final digital models to digital models of initial setups, a second sample consisting of models of five patients was randomly selected from the population of 94 consecutive treated patients<sup>30</sup>. For each patient two sets of models were available: final models post-orthodontic treatment obtained the day of bracket de-bonding and setup model made on a duplicate of the malocclusion models before orthodontic treatment. Models were scanned with an ATOS optical scanner (GOM mbH, Braunschweig, Germany) at a spatial resolution of 20 microns.

### Software

Models were repositioned in space to reproduce their occlusion relationship using method described in the first part of this article. The surfaces were simplified to 50,000 points using the Qslim 2.0 tool<sup>31</sup> and then cleaned to delete the gingival tissues. Once simplified, the upper setup model was registered to the upper final model using eModel 9.0 software (Geodigm Corporation, Chanhassen, MN), to combine both models in the same coordinate system. The same process was followed for the lower setup model.

The registration process was repeated 3 times per dental arch, per patient, rendering three relative positions of the upper and lower setup arches to the final models (Figure 5.4). Setup and final dental arch positions were compared pair-wise and average surface distance was computed between homologous record arches. The variable of interest was the absolute value of the standard deviation surface distance between final and setup models as a proxy of the average discrepancy due to the registration process.

### Statistical analysis

In order to assess whether the error in replicate positioning varies by dental arch, the standard deviation was used to summarize the deviation between replicates. A repeated measures analysis was performed, allowing for different compound symmetry covariance structures for each dental arch.

## RESULTS

The estimated maximum difference in replicate positioning is shown in Table 5.3. The average difference in absolute value of the standard deviation was not significantly different from zero for the upper jaw ( $p=0.08$ ) or for the lower jaw ( $p=0.22$ ). The summary of the statistical model analysis is displayed in Table 5.4.

This data suggests that there is no statistically significant difference between the upper and lower arches in the average discrepancy in replicate positioning and no statistically significant differences between replicate positioning across the entire sample.

## DISCUSSION

Longitudinal change assessment using sequential digital models is based in the following process: first a coordinate system has to be defined; second models from different time points must be registered to that coordinate system; and third, models are superimposed and the differences among them are evaluated. In order to combine different records in the same coordinate system, stable structures – which did not change with time or treatment – are defined and used as registration regions. Once registered, structures that did change can be qualitatively and quantitatively described.

While the orthodontic community is waiting for a reliable longitudinal registration of sequential dental models to assess tooth movement, other methods to assess treatment outcomes are being used. The ABO OGS is a validated tool to assess orthodontic outcomes. Even though at this point it is one of the best methods we have, it depends on fixed anatomical relationships rather than on actual tooth movement. Due to that, its results are often influenced by the tooth anatomy.

Researchers have been looking for stable structures within the dental models to be used as registration landmarks or surfaces<sup>32-35</sup>. The main problem using rugae as stable registration surfaces is that – as in any registration process – the further away from the registration surface a point is, the greater the registration error becomes<sup>21,25</sup>. While the rugae may be reliable to assess tooth movement in the premolar region (mainly in cases treated with no extractions), it may not be precise enough to assess changes in the molar region. In addition, small changes in rugae

morphology will have great effects on the relative vertical position of molars between time points. Recently Jang et al. compared the rugae registration method with registration on miniscrews placed in the maxilla and concluded that the medial points of the third palatal rugae and the palatal vault could be used as reference landmarks<sup>28</sup>.

An efficient way to assess treatment outcomes – not tooth movement – would be to register and superimpose the models obtained after orthodontic treatment on the setup or planned correction. While this method does not allow for calculation of tooth movement due treatment and growth, it does allow for calculation in the discrepancy between planned position and obtained position relative to intra-arch tooth alignment. The first step for such method is the establishment of reproducible registration method. Iterative closest point registration does not depend on stable structures and rather utilizes the whole surface during the computation of the registration parameters. Given that the differences between surfaces (final treatment and planned setup) are relatively small, the registration error is divided among all teeth based on their size.

The reliability of this method depends on the relative initial position of the surfaces before registration process, because ICP registration uses optimization methods to identify a minimum surface distance value between surfaces. Given that the surfaces that we register are similar but not equal, we have chosen the standard deviation as a proxy variable for the registration variability. If we would use the average surface distance between surfaces we would underestimate the error in registration, because positive errors would cancel negative ones. The absolute value

of the maximum distance between surfaces is also not representative of the discrepancy between registration instances given that the surfaces are not equal.

#### CONCLUSION:

Based on the data presented above, it is reliable to register independently scanned models to a scanned surface of the models in occlusion. Surface to surface registration of final orthodontic digital models to planned setup models is also reproducible.

Further research is needed to establish the most stable landmarks/surfaces for longitudinal registration of sequential digital models. Once surfaces are registered the difference between positions of individual teeth can be measured and expressed in terms of six degrees of freedom (Figure 5.5).

## REFERENCES

1. McKeown HF, Murray AM, Sandler PJ. How to avoid common errors in clinical photography. *J Orthod* 2005;32:43-54.
2. Bjork A. Sutural growth of the upper face studied by the implant method. *Acta Odontol Scand* 1966;24:109-127.
3. Johnston LE, Jr. Balancing the books on orthodontic treatment: an integrated analysis of change. *Br J Orthod* 1996;23:93-102.
4. Hunter WS, Baumrind S, Moyers RE. An inventory of United States and Canadian growth record sets: preliminary report. *Am J Orthod Dentofacial Orthop* 1993;103:545-555.
5. Han UK, Vig KW, Weintraub JA, Vig PS, Kowalski CJ. Consistency of orthodontic treatment decisions relative to diagnostic records. *Am J Orthod Dentofacial Orthop* 1991;100:212-219.
6. Casco JS, Vaden JL, Kokich VG, Damone J, James RD, Cangialosi TJ et al. Objective grading system for dental casts and panoramic radiographs. American Board of Orthodontics. *Am J Orthod Dentofacial Orthop* 1998;114:589-599.
7. Hildebrand JC, Palomo JM, Palomo L, Sivik M, Hans M. Evaluation of a software program for applying the American Board of Orthodontics objective grading system to digital casts. *Am J Orthod Dentofacial Orthop* 2008;133:283-289.
8. Okunami TR, Kusnoto B, BeGole E, Evans CA, Sadowsky C, Fadavi S. Assessing the American Board of Orthodontics objective grading system: digital vs plaster dental casts. *Am J Orthod Dentofacial Orthop* 2007;131:51-56.
9. Rheude B, Sadowsky PL, Ferriera A, Jacobson A. An evaluation of the use of digital study models in orthodontic diagnosis and treatment planning. *Angle Orthod* 2005;75:300-304.
10. Whetten JL, Williamson PC, Heo G, Varnhagen C, Major PW. Variations in orthodontic treatment planning decisions of Class II patients between virtual 3-dimensional models and traditional plaster study models. *Am J Orthod Dentofacial Orthop* 2006;130:485-491.
11. Sjogren AP, Lindgren JE, Huggare JA. Orthodontic Study Cast Analysis- Reproducibility of Recordings and Agreement Between Conventional and 3D Virtual Measurements. *J Digit Imaging* 2009.
12. Leifert MF, Leifert MM, Efstratiadis SS, Cangialosi TJ. Comparison of space analysis evaluations with digital models and plaster dental casts. *Am J Orthod Dentofacial Orthop* 2009;136:16 e11-14; discussion 16.

13. Bell A, Ayoub AF, Siebert P. Assessment of the accuracy of a three-dimensional imaging system for archiving dental study models. *J Orthod* 2003;30:219-223.
14. Gracco A, Buranello M, Cozzani M, Siciliani G. Digital and plaster models: a comparison of measurements and times. *Prog Orthod* 2007;8:252-259.
15. Motohashi N, Kuroda T. A 3D computer-aided design system applied to diagnosis and treatment planning in orthodontics and orthognathic surgery. *Eur J Orthod* 1999;21:263-274.
16. Mullen SR, Martin CA, Ngan P, Gladwin M. Accuracy of space analysis with emodels and plaster models. *Am J Orthod Dentofacial Orthop* 2007;132:346-352.
17. Quimby ML, Vig KW, Rashid RG, Firestone AR. The accuracy and reliability of measurements made on computer-based digital models. *Angle Orthod* 2004;74:298-303.
18. Stevens DR, Flores-Mir C, Nebbe B, Raboud DW, Heo G, Major PW. Validity, reliability, and reproducibility of plaster vs digital study models: comparison of peer assessment rating and Bolton analysis and their constituent measurements. *Am J Orthod Dentofacial Orthop* 2006;129:794-803.
19. Tomassetti JJ, Taloumis LJ, Denny JM, Fischer JR, Jr. A comparison of 3 computerized Bolton tooth-size analyses with a commonly used method. *Angle Orthod* 2001;71:351-357.
20. Zilberman O, Huggare JA, Parikakis KA. Evaluation of the validity of tooth size and arch width measurements using conventional and three-dimensional virtual orthodontic models. *Angle Orthod* 2003;73:301-306.
21. Choi DS, Jeong YM, Jang I, Jost-Brinkmann PG, Cha BK. Accuracy and reliability of palatal superimposition of three-dimensional digital models. *Angle Orthod* 2010;80:497-503.
22. Almeida MA, Phillips C, Kula K, Tulloch C. Stability of the palatal rugae as landmarks for analysis of dental casts. *Angle Orthod* 1995;65:43-48.
23. Ashmore JL, Kurland BF, King GJ, Wheeler TT, Ghafari J, Ramsay DS. A 3-dimensional analysis of molar movement during headgear treatment. *Am J Orthod Dentofacial Orthop* 2002;121:18-29; discussion 29-30.
24. Bailey LT, Esmailnejad A, Almeida MA. Stability of the palatal rugae as landmarks for analysis of dental casts in extraction and nonextraction cases. *Angle Orthod* 1996;66:73-78.
25. Cha BK, Lee JY, Jost-Brinkmann PG, Yoshida N. Analysis of tooth movement in extraction cases using three-dimensional reverse engineering technology. *Eur J Orthod* 2007;29:325-331.

26. Christou P, Kiliaridis S. Vertical growth-related changes in the positions of palatal rugae and maxillary incisors. *Am J Orthod Dentofacial Orthop* 2008;133:81-86.
27. Hoggan BR, Sadowsky C. The use of palatal rugae for the assessment of anteroposterior tooth movements. *Am J Orthod Dentofacial Orthop* 2001;119:482-488.
28. Jang I, Tanaka M, Koga Y, Iijima S, Yozgatian JH, Cha BK et al. A novel method for the assessment of three-dimensional tooth movement during orthodontic treatment. *Angle Orthod* 2009;79:447-453.
29. van der Linden FP. Changes in the position of posterior teeth in relation to ruga points. *Am J Orthod* 1978;74:142-161.
30. Grauer D. 3D-orthodontic change assessment with CAD/CAM lingual technique (Part I: accuracy). In Press.
31. Garland M, Heckbert PS. Surface Simplification Using Quadric Error Metrics. *SIGGRAPH* 1997.
32. Baumrind S, Carlson S, Beers A, Curry S, Norris K, Boyd RL. Using three-dimensional imaging to assess treatment outcomes in orthodontics: a progress report from the University of the Pacific. *Orthod Craniofac Res* 2003;6 Suppl 1:132-142.
33. Beers AC, Choi W, Pavlovskaja E. Computer-assisted treatment planning and analysis. *Orthod Craniofac Res* 2003;6 Suppl 1:117-125.
34. Kravitz ND, Kusnoto B, BeGole E, Obrez A, Agran B. How well does Invisalign work? A prospective clinical study evaluating the efficacy of tooth movement with Invisalign. *Am J Orthod Dentofacial Orthop* 2009;135:27-35.
35. Miller RJ, Kuo E, Choi W. Validation of Align Technology's Treat III digital model superimposition tool and its case application. *Orthod Craniofac Res* 2003;6 Suppl 1:143-149.

TABLE 5.1

Table 5.1: Estimated Maximum Difference in Replicate Positioning By Dental Arch		
Dental Arch	Estimate (mm)	Standard Error (mm)
Upper	0.007	0.003
Lower	0.009	0.004

TABLE 5.2

Table 5.2 Statistical model analysis: Type 3 Tests of Fixed Effects			
Effect	DF	F-Statistic	P-Value
Dental Arch	1,24	0.21	0.65

TABLE 5.3

Table 5.3 Estimated Standard Deviation By dental arch		
Dental arch	Estimate (mm)	Standard Error (mm)
Upper	0.07	0.04
Lower	0.05	0.03

TABLE 5.4

Table 5.4 Statistical model analysis: Type 3 Tests of Fixed Effects			
Effect	DF	F-Statistic	P-Value
Dental Arch	1,24	0.15	0.71

FIGURE 5.1

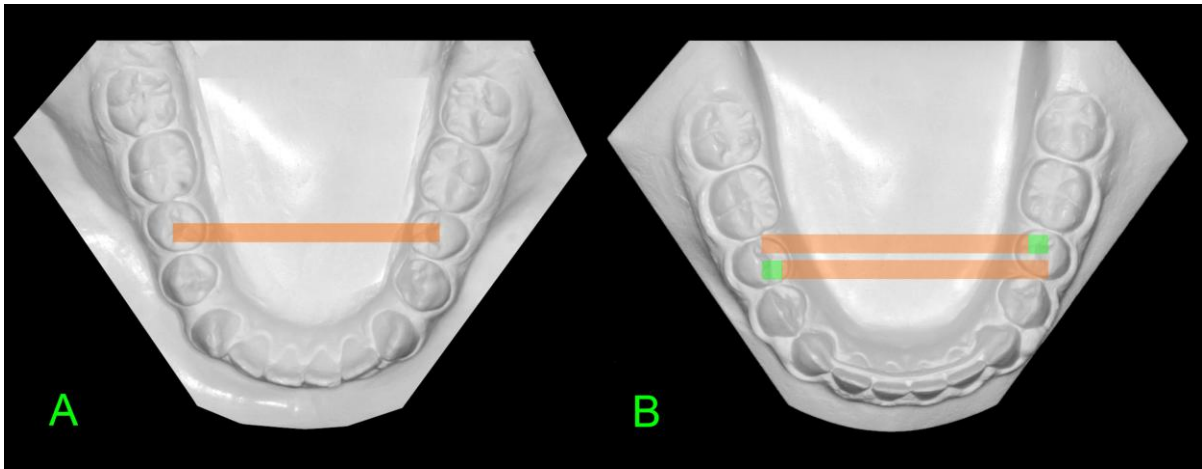


Figure 5.1 During treatment the width between the premolars and molars was increased. Dental casts allow for measurement of linear distances but not relative measurements. The orange bar represents the initial distance between second premolars (A). The green box represents the increase in interpremolar width (B). Measurements on dental casts do not allow for determination of whether interpremolar expansion occurred by the right premolar moving facially, the left premolar moving facially or most likely both premolars moving facially.

FIGURE 5.2

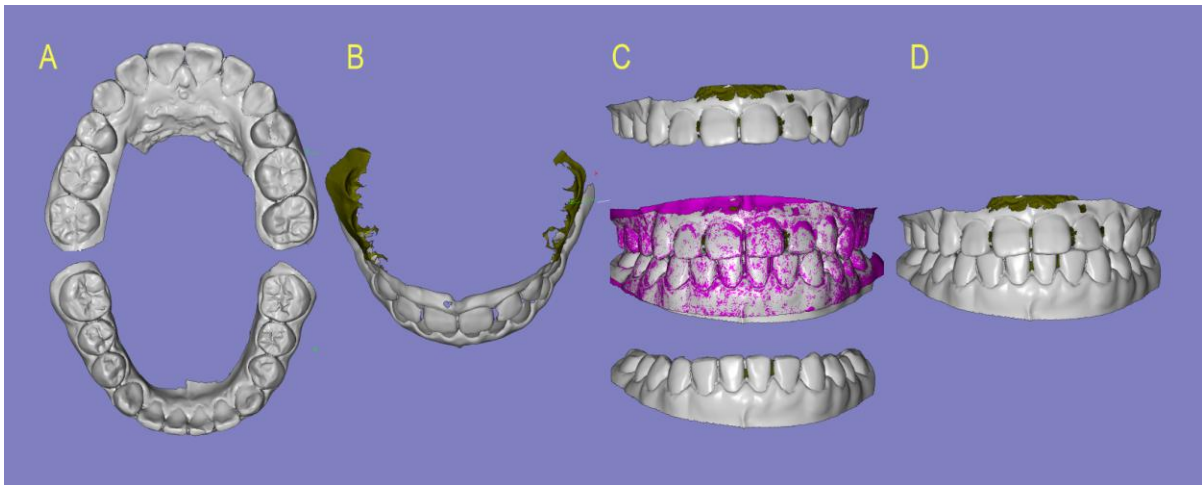


Figure 5.2 Independently scanned models (A) are registered using a scanned surface of the facial aspect of the models in occlusion (B). The scan of the models in occlusion is used only for the registration of the upper and lower models in occlusion (C, D)

FIGURE 5.3

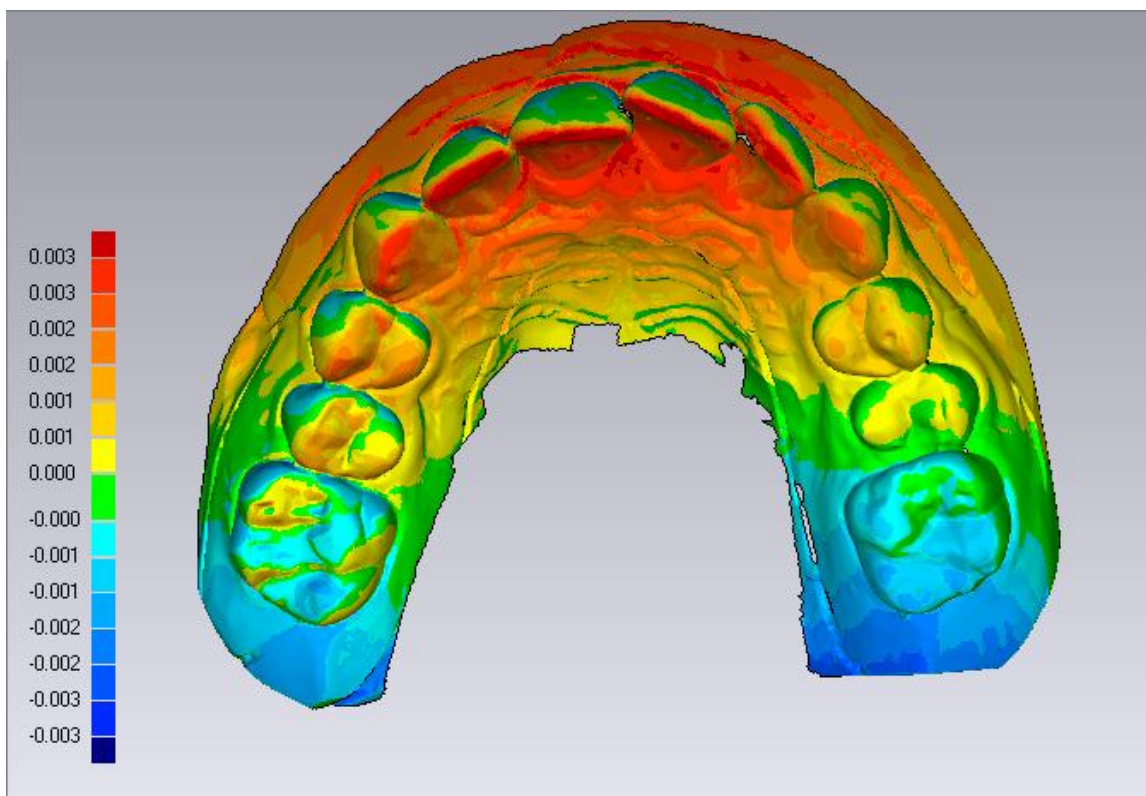


Figure 5.3 Three-dimensional comparison of the models is performed by Geomagic Studio 10.0 (Geomagic U.S., North Carolina, USA). Replicate positions are compared based on the absolute value of the maximum distance between surfaces and graphically displayed as color maps. Color segments correspond to distance (mm) between surfaces.

FIGURE 5.4

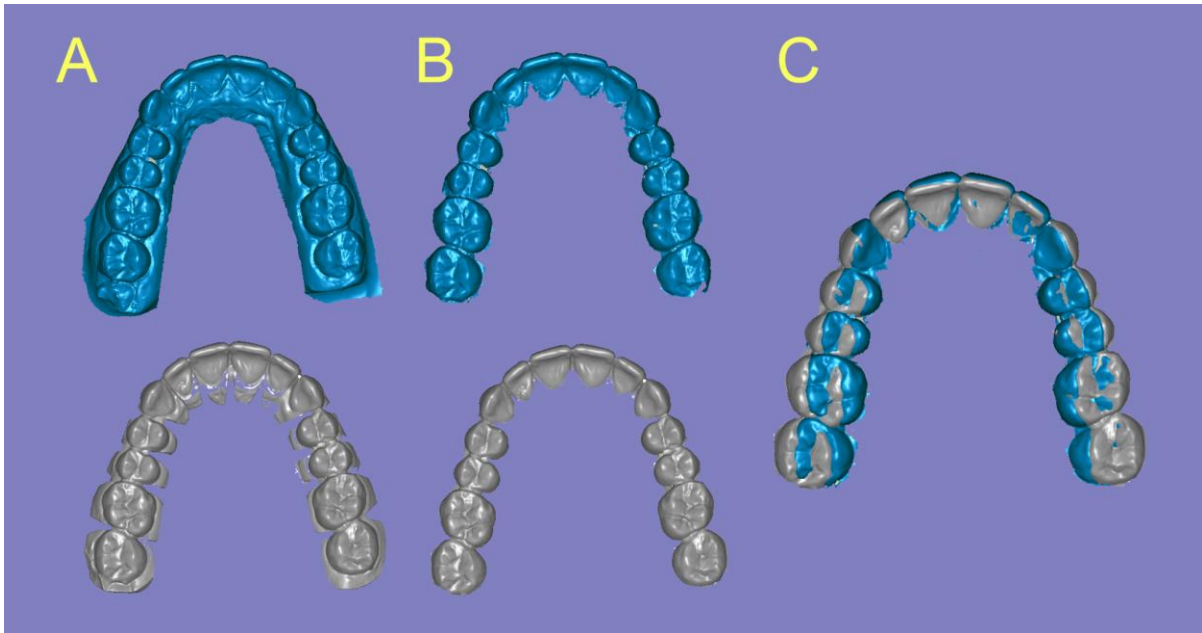


Figure 5.4 Final and setup orthodontic digital models are registered (A). The surfaces corresponding to the gingival tissues are removed (B) Registered digital models can be superimposed in space (C).

FIGURE 5.5

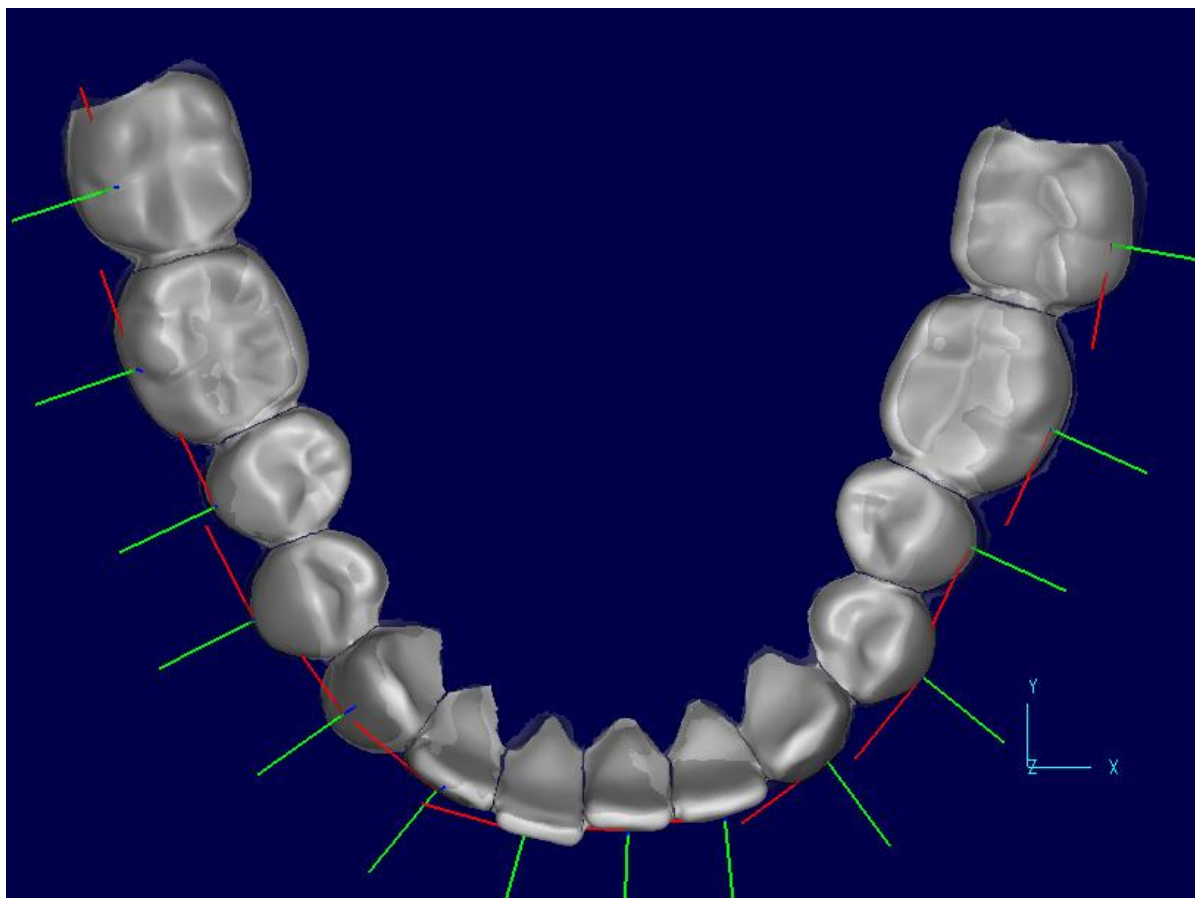


Figure 5.5 Once registered in the same coordinate system the six degrees of freedom describing tooth movement can be computed (Euler system). Computation of translation is based on the relative position of the tooth centroid. From eModel software (Geodigm Corporation, Chanhassen, MN). Computation of rotation is based on the relation of the local coordinate system of each tooth and the general coordinate system.

## CHAPTER 6

### ACCURACY IN TOOTH POSITIONING WITH FULLY CUSTOMIZED LINGUAL ORTHODONTIC APPLIANCES

#### ABSTRACT

Background. In order to understand orthodontic tooth movement, a method of quantification of tooth position discrepancies in three dimensions is needed. While the registration of sequential orthodontic digital models is still controversial, setup models of the planned correction can be registered to the final obtained correction after orthodontic treatment. Today, brackets and wires can be fabricated by CAD/CAM technology on a setup made at the beginning of treatment, so that treatment should produce a reasonably precise duplicate of the setup.

Method. In order to assess the accuracy of a CAD/CAM lingual orthodontic technique, dental casts of 94 patients from a single practice, representing a broad range of orthodontic problems, were evaluated. The casts for the planned outcome (setup) and actual outcome after treatment (final) were scanned to create digital models, and then the setup and final models for each patient were registered individually for the maxillary and mandibular dental arches. The planned and achieved tooth position was compared for each tooth. Individual tooth discrepancies were computed and expressed in terms of a six-degrees-of-freedom rectangular coordinate system (XYZ).

Results. Translational and rotational discrepancies were quite small for all teeth (generally less than 1 mm and than 6 degrees) except for 2<sup>nd</sup> molars, where some larger discrepancies were observed. Labio-lingual expansion in the posterior teeth was greater in the setup than in the final models, especially at the 2<sup>nd</sup> molars. Linear mixed models showed that age, type of tooth, jaw, initial crowding, time in slot-filling wire, use of elastics, days in treatment, interproximal reduction and rebonding all were influences on the setup/ final differences, but for some of these factors, the influence was small, explaining only a small amount of the discrepancy between planned and actual outcomes.

Conclusion. The presented methodology represents the first step towards understanding and measurement of tooth movement in three dimensions. These fully customized lingual orthodontic appliances were very accurate in achieving the goals planned at the initial setup, except for the full amount of planned expansion and inclination at the 2<sup>nd</sup> molars.

## BACKGROUND

In order to assess change in orthodontic treatment, sequential records obtained at different time points are compared. Historically most quantitative comparisons in orthodontics were made on cephalograms<sup>1,2</sup>, which generate a two-dimensional projection of three-dimensional structures. Due to the overlapping of the left and right sides of the dental arches it is particularly difficult to obtain a precise assessment of tooth movement<sup>3,4</sup>. During the last ten years numerous three dimensional record modalities have been introduced. These include digital

orthodontic models, cone-beam computed tomography (CBCT) and three-dimensional photography<sup>5</sup>. The new modalities allow for assessment of changes in three dimensions<sup>6</sup> and for customization of treatment planning, brackets and wires by means of CAD/CAM technology.

Digital models are comparable to conventional dental casts when qualitatively compared, for instance in terms of decision making<sup>7,8</sup>. Quantitatively, when linear measurements are compared between digital models and dental casts, some statistically significant differences are found but these differences do not reach clinical significance<sup>9-18</sup>. Among the many advantages of digital models over conventional dental casts is the possibility of spatial registration. Digital models from different time points can be combined in the same coordinate system. Baumrind et al. described three types of registration of digital models<sup>19</sup>. Type I consist of tooth by tooth registration, in which pre-to-post position of individual teeth are taken into account. Type II and Type III registrations are based on positional information of stable structures external to the dental arches. The stable structure most frequently used in Type II registrations is the palatal rugae, which has been used by many authors to assess tooth movement<sup>20-28</sup>. Type III registration incorporates information from a two-dimensional source – change measured on superimposed sequential cephalograms – to the three-dimensional digital models.

Previous studies measuring three-dimensional tooth movement or tooth positional discrepancy can be classified into three categories based on their reported outcome. Group I includes all studies reporting tooth movement as the three-dimensional translation of a chosen landmark in a XYZ system<sup>22,24,26,28-30</sup>. In a study

of this type, Ashmore et al. registered bimonthly serial models on palatal rugae landmarks and described the translational movements of the molars subjected to a headgear force. In order to compute the molar translational parameters these authors digitized four landmarks on each molar at each time point, and constructed a centroid. They reported good reliability for the translational movements and not so good reliability for the rotational parameters<sup>24</sup>.

Group II is comprised of studies reporting both translation and rotation parameters based on the calculation of a transformation matrix in a XYZ system<sup>31-34</sup>. This transformation matrix is computed through an iterative closest point registration between homologous teeth at different time points. Chen et al. applied this method to measure simulated tooth movement on cone-beam CT images<sup>33</sup>. This methodology can also be used to compare planned tooth positions to the achieved tooth positions<sup>34,35</sup>.

Group III studies describe rotational parameters and translation relative to a finite helical axis system (FHA)<sup>36-38</sup>. Hayashi et al. compared the FHA system and the XYZ system and found no statistically significant differences in absolute tooth movement measurements, but noted differences in the description of the rotational parameters<sup>39</sup>.

In order to understand orthodontic tooth movement, a method of quantification of tooth position discrepancies in three dimensions is needed. While the registration of sequential orthodontic digital models is still controversial, setup models of the planned correction can be registered to the final obtained correction after orthodontic treatment. Current technology allows for the establishment of

precise treatment goals and mechanics before initiation of treatment. Treatment goals are established in virtual space and custom appliances are manufactured to produce the desired tooth movement<sup>40-43</sup>. The use of goal-driven orthodontic techniques has not been validated, and it is not known how close the final treatment results are to the planned correction<sup>44-46</sup>. Digital models allow for superimpositions in space and hence for measurement of the possible discrepancy between planned and achieved tooth movement.

Based on the above considerations, a new method for: (1) registration and superimposition of setup and final models, and (2) assessment of tooth positional discrepancy, was developed and validated<sup>35</sup>. It consists of a two-step registration of digital models: first, dental arches from different time points are registered in the same coordinate system, and second, homologous teeth in different positions are registered in order to compute the transformation matrix between time points. This method allows for computation and description of differences between planned tooth positions - used for appliances fabrication - and achieved tooth positions by means of these appliances. The obtained differences in translation and rotation between teeth at two time points can be translated into translation and rotation parameters around the dental arches, and this information can be applied in refinement of orthodontic appliances fabrication. To this day, there is no evidence to support that the orthodontic planned changes will be delivered by the CAD/CAM orthodontic appliances.

The aim of this study is to assess the accuracy in translational and rotational tooth positioning of a CAD/CAM lingual orthodontic technique.

## MATERIALS AND METHODS

### Sample

A sample was collected at an orthodontic office in Bad Essen, Germany, dedicated almost exclusively to lingual orthodontics. Incognito is a lingual orthodontic technique in which brackets and wires are CAD/CAM customized on a scanned model of the patient's setup at the beginning of treatment<sup>41,47,48</sup>. Laboratory technicians fabricate a setup model according to the orthodontist prescription. These models are scanned and used as a template to design virtual brackets and wires. Virtual brackets are printed in wax and cast in a gold alloy. Arch wires are formed by a wire-bending robot. Dental casts, brackets and wires are delivered to the orthodontist (Figure 6.1). Inclusion criteria were patients treated with Incognito lingual technique for both upper and lower dental arches and debonded between January 2008 and January 2009. Initial sample was composed of 118 patients. Exclusion criteria were: surgical or skeletal anchorage treatment, unavailability of diagnostic records and lack of compliance defined as no appointment in three consecutive months. After application of exclusion criteria the final sample was composed of 94 patients (tables 6.1 and 6.2). The average age for the sample was 27.7 years, and it ranged from 15.51 to 61.64 years. The ratio female to male was 2 to 1.

For each individual the following records were collected: pre-treatment dental casts (initial), pre-treatment setup (setup), post-treatment dental casts (final), pre and post-treatment cephalogram and panoramic radiographs, and pre and post-treatment photos. The following information was also collected: gender, age,

ethnicity, days in treatment, arch wire sequence, use of intermaxillary elastics, and use of extractions and/or interproximal reduction.

#### Scanning of dental casts and establishment of occlusion

Dental casts were created from poly-vinyl siloxane impressions made with Bisico impression material (Bielefelder Dentsilicone GmbH & Co. KG, Bielefeld, Germany) and poured with Type IV extra hard white stone. Dental casts were scanned with an ATOS optical scanner (GOM mbH, Braunschweig, Germany) at a spatial resolution of 20 microns. For each patient and time point three scans or surfaces were created: one surface of the upper arch, one surface of the lower arch and one surface of the models in occlusion. The latter one included only the facial aspect of the models in occlusion.

The upper and lower arch surfaces were registered to the corresponding upper and lower portions of the surface of the models in occlusion using Occlusomatch software (TopService, 3M, Bad Essen Germany). An automatic registration process selected 2500 points on each surface (search radius of 1 mm reduced to 0.25 mm, factor of 0.50 mm), and iterations were performed until the success threshold was reached at 0.06 mm. Once the occlusal position of the upper and lower arches was established the surface of the models in occlusion was deleted. The variability introduced by this two-step process was quite small and its validation is reported elsewhere<sup>35</sup>. This process was used for the initial, setup and final models, generating three pairs of digital models.

#### Removal of the gingival tissue and surface-to-surface registration

Digital models corresponding to the setup and final time points were loaded into Geomagic Studio10.0 software (Geomagic U.S., Research Triangle Park, NC, USA), and the surfaces corresponding to the gingival tissue were removed. The remaining surfaces corresponding to the dental arches were simplified to 50,000 points using the Qslim 2.0 tool<sup>49</sup>. Once simplified, the upper setup model was registered to the upper final model using emodel 8.05 software (Geodigm Corporation, Chanhassen, MN), to combine both models in the same coordinate system.

The same process was followed for the lower setup model. The surface-to-surface registration of the setup dental arch to the final dental arch was independently performed for upper and lower dental arches. 1500 points were selected on each surface with a search radius of 0.5 mm. 30 iterations were automatically performed until the best fit of the surfaces was obtained (Figure 6.2). The small and not statistically significant variability introduced by this registration process and its good reliability are reported elsewhere<sup>35</sup>.

#### Segmentation of teeth and measurement of tooth discrepancy in position

Once setup and final digital models were combined in the same coordinate system, the individual teeth were segmented with emodel 8.05 software (Geodigm Corporation, Chanhassen, MN). Both the setup and final digital models were loaded into emodel Compare software. The long axis of each tooth was located and a local coordinate system was assigned to each individual tooth. The rigid transformation matrix (translation and rotation) between teeth at different time points was calculated by means of an iterative closest point registration of homologous teeth in the setup

and final models. The difference in translational components (mesio/distal, labio/lingual and vertical) was computed by comparing the position of the center of coordinates between homologous teeth at different time points. The difference in rotational components (inclination, angulation and rotation) was computed by projecting the local coordinate systems onto the world coordinate systems. (Figure 6.3)

### Statistical analysis

The translational and rotational discrepancies were used as the outcome variables. Demographical, initial malocclusion and treatment variables were considered as covariates. Linear mixed effects models were constructed for each of the six outcome variables. The level of significance was set at 0.05.

Translational and rotational discrepancies for homologous teeth from the right and left sides were aggregated by tooth type. Age was centered on its mean value. Days in treatment was centered on its mean value and standardized to 120-day intervals. Days in slot-filling wire (0.0182x0.0182 inches) was categorized into three groups: 1). No slot-filling wire, 2). 1-180 days in slot-filling wire and 3). More than 181 days in slot-filling wire.

The final model for each of the translational and rotational discrepancies had the form of:

$$Y_{ijkl} = \beta_0 + b_i + b_{ij} + x_{ijk}\beta + e_{ijkl} \quad (1)$$

where  $Y_{ijkl}$  is one of the discrepancies,  $\beta_0$  is an intercept term,  $\beta$  is a vector of fixed effect coefficients,  $x_{ijk}$  is a vector of fixed effect covariates,  $b_i$  is a random effect for a

patient,  $b_{ij}$  is a random effect for the jaw within a patient, and  $e_{ijkl}$  is a random error. (1, see Appendix B)

## RESULTS

### Clinical outcomes

As depicted by the dispersion values in Table 6.1, variability in age and malocclusion characteristics in the final sample was large enough to represent the orthodontic patients' population. Note the range of Overjet [-4.70, 11.50] mm and overbite [-6.70, 7.60] mm.

Malocclusion characteristics, as a proxy for malocclusion complexity, were: upper and lower crowding calculated as the difference between the available and needed space, overjet, overbite and ANB angle. Treatment variables included treatment time, time in slot-filling wire for upper and lower dental arch, interproximal reduction, number of brackets rebonded and use of elastics (Class II and vertical). Two other variables, extractions and missing premolars at the beginning of treatment were recorded but not included in the study given that their distribution rendered some groups with less than 5 individuals and would cause a decrease in stability in statistical outcomes (table 6.1 and 6.2).

A clinical example is shown in figure 6.4, 6.5 and 6.6. For this patient the dental Class II malocclusion was corrected by extraction of upper first premolars and retraction of the upper front teeth into the extraction space (figure 6.4). Digital models corresponding to the initial, setup and final time points are depicted in figure 6.5. Note the difference in arch form and overjet between initial and final time points.

Using the described method the setup models were registered and superimposed on the final models (figure 6.6). Surfaces corresponding to the setup and final time points were similar with some differences in the molar region.

Discrepancies between planned and actual tooth position: translational discrepancies

Means of absolute translational discrepancies were small, with the greatest discrepancy and variability shown at the upper and lower second molars (Table 6.3 and 6.4, and figure 6.7 A-C). For all three translational discrepancies, and for all teeth except second molars, most teeth were positioned within 1 mm of their planned positions (-1mm to +1mm). Mesio-distal discrepancies were greatest at the second molars with upper second molars positioned mesially relative to their planned position and lower second molars positioned distally relative to their planned position (Figure 6.7 A). A pattern was observed in the labio-lingual translational discrepancies (Figure 6.7 B) where the molars and posterior segments were in a more lingual position relative to the planned positions and the incisors were in a more labial position relative to their planned position. The setup was on average wider in terms of expansion than the final model.

Vertical discrepancies were the smallest and the least variable among the translational discrepancies (Figure 6.7, C) Once again, second molars displayed the greatest discrepancy with upper second molars in a more apical position and the lower second molars in more coronal position relative to their positions in the setup models.

### Discrepancies between planned and actual tooth position: rotational discrepancies

Rotational discrepancies were also small, and their mean was close to zero (Table 6.3 and 6.4, and figure 6.7 D-F). Upper teeth except upper second molars were on average within 4 degrees of their planned inclination (Figure 6.7, D). Second molars displayed the greatest and most variable discrepancies in inclination, with upper second molars showing more inclination at their final position than the setup, and lower second molars showing less inclination at their final position relative to their planned inclination. A pattern was detected in the lower arch where the average discrepancy in inclination increased from posterior teeth to anterior teeth. Angulation discrepancies were small. Upper second molars were slightly distally angulated and lower second molars were mesially angulated in comparison with their planned positions (Figure 6.7, E). Variability in rotation discrepancy was greater than inclination and angulation variability (Figure 6.7, F).

### Relation between covariates and outcome variables (Table 6.5)

When all variables were considered in a general model, age was statistically related to an increase of labio-lingual discrepancy and almost reached statistical significance in mesio-distal and vertical positioning and in inclination; however, parameter estimates were not clinically significant. Gender displayed no statistically significant relationship to any rotational or translational dependent variables.

Both the rotational and translational discrepancies were statistically different between upper and lower jaw, and among tooth types with the only exception of rotation between upper and lower jaw. These positive or negative statistically

significant relationships vary among the discrepancies and will be addressed in each translational and rotational discrepancy further below. Clinical significance criteria depended on the center value and standardization of continuous variables and on the reference group and categorization for categorical variables. (Appendix B)

Discrepancy in mesio-distal positioning was statistically related to initial crowding in the upper arch, to interproximal reduction, to rebonding, to jaw and to tooth type while accounting for all other covariates. The achievement of the setup goals in terms of mesio-distal positioning was better for the mandible than the maxilla. Parameter estimates were not clinically significant except for interproximal reduction where a 0.2 mm reduction of mesio-distal discrepancy was found when IPR was performed (Table 6.5 and Appendix B).

Discrepancy in labio-lingual positioning was statistically related to an increase in age and days in treatment, to the use of vertical elastics, to jaw and to tooth type while accounting for all other covariates. The achievement of the setup goal in terms of labio-lingual positioning was better for the maxilla than the mandible. Parameter estimates were not clinically significant except for the use of vertical elastics, where a average of 0.2 mm increase in labio-lingual discrepancy was noted when these were used (Table 6.5 and Appendix B).

Discrepancy in vertical positioning was statistically related to use of Class II elastics (increased discrepancy), rebonding (increased discrepancy), to jaw and to tooth type while accounting for all other covariates. The achievement of the setup goal in terms of vertical positioning was better for the maxilla than the mandible. An

average increase of 0.1 mm in vertical discrepancy was found when Class II elastics were employed (Table 6.5 and Appendix B).

Discrepancy in inclination was statistically related to initial crowding in the lower arch, to jaw and to tooth type while accounting for all other covariates. The achievement of the setup goal in terms of inclination was better for the mandible than the maxilla. A reduction of 0.4 degrees in inclination discrepancy was observed per 1 mm increase in initial crowding. Some of the covariates did not reach statistical significance in the statistical model, but their parameter estimates were clinically significant. In terms of inclination, the achievement of the setup goals was better when slot-filling wires and vertical elastics were used; and was worse when treatment time was shorter, and when Class II elastics and interproximal reduction were employed (Table 6.5 and Appendix B).

Discrepancy in angulation was statistically related to initial crowding in the upper arch, to the use of vertical elastics, to jaw and to tooth type while accounting for all other covariates. The achievement of the setup goal in terms of angulation was better for the maxilla than the mandible. The use of vertical elastics led to a 0.7 mean decrease in angulation discrepancy. Other covariates that did not reach statistical significance by themselves while accounting for all other covariates but were related to a decrease in angulation discrepancy are: use of Class II elastics and interproximal reduction (table 6.5 and Appendix B).

Discrepancy in rotation was statistically related to initial upper and lower crowding, to ANB angle, to lower slot-filling wire and to tooth type while all other covariates were considered. Discrepancy in rotation was smaller when upper slot-

filling wire was used (but did not reach statistical significance). Conversely the use of the lower slot-filing wire was related to an increase in rotational discrepancy (Table 6.5 and Appendix B).

## DISCUSSION

### Sample characteristics

The lack of clinical relevance of age and gender on the amount of translational or rotational discrepancy can be explained by the fact that severity of the malocclusion, and hence needed correction, was not correlated to age and gender, and was homogeneously distributed among individuals; it makes sense that the discrepancy between planned and achieved results would be related to the severity of the malocclusion rather than to demographical variables. Ethnicity was not included in the study given that the sample originated in a region in Germany where almost all individuals were Saxons.

A possible explanation for the lack of statistical relationship between discrepancy and interarch variables (overjet, overbite and ANB angle) is that the presented method measures discrepancies in intra-arch translation and rotation independently of the occlusal relationship. The registration of the setup models to the final models was performed as a two registrations with upper and lower dental arches independently registered. Inter-arch variables (overjet, overbite and ANB angle) could have only an indirect effect on the translational and rotational discrepancies due to the use of inter-arch elastics; that was the case when all variables were accounted for in the six statistical models.

### Influences on translational accuracy

Mesio-distal translational discrepancies were small, with most of the sample within 1 mm of the planned position. This was expected given that the differences in arch form have only small effect in the mesio-distal position of a tooth. Second molars exhibit the greatest translational discrepancy between planned and achieved positions, probably due to being the terminal molar where the arch wire is performing as a cantilever as opposed to a supported beam. Estimated parameters for all covariates were not clinically relevant (see Appendix B). The use of interproximal reduction was expected to be related to a smaller mesio-distal discrepancy between setup and final models given that interproximal reduction was also performed on the setup model. Thalheim et al. compared the intercanine distance planned on the setup model with the one obtained after treatment with Incognito lingual technique. The authors reported a difference smaller than 0.5 mm (range of -0.8 to 0.9 mm). They concluded that the realization of the planned intercanine distance with Incognito technique is predictable<sup>50</sup>. These results are expected given that if the treatment is finished without spacing between lower canines the arch form would have only a small effect on the lineal distance between canines' cusps. These results are comparable to the mesio-distal positioning discrepancies presented in the present study.

The data regarding labio-lingual discrepancy displayed a trend, with the molars in a more constricted position and the incisors in a more proclined position. This was probably due to the fact that the arch form change was not entirely achieved by the slot-filling wire, and could be explained because dental arch

expansion is proportional to the arch wire expansion until a threshold is reached, and after that point a greater torsional stiffness of the wire would be necessary. The last wire used in over two-third of patients is a 0.0182x0.0182 TMA wire, the torsional stiffness of this wire is around 40% of the rigidity of a similarly-sized stainless steel wire<sup>51</sup>. Maybe overcorrection in the customized prescription should be added to second molar brackets to reduce discrepancy between planned and achieve tooth positioning. Covariate statistically related to labio-lingual discrepancy displayed: either not clinically relevant parameter estimates, (age and days in treatment), or slight negative effect on the achievement of the setup goals (use of vertical elastics). The use of vertical elastics could be the consequence rather than the cause of the discrepancy in labio-lingual positioning. Perhaps the clinician instructed the patient to wear vertical elastics in an attempt to correct labio-lingual as well as vertical discrepancies.

Vertical discrepancies could be explained by three factors: first, one third of the individuals in our sample were still growing and second molars were still in active eruption process – note vertical discrepancies in position for second molars (see figure 6.7 C). The second factor that may have introduced a greater variability at the second molar region is the iterative-closest-point registration of setup and final models. If the final relative position of the setup and the final models depends on the average of the surface differences, the greatest discrepancies would be expected at the terminal end of the surface, in this case at the second molars. Finally, arch wires are less efficient in producing orthodontic tooth movement and controlling vertical position when they function as a cantilever, which is the case for second molars. It is

important to note that almost half of the sample used Class II elastics, and these were statistically related to the vertical discrepancies. Rebonding was also related to greater vertical discrepancies but the parameter estimate was not relevant (see Table 6.5 and Appendix B).

#### Influences on rotational accuracy

Rotational discrepancies were also small for all teeth except second molars. This fully customized lingual technique was very predictable in achieving the rotational changes (inclination, angulation and rotation) planned in the setup.

Discrepancies in inclination for the upper teeth were small, but on average upper teeth (except central incisors) displayed more inclination than planned. This may be due to the fact that the force application is in lingual position relative to the center of resistance of the teeth. Any labially directed force applied in a lingual position to the center of resistance of a tooth will produce a moment that will tend to rotate the tooth crown facially and root palatally.

A pattern at the lower teeth was observed where posterior teeth displayed less inclination than planned and anterior teeth matched the planned inclination. A possible explanation for this phenomenon is that almost half of the sample used Class II elastics which are attached to a facial button bonded on the lower second molars and to a hook on the canine lingual bracket. In the mandible, the force application is labial to the center of resistance of the tooth and would have the tendency to decrease inclination.

Even though covariates were not statistically related to the inclination discrepancies, it makes sense that the use of a slot-filling wire and a longer

treatment time would decrease them. An inter-arch mesio-distal force, like use of Class II elastics, would increase the discrepancies in inclination by interfering with the intra-arch torque expression. Vertical elastics decreased the inclination discrepancy and that could be explained by the effect of pulling the tooth and compressing the wire into the slot and facilitating torque expression. Anterior teeth brackets employ a vertical insertion of the wire, and a common approach to increase the torque expression is the use of power-ties to compress the wire into the slot. Interproximal reduction was related to an increase in inclination discrepancy, even though this relationship was not statistically significant. After interproximal reduction an elastic chain is employed to close the spaces between anterior teeth. This chain may have a negative effect on the torque expression during the space closure period.

Wiechmann et al found no statistically significant difference between planned lower incisor inclination and achieved lower incisor inclination in 12 patients treated with Incognito technique combined with Herbst appliance. The mean difference between planned and obtained incisor inclination was 2.2 degrees (+/- 1.0 degrees). Absolute comparison with the present study is not possible because the studies employed a slightly different registration method. In Wiechmann's study the common coordinate system was based on a horizontal plane constructed in relation to landmarks positioned on the middle of the crowns; while in our study a full surface to surfaces registration was utilized in order to combine both setup and final models in the same coordinate system. Nevertheless, both studies are confirming the accuracy in inclination with This fully customized lingual technique<sup>43</sup>.

Angulation discrepancies were close to zero except for second molars. Once again it is believed that the arch wire is not efficient in controlling second molar position when employed as a cantilever. When compared with the setup planned angulations, upper second molars were distally angulated and lower second molars were mesially angulated. It is important to note that these angulation characteristics follow the trend of normal development of the dentition and it is likely that the appliance effects in angulation was superimposed to the changes in angulation of erupting second molars in growing patients. This is especially important at the upper second molar root area where excessive distal root angulation could interfere with the development of the third molar<sup>52</sup>. Use of vertical or Class II elastics and interproximal reduction improved the achievement of the planned angulation, even though the relationship was not statistically significant. This was expected given that the inter-arch elastic force in the mesio-distal plane is intended to correct both medio-distal positioning and angulation problems in addition to the intra-arch correction provided by the appliances. Interproximal reduction can facilitate the achievement of the desired angulation by allowing the incisors and canines to rotate around their labio-lingual axis.

Average discrepancies in rotation were close to zero, but were more variable than other rotational discrepancies. This is probably due to the difficulty of measuring rotation around the long axis of a tooth. Some teeth were anatomically round and lack morphological traits to allow for measurement of rotation around their long axis.

#### Other considerations

The present study belongs to the group II type of studies given that an iterative-closest point registration is performed between tooth positions; and the obtained transformation matrix is described in terms of rotation and translation in a six-degrees-of-freedom rectangular coordinate system. The first limitation of this type of studies is that the description changes depending on the position of the coordinate origin, the sequence of rotations and the timing of translation<sup>39</sup>. In the present study the translational and rotational discrepancies were translated into translation and rotation parameters around the dental arches, which are easily interpreted by orthodontists.

Surface-to-surface registration: In order to combine setup and final models in the same coordinate system a registration process was necessary. The rationale behind this registration is that we wanted to investigate how close the final positions of the teeth were to the planned correction, regardless of their absolute position in space. Given that in the setup model there were no positionally stable structures - as the palatal rugae<sup>22</sup> – and that the differences between both setup and final are relatively small, the best fit between surfaces was used. We are aware that when registering homologous but not identical surfaces, the final relative position depends on the average of the surface differences; this method has proven to be reliable, and the variability introduced by this method is below our measurement threshold<sup>35</sup>.

Computation of the transformation matrix between teeth positions: In order to compute the differences in tooth position a second registration is performed – this time between surfaces belonging to homologous teeth in different positions. Our models were simplified to 50.000 points per dental arch. Each tooth was represented

by approximately 2000 points that were used in this second registration process. Similar to Chen et al, the resulting transformation matrix was translated into translation and rotation components around a center of rotation<sup>33</sup>.

Positioning of center of rotation: There is no consensus on the ideal location of the local coordinate system for each tooth. An automated method incorporated in the emodel Compare Software was used. In this method the long axis of the tooth is computed and then a centroid is defined 10mm below the most incisal point on the long axis of the tooth. An automated process was chosen because our previous attempts to locate the coordinate system on a user-selected landmark on the tooth surface rendered poor reliability. For more information on the determination of local coordinate system and comparison of tooth position the reader is referred to the emodel Compare manual (Geodigm Corporation, Chanhassen, MN). Different positions of the center of coordinates would render different computed values in terms of six degrees of freedom for the same displacement. The solution to this problem is to express the displacements in a finite helical axis system; however the clinical interpretation of a rotation and translation along an axis in space is difficult<sup>38</sup>. Chen et al. used computed local coordinate systems based on a boxing-algorithm<sup>33</sup>. The main problem with this process is that it depends on the tooth segmentations – small changes in geometry could have a big impact on the position of the local coordinate system. Other studies described tooth movement based on the movement of a landmark or a set of landmarks on a tooth. Some authors employed cusp tips and incisal edges. While in theory it is reliable to locate a landmark on a cusp tip, its displacement only represents the displacement of that landmark, and not

the displacement of the whole tooth<sup>22,28,29</sup>. Studies employing landmarks averaged to a centroid were able to describe the translational movements of teeth but did not report rotational changes<sup>24,26,30</sup>.

Tooth position accuracy: In terms of accuracy of tooth positioning, direct comparison of these results with other studies is not possible given the different criteria employed to describe the accuracy in tooth positioning. Kravitz et al, reported a mean accuracy of tooth movement with Invisalign technique of 41%. This percentage corresponds to the comparison between planned displacement and obtained displacement. The main difference between studies is that the present one reports the discrepancy between the planned position and the obtained one in absolute terms, and Kravitz et al. reported the percentage of change obtained relative to the overall planned change<sup>34</sup>.

## CONCLUSIONS

The presented method of comparison between planned and obtained tooth positions is applicable to any orthodontic technique where appliances are designed on a setup at the beginning of treatment. Assessment of translational and rotational discrepancies between planned and achieved tooth positions, and the correlation of these finding with demographical, initial malocclusion and treatment characteristics will improve our understanding of tooth movement, appliance design and manufacturing and biological limits of orthodontic treatment. Further research incorporating root information from cone-beam computerized tomography will allow creating models to predict tooth movement.

For both translation and rotation, this customized lingual technique was very accurate in achieving the tooth position planned in the setup. Age, type of tooth, jaw, initial crowding, time in slot-filling wire, use of elastics, days in treatment, interproximal reduction and rebonding were statistically related to the amount of rotational and translational discrepancy while accounting for all other covariates.

In the future, this method could be applied to assess tooth movement without radiation if rugae registration is validated as stable in the vertical dimension (figure 6.8). Further research into three-dimensional description of tooth movement is necessary to reach consensus on the type of description – rectangular coordinate system or finite-helical axis system – and on the position of the local coordinate systems.

## REFERENCES

1. Bjork A. Sutural growth of the upper face studied by the implant method. *Acta Odontol Scand* 1966;24:109-127.
2. Johnston LE, Jr. Balancing the books on orthodontic treatment: an integrated analysis of change. *Br J Orthod* 1996;23:93-102.
3. Lee KH, Hwang HS, Curry S, Boyd RL, Norris K, Baumrind S. Effect of cephalometer misalignment on calculations of facial asymmetry. *Am J Orthod Dentofacial Orthop* 2007;132:15-27.
4. Malkoc S, Sari Z, Usumez S, Koyuturk AE. The effect of head rotation on cephalometric radiographs. *Eur J Orthod* 2005;27:315-321.
5. Grauer D, Cevidanes LS, Proffit WR. Working with DICOM craniofacial images. *Am J Orthod Dentofacial Orthop* 2009;136:460-470.
6. De Vos W, Casselman J, Swennen GR. Cone-beam computerized tomography (CBCT) imaging of the oral and maxillofacial region: a systematic review of the literature. *Int J Oral Maxillofac Surg* 2009;38:609-625.
7. Rheude B, Sadowsky PL, Ferriera A, Jacobson A. An evaluation of the use of digital study models in orthodontic diagnosis and treatment planning. *Angle Orthod* 2005;75:300-304.
8. Whetten JL, Williamson PC, Heo G, Varnhagen C, Major PW. Variations in orthodontic treatment planning decisions of Class II patients between virtual 3-dimensional models and traditional plaster study models. *Am J Orthod Dentofacial Orthop* 2006;130:485-491.
9. Bell A, Ayoub AF, Siebert P. Assessment of the accuracy of a three-dimensional imaging system for archiving dental study models. *J Orthod* 2003;30:219-223.
10. Gracco A, Buranello M, Cozzani M, Siciliani G. Digital and plaster models: a comparison of measurements and times. *Prog Orthod* 2007;8:252-259.
11. Leifert MF, Leifert MM, Efstratiadis SS, Cangialosi TJ. Comparison of space analysis evaluations with digital models and plaster dental casts. *Am J Orthod Dentofacial Orthop* 2009;136:16 e11-14; discussion 16.
12. Motohashi N, Kuroda T. A 3D computer-aided design system applied to diagnosis and treatment planning in orthodontics and orthognathic surgery. *Eur J Orthod* 1999;21:263-274.
13. Mullen SR, Martin CA, Ngan P, Gladwin M. Accuracy of space analysis with emodels and plaster models. *Am J Orthod Dentofacial Orthop* 2007;132:346-352.

14. Quimby ML, Vig KW, Rashid RG, Firestone AR. The accuracy and reliability of measurements made on computer-based digital models. *Angle Orthod* 2004;74:298-303.
15. Sjogren AP, Lindgren JE, Huggare JA. Orthodontic Study Cast Analysis- Reproducibility of Recordings and Agreement Between Conventional and 3D Virtual Measurements. *J Digit Imaging* 2009.
16. Stevens DR, Flores-Mir C, Nebbe B, Raboud DW, Heo G, Major PW. Validity, reliability, and reproducibility of plaster vs digital study models: comparison of peer assessment rating and Bolton analysis and their constituent measurements. *Am J Orthod Dentofacial Orthop* 2006;129:794-803.
17. Tomassetti JJ, Taloumis LJ, Denny JM, Fischer JR, Jr. A comparison of 3 computerized Bolton tooth-size analyses with a commonly used method. *Angle Orthod* 2001;71:351-357.
18. Zilberman O, Huggare JA, Parikakis KA. Evaluation of the validity of tooth size and arch width measurements using conventional and three-dimensional virtual orthodontic models. *Angle Orthod* 2003;73:301-306.
19. Baumrind S, Carlson S, Beers A, Curry S, Norris K, Boyd RL. Using three-dimensional imaging to assess treatment outcomes in orthodontics: a progress report from the University of the Pacific. *Orthod Craniofac Res* 2003;6 Suppl 1:132-142.
20. Almeida MA, Phillips C, Kula K, Tulloch C. Stability of the palatal rugae as landmarks for analysis of dental casts. *Angle Orthod* 1995;65:43-48.
21. Bailey LT, Esmailnejad A, Almeida MA. Stability of the palatal rugae as landmarks for analysis of dental casts in extraction and nonextraction cases. *Angle Orthod* 1996;66:73-78.
22. Jang I, Tanaka M, Koga Y, Iijima S, Yozgatian JH, Cha BK et al. A novel method for the assessment of three-dimensional tooth movement during orthodontic treatment. *Angle Orthod* 2009;79:447-453.
23. van der Linden FP. Changes in the position of posterior teeth in relation to ruga points. *Am J Orthod* 1978;74:142-161.
24. Ashmore JL, Kurland BF, King GJ, Wheeler TT, Ghafari J, Ramsay DS. A 3-dimensional analysis of molar movement during headgear treatment. *Am J Orthod Dentofacial Orthop* 2002;121:18-29; discussion 29-30.
25. Hoggan BR, Sadowsky C. The use of palatal rugae for the assessment of anteroposterior tooth movements. *Am J Orthod Dentofacial Orthop* 2001;119:482-488.

26. Christou P, Kiliaridis S. Three-dimensional changes in the position of unopposed molars in adults. *Eur J Orthod* 2007;29:543-549.
27. Christou P, Kiliaridis S. Vertical growth-related changes in the positions of palatal rugae and maxillary incisors. *Am J Orthod Dentofacial Orthop* 2008;133:81-86.
28. Cha BK, Lee JY, Jost-Brinkmann PG, Yoshida N. Analysis of tooth movement in extraction cases using three-dimensional reverse engineering technology. *Eur J Orthod* 2007;29:325-331.
29. Choi DS, Jeong YM, Jang I, Jost-Brinkmann PG, Cha BK. Accuracy and reliability of palatal superimposition of three-dimensional digital models. *Angle Orthod* 2010;80:497-503.
30. Lai EH, Yao CC, Chang JZ, Chen I, Chen YJ. Three-dimensional dental model analysis of treatment outcomes for protrusive maxillary dentition: comparison of headgear, miniscrew, and miniplate skeletal anchorage. *Am J Orthod Dentofacial Orthop* 2008;134:636-645.
31. Beers AC, Choi W, Pavlovskaja E. Computer-assisted treatment planning and analysis. *Orthod Craniofac Res* 2003;6 Suppl 1:117-125.
32. Miller RJ, Kuo E, Choi W. Validation of Align Technology's Treat III digital model superimposition tool and its case application. *Orthod Craniofac Res* 2003;6 Suppl 1:143-149.
33. Chen J, Li S, Fang S. Quantification of tooth displacement from cone-beam computed tomography images. *Am J Orthod Dentofacial Orthop* 2009;136:393-400.
34. Kravitz ND, Kusnoto B, BeGole E, Obrez A, Agran B. How well does Invisalign work? A prospective clinical study evaluating the efficacy of tooth movement with Invisalign. *Am J Orthod Dentofacial Orthop* 2009;135:27-35.
35. Grauer D, Cevidanes LH, Tyndall D, Styner MA, Flood PM, Proffit WR. Registration of Orthodontic Digital Models. In: McNamara JA Jr, Hatch N, Kapila SD, eds. *Effective and Efficient Orthodontic Tooth Movement*. Monograph 48, Craniofacial Growth Series, Department of Orthodontics and Pediatric Dentistry and Center for Human Growth and Development, The University of Michigan, Ann Arbor, 2011.
36. Hayashi K, Uechi J, Murata M, Mizoguchi I. Comparison of maxillary canine retraction with sliding mechanics and a retraction spring: a three-dimensional analysis based on a midpalatal orthodontic implant. *Eur J Orthod* 2004;26:585-589.
37. Hayashi K, Uechi J, Mizoguchi I. Three-dimensional analysis of dental casts based on a newly defined palatal reference plane. *Angle Orthod* 2003;73:539-544.

38. Hayashi K, Araki Y, Uechi J, Ohno H, Mizoguchi I. A novel method for the three-dimensional (3-D) analysis of orthodontic tooth movement-calculation of rotation about and translation along the finite helical axis. *J Biomech* 2002;35:45-51.
39. Hayashi K, Uechi J, Lee SP, Mizoguchi I. Three-dimensional analysis of orthodontic tooth movement based on XYZ and finite helical axis systems. *Eur J Orthod* 2007;29:589-595.
40. Scholz RP, Sarver DM. Interview with an Insignia doctor: David M. Sarver. *Am J Orthod Dentofacial Orthop* 2009;136:853-856.
41. Wiechmann D, Rummel V, Thalheim A, Simon JS, Wiechmann L. Customized brackets and archwires for lingual orthodontic treatment. *Am J Orthod Dentofacial Orthop* 2003;124:593-599.
42. Wiechmann D, Schwestka-Polly R, Hohoff A. Herbst appliance in lingual orthodontics. *Am J Orthod Dentofacial Orthop* 2008;134:439-446.
43. Wiechmann D, Schwestka-Polly R, Pancherz H, Hohoff A. Control of mandibular incisors with the combined Herbst and completely customized lingual appliance--a pilot study. *Head Face Med* 2010;6:3.
44. Djeu G, Shelton C, Maganzini A. Outcome assessment of Invisalign and traditional orthodontic treatment compared with the American Board of Orthodontics objective grading system. *Am J Orthod Dentofacial Orthop* 2005;128:292-298; discussion 298.
45. Lagravere MO, Flores-Mir C. The treatment effects of Invisalign orthodontic aligners: a systematic review. *J Am Dent Assoc* 2005;136:1724-1729.
46. Turpin DL. Clinical trials needed to answer questions about Invisalign. *Am J Orthod Dentofacial Orthop* 2005;127:157-158.
47. Wiechmann D. A new bracket system for lingual orthodontic treatment. Part 1: Theoretical background and development. *J Orofac Orthop* 2002;63:234-245.
48. Wiechmann D. A new bracket system for lingual orthodontic treatment. Part 2: First clinical experiences and further development. *J Orofac Orthop* 2003;64:372-388.
49. Garland M, Heckbert PS. *Surface Simplification Using Quadric Error Metrics SIGGRAPH*. Los Angeles, CA; 1997.
50. Thalheim, A, Schwestka P, R. *Clinical Realisation of a Setup in Lingual Orthodontics*. Stuttgart, ALLEMAGNE: Thieme; 2008.
51. Kusy RP. On the use of nomograms to determine the elastic property ratios of orthodontic arch wires. *Am J Orthod* 1983;83:374-381.

52. Radlanski RJ, van der Linden FP, Ohnesorge I. 4D-computerized visualisation of human craniofacial skeletal growth and of the development of the dentition. *Ann Anat* 1999;181:3-8.

TABLE 6.1

Table 6.1 Descriptive statistics for continuous variables

Variable	Mean	S.D.	Min	Max
ANB (degrees)	3.49	2.37	-1.60	9.10
Overjet (mm)	4.80	2.40	-4.70	11.50
Overbite (mm)	3.58	2.23	-6.70	7.60
Age (years)	27.70	12.51	15.51	61.64
Days in treatment	601.44	213.33	145.00	1159.00
Rebondings	1.78	2.10	0.00	9.00
Crowding U arch (mm)	-2.48	4.07	-9.74	12.51
Crowding L arch (mm)	-2.76	3.30	-8.85	7.90

TABLE 6.2

Table 6.2 Descriptive statistics for categorical variables

Variable	Frequency	Percent
Gender		
F	63	67.02
M	31	32.98
Interproximal reduction		
0	74	78.72
1	20	21.28
Class_II		
0 (No C_II elastics)	38	40.43
1 (from 1 to 120 days)	10	10.64
2 (more than 121 days)	46	48.94
Vertical_elastics		
0	76	80.85
1	18	19.15
Days_U18_2		
No Slot_filling_W	28	29.79
1-180 days	28	29.79
More than 181 days	38	40.43
Days_L18_2		
No Slot_filling_W	33	35.11
1-180 days	30	31.91
More than 181 days	31	32.98

TABLE 6.3

Table 6.3: Mean of absolute discrepancies (10%, 90% quantiles) for maxilla.

Tooth type	Measurement					
	Mesial	Facial	Vertical	Torque	Tip	Rotation
2M	0.74 (-0.43, 1.34)	2.01 (-3.42, -0.41)	0.73 (-1.58, 0.31)	5.80 (-1.51, 11.55)	5.12 (-10.31, 3.72)	4.01 (-7.53, 4.49)
1M	0.54 (-0.68, 0.86)	1.24 (-2.35, 0.12)	0.31 (-0.49, 0.39)	3.62 (-3.80, 7.77)	2.59 (-4.20, 3.78)	4.50 (-8.99, 1.90)
2PM	0.50 (-0.53, 0.96)	1.03 (-1.92, 0.44)	0.22 (-0.33, 0.41)	4.37 (-4.53, 8.93)	3.00 (-5.20, 3.60)	3.64 (-6.23, 4.39)
1PM	0.48 (-0.29, 0.9)	0.82 (-1.43, 0.21)	0.24 (-0.35, 0.36)	4.18 (-4.50, 7.56)	3.23 (-6.23, 1.76)	4.00 (-6.56, 4.73)
C	0.54 (-0.13, 1.03)	0.49 (-0.95, 0.29)	0.29 (-0.47, 0.36)	3.78 (-4.06, 7.28)	3.15 (-6.14, 3.06)	3.91 (-7.00, 3.12)
LI	0.54 (-0.09, 1.01)	0.41 (-0.68, 0.51)	0.33 (-0.48, 0.57)	3.61 (-3.83, 6.30)	2.59 (-4.63, 2.4)	3.36 (-6.39, 1.90)
CI	0.30 (-0.23, 0.60)	0.49 (-0.17, 1.00)	0.39 (-0.27, 0.72)	3.35 (-5.79, 4.90)	1.83 (-3.30, 2.46)	2.12 (-4.03, 2.33)

TABLE 6.4

Table 6.4: Mean of absolute discrepancies (10%, 90% quantiles) for mandible.

Tooth type	Measurement					
	Mesial	Facial	Vertical	Torque	Tip	Rotation
2M	0.86 (-1.45, 0.38)	0.95 (-1.77, 1.09)	0.81 (-0.10, 1.73)	7.48 (-14.23, 1.80)	5.35 (-0.66, 9.90)	3.94 (-6.19, 5.82)
1M	0.57 (-0.89, 0.35)	0.82 (-1.59, 0.55)	0.25 (-0.23, 0.48)	3.94 (-7.50, 3.58)	2.48 (-1.82, 4.60)	3.77 (-7.10, 2.80)
2PM	0.41 (-0.75, 0.52)	0.62 (-1.18, 0.51)	0.26 (-0.26, 0.51)	3.64 (-7.04, 4.10)	2.39 (-3.00, 4.08)	3.35 (-6.60, 3.40)
1PM	0.39 (-0.54, 0.65)	0.55 (-0.96, 0.72)	0.30 (-0.34, 0.49)	4.04 (-8.00, 5.50)	2.79 (-4.60, 4.10)	4.13 (-7.80, 3.70)
C	0.45 (-0.41, 0.84)	0.39 (-0.59, 0.53)	0.29 (-0.38, 0.55)	3.61 (-5.12, 6.30)	2.85 (-4.03, 4.43)	4.71 (-8.93, 1.16)
LI	0.44 (-0.41, 0.84)	0.41 (-0.5, 0.73)	0.35 (-0.22, 0.75)	3.70 (-4.83, 6.36)	2.76 (-5.03, 2.96)	2.90 (-5.26, 2.50)
CI	0.34 (-0.46, 0.51)	0.47 (-0.47, 0.87)	0.37 (-0.26, 0.83)	3.83 (-4.60, 7.10)	2.35 (-3.26, 3.30)	2.29 (-4.02, 3.10)

TABLE 6.5

Table 6.5: Type III mixed effect models for each one of the six rotational and translational discrepancies. Level of significance was set at 0.05 and significant cells are depicted in yellow.

Effect	Mesio-Distal	Labio-Lingual	Vertical	Inclination	Angulation	Rotation
Age	0.06	0.02	0.05	0.06	0.11	0.53
Gender	0.98	0.99	0.31	0.45	0.95	0.95
Crowding U arch	0.02	0.39	0.24	0.85	0.00	0.02
Crowding L arch	0.81	0.06	0.45	0.00	0.27	0.02
Overbite	1.00	0.27	0.82	0.86	0.06	0.35
Overjet	0.09	0.23	0.82	0.73	0.41	0.76
ANB	1.00	0.69	0.08	0.33	0.16	0.02
Days in treatment	0.06	0.02	0.95	0.10	0.06	0.33
Days in U slot_filling_W	0.64	0.33	0.73	0.48	0.66	0.16
Days in L slot_filling_W	0.26	0.98	0.65	0.74	0.02	0.04
Class_II_Elastics	0.63	0.72	0.02	0.54	0.35	0.33
Vertical_Elastics	0.38	0.04	0.07	0.07	0.03	0.52
Interproximal reduction	0.01	0.25	0.61	0.12	0.15	0.98
Rebondings	0.03	0.70	0.02	0.33	0.63	0.98
Jaw	<.0001	<.0001	<.0001	<.0001	<.0001	0.45
Tooth_type	<.0001	<.0001	<.0001	<.0001	<.0001	<.0001

FIGURE 6.1

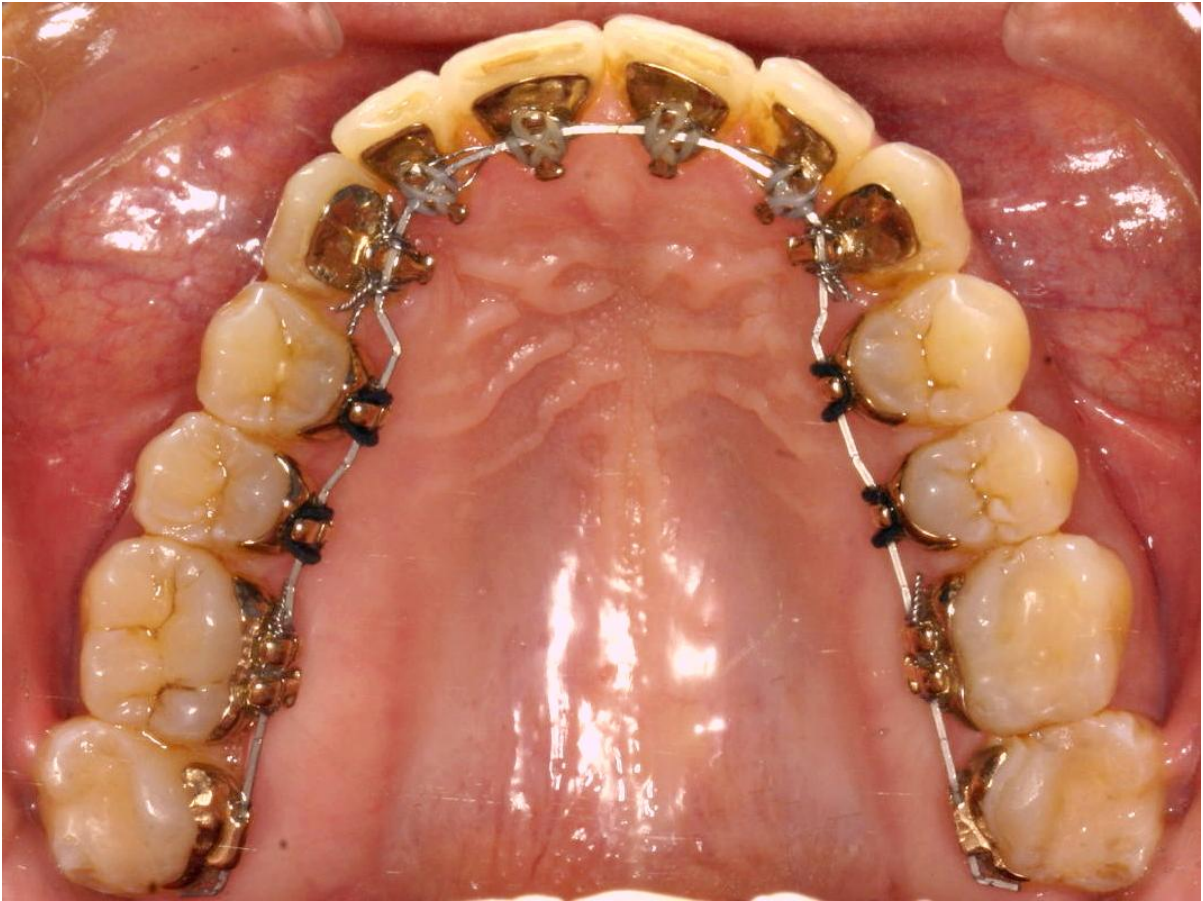


Figure 6.1. Incognito is a CAD/CAM lingual orthodontics technique. Brackets are custom-designed on a setup digital model and wires are bent by a robot based on the planned position for each tooth.

FIGURE 6.2

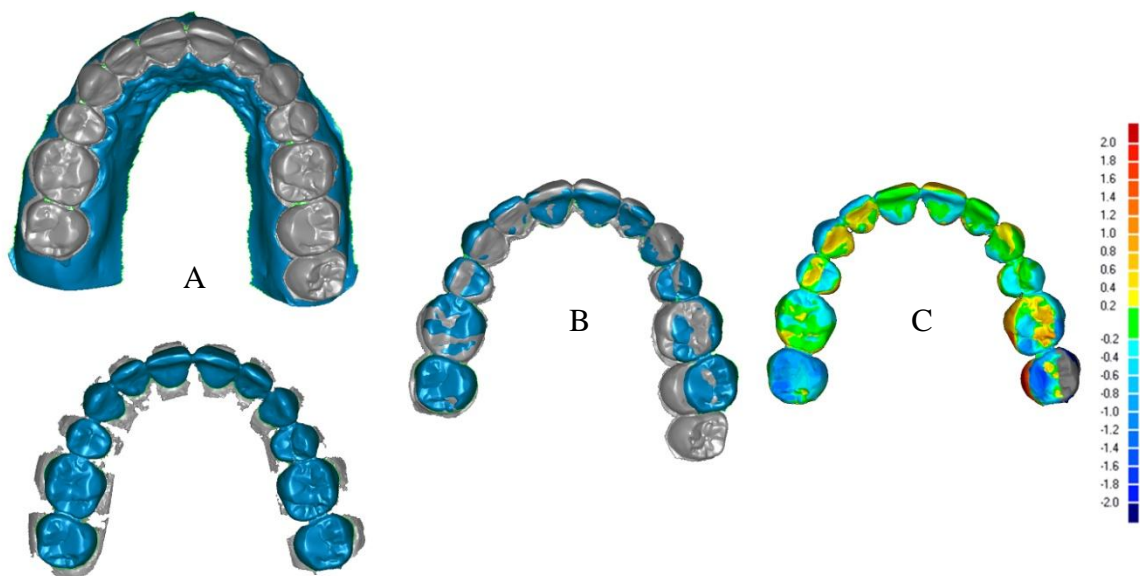


Figure 6.2. Final and setup models are cleaned by eliminating the surfaces corresponding to the gingival tissues (A); and are registered by an iterative closest point registration algorithm (B). Once registered, the difference between surfaces can be visualized as superimposed models or by means of color maps (C). Distances are in mm.

FIGURE 6.3

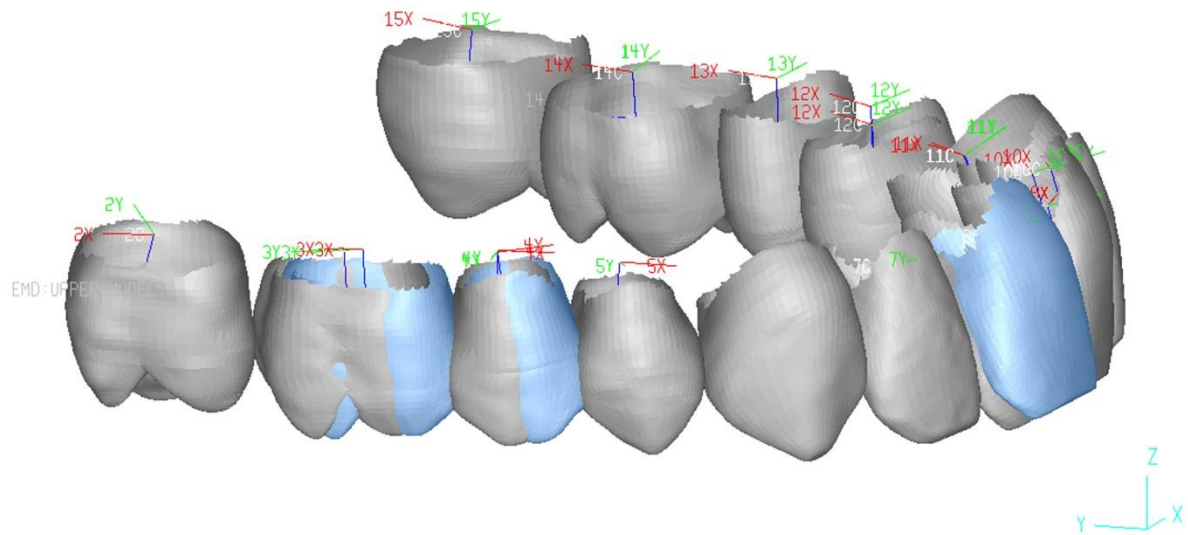


Figure 6.3 A local coordinate system is assigned to each tooth. For each pair of homologous teeth at different time points, an iterative closest point is performed to calculate the transformation matrix between positions. In this example the upper right first molar was displaced 1mm mesially, the right second premolar was tipped mesially 10 degrees and the right central incisor was torqued (crown-facial) 10 degrees. Rotational displacements are around a center of rotation located 10 mm apically to the occlusal plane on the long axis of each tooth.

FIGURE 6.4

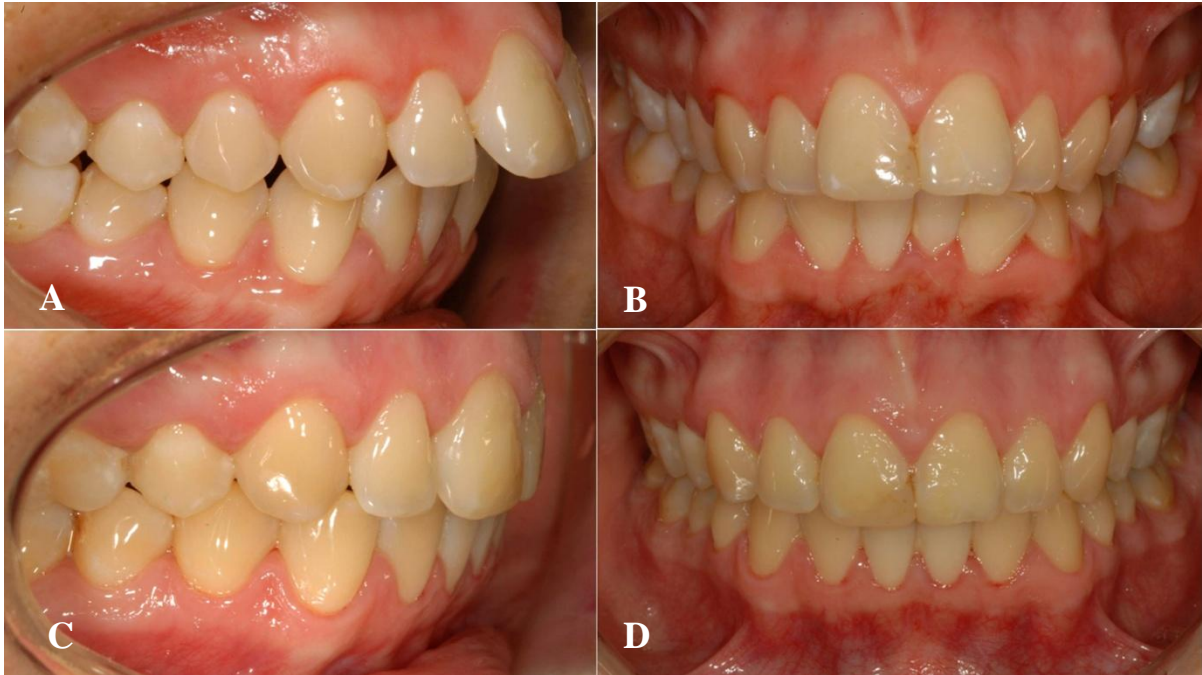


Figure 6.4. This patient displayed a dental Class II malocclusion and required extractions of her upper first premolars in order to retract her front teeth. Photographs are obtained before treatment (A, B) and after treatment (C, D).

FIGURE 6.5

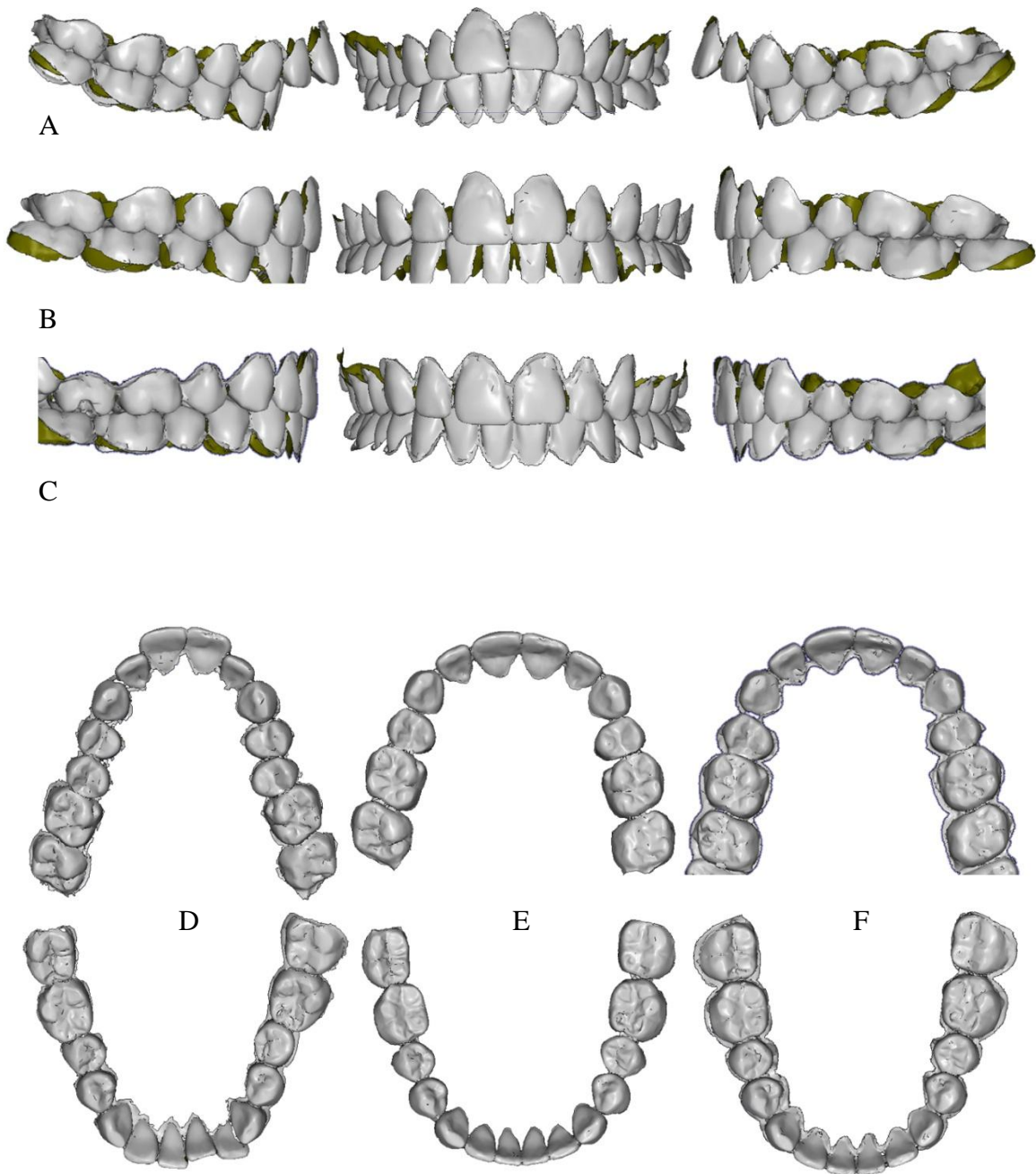


Figure 6.5. Digital models for the patient in figure 6.4 are depicted in right lateral, frontal, left lateral and occlusal views. These models correspond to three time points: initial (A and D), setup (B and E) and final (C and F). Note the change in overjet and arch form between initial and final time points.

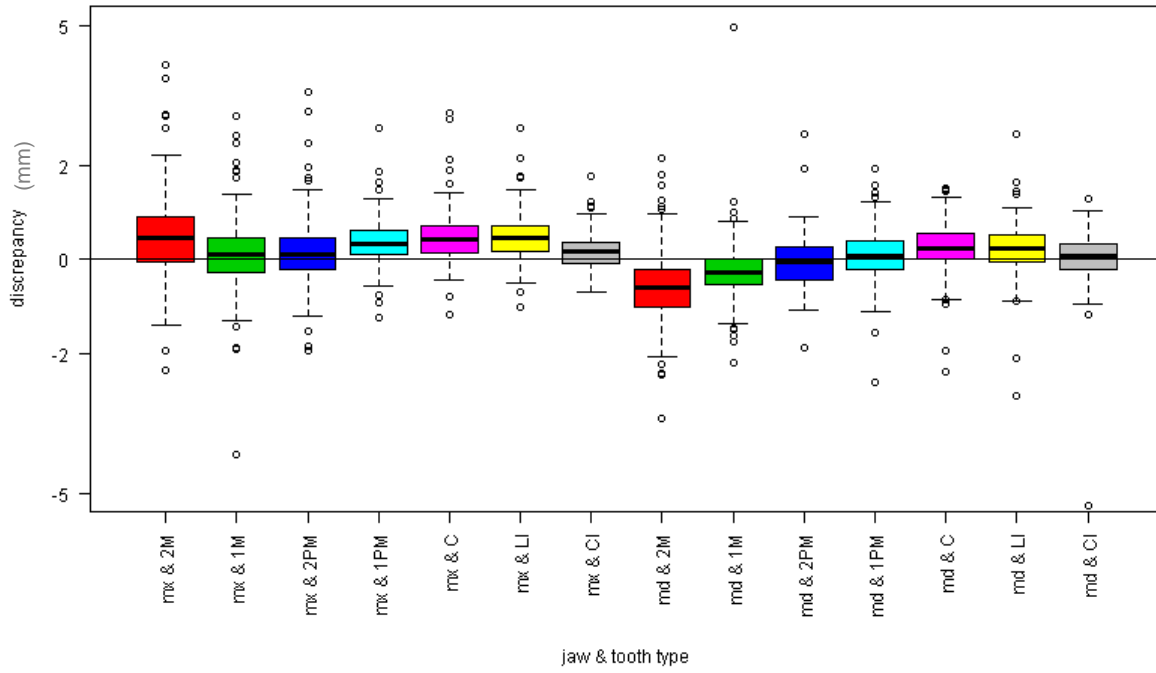
FIGURE 6.6



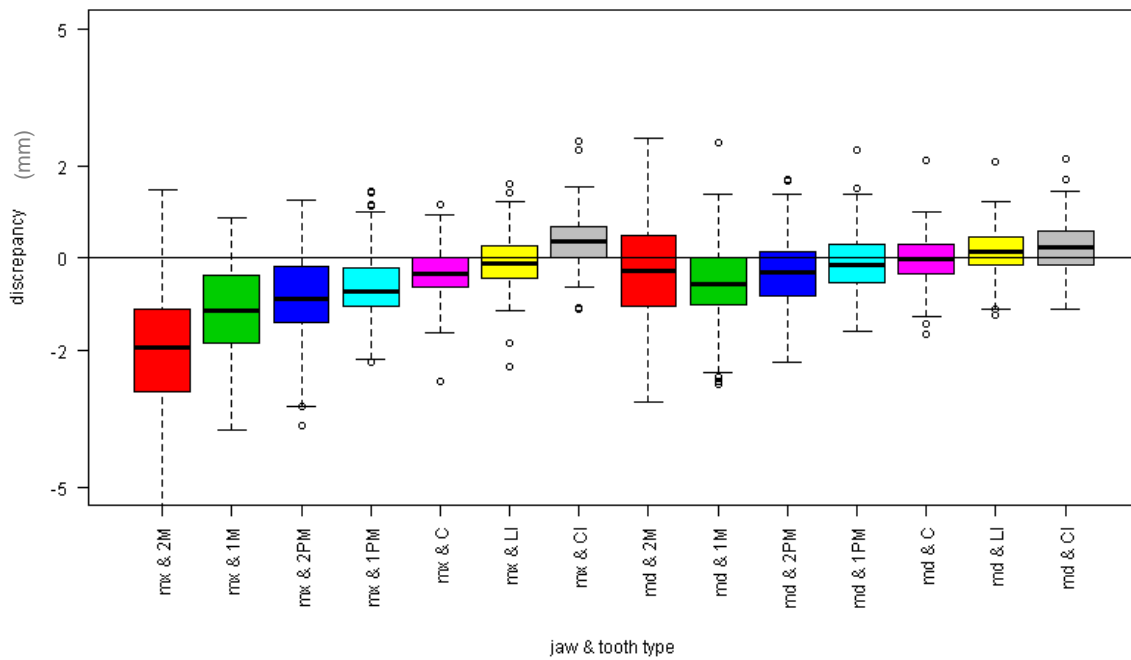
Figure 6.6. These digital models belong to the patient in figures 6.4 and 6.5 and correspond to the setup and final time points. Planned dental positions (orange) are superimposed to final tooth positions (blue). Note that both surfaces are similar. Some differences can be observed at the molar labio-lingual position.

FIGURE 6.7

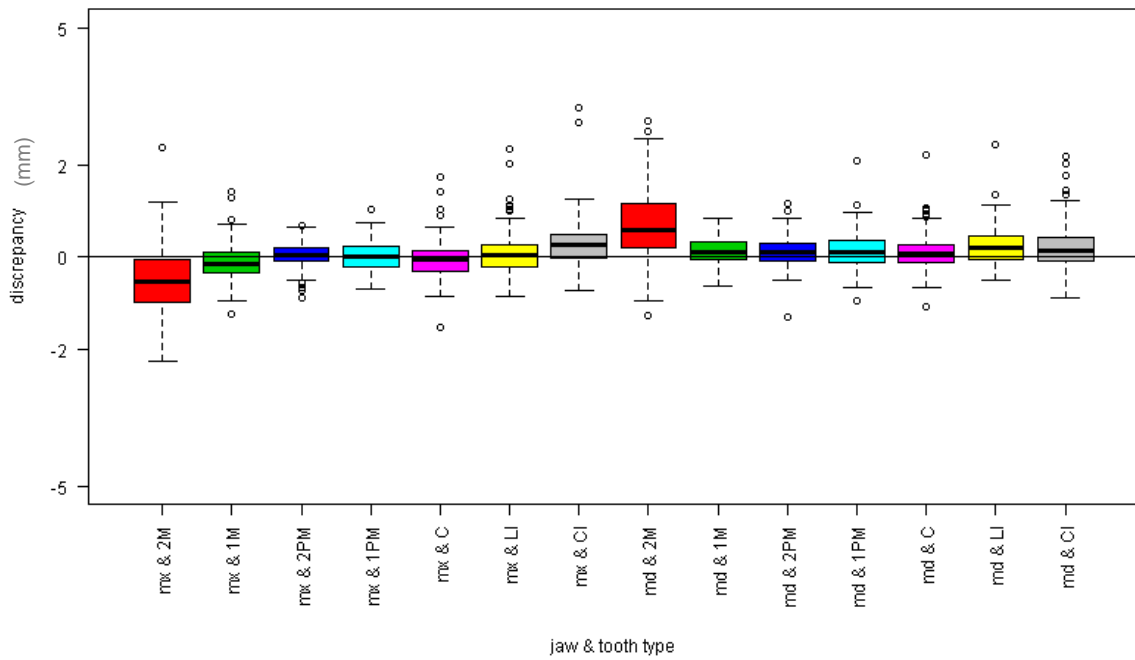
A. Mesio-Distal discrepancies



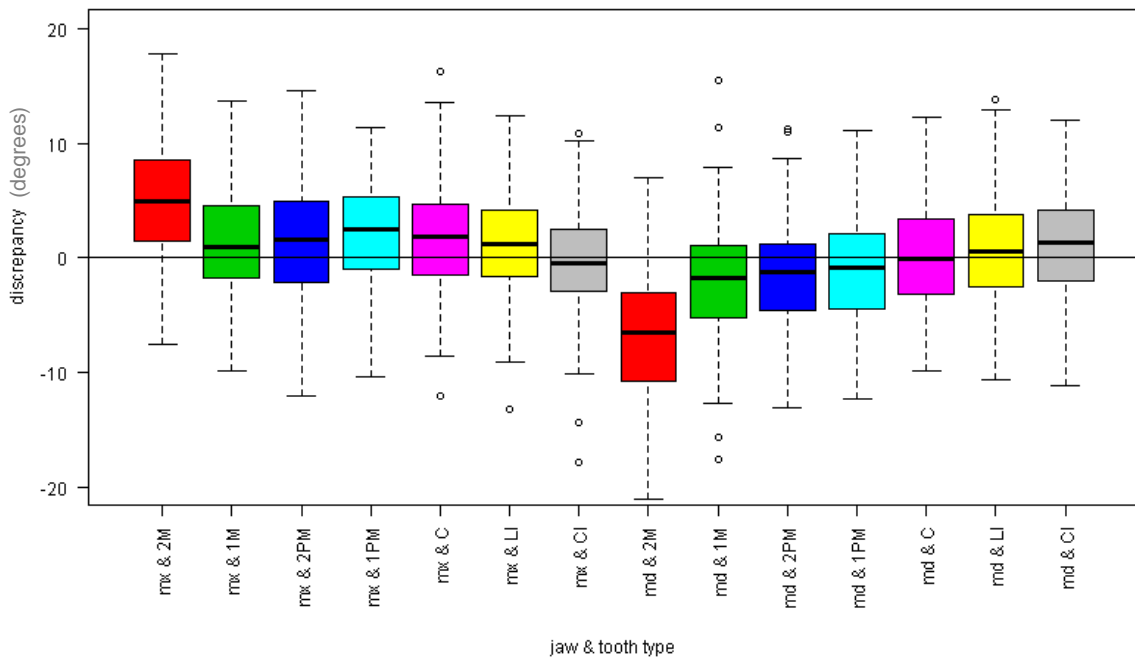
B. Labio-Lingual discrepancies



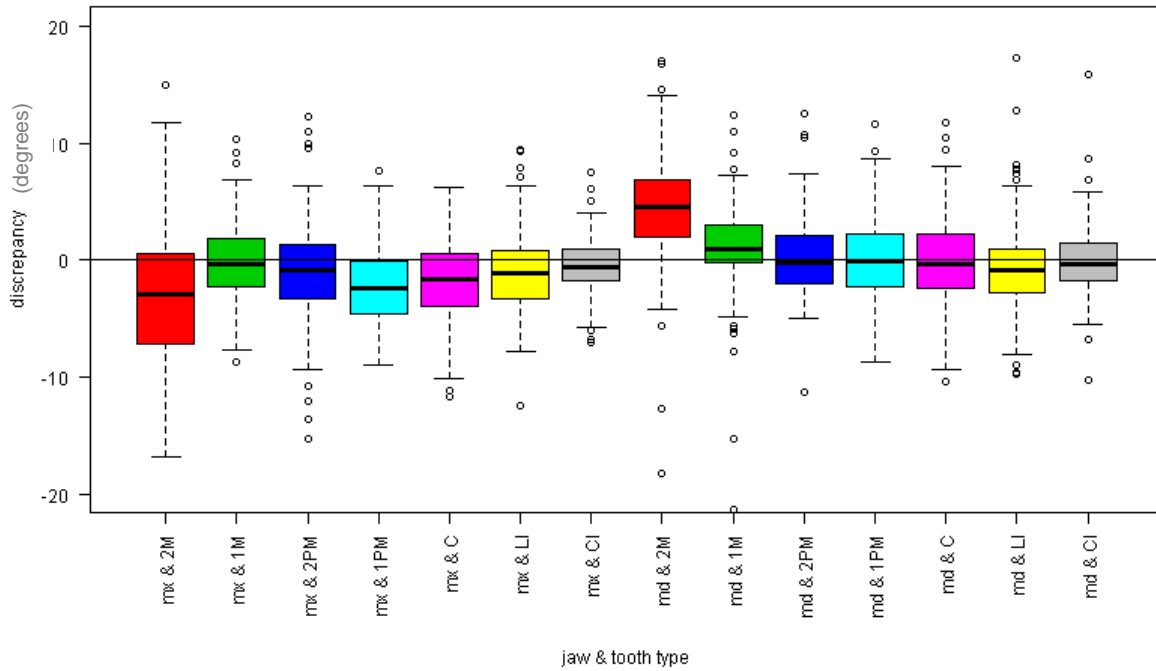
### C. Vertical discrepancies



### D. Inclination discrepancies.



### E. Angulation discrepancies



### F. Rotation discrepancies

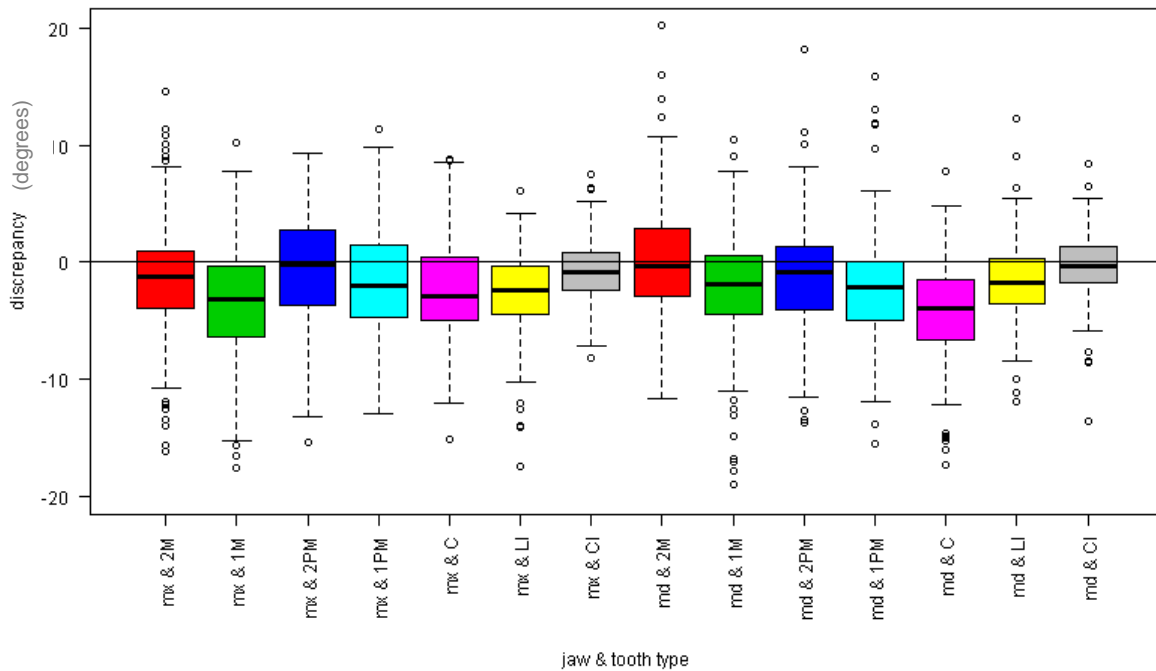


Figure 6.7 Boxplot diagrams for each discrepancy: mesio-distal, labio-lingual, vertical, inclination, angulation and rotation by tooth type and jaw.

FIGURE 6.8

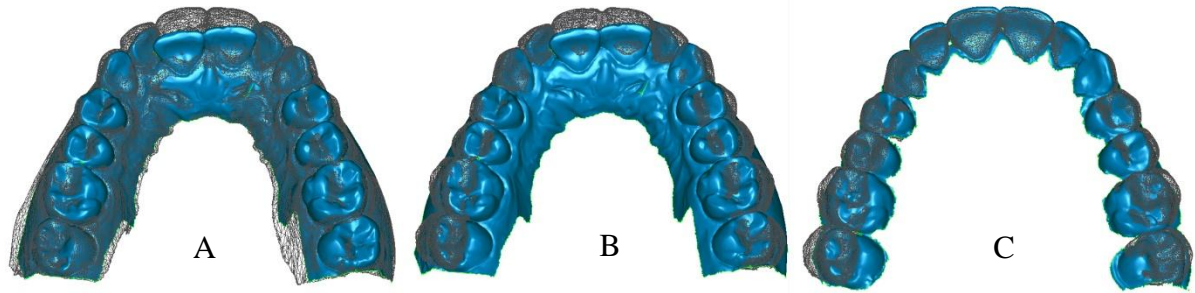


Figure 6.8. Final (black) and initial (blue) models are registered on the palatal rugae (A). The planned correction or setup (black) is registered to the initial (blue) model through iterative-closest point to the final model (B). The planned correction or setup (black) is registered to the final (blue) model through iterative closest-point registration (C). Note the differences in expansion at the molar region and the small differences in incisor positions.

## CHAPTER 7

### CONCLUSIONS

Orthodontics is facing a paradigm change. Concepts based on two-dimensional premises may not be valid anymore from a three-dimensional perspective. New research is being conducted to establish new diagnosis/prognosis classifications, to validate new procedures and techniques and to generate knowledge databases in three dimensions.

Airway dimensions in orthodontic patients who have skeletal problems are potentially important because airway maintenance has a high physiologic priority. This study showed that although there is a great variability in airway shape among individuals the patients with a Class II jaw relationship had a statistically significant smaller volume of their lower airway. Further research in this area should include assessment of changes in airway volume and shape in relation to treatment; use of stable structures as registration surfaces to combine airway segmentations from different time points; and studies to relate the morphological findings to functional assessments and to a diagnosis and prognosis scheme. This technology will allow for inter-and intra-patient comparisons and in the future we can expect a much better understanding of adaptive changes in the airway shape and volume.

At present, clinicians find themselves in a period where 3D technology precedes the evidence to support its use. Because of the advances in both CBCT

scanners and software designed to manage CBCT data, it is possible to take advantage of CBCT information in a clinical setting. However, clinicians should be careful in 2 areas: first, most morphological information gathered with these systems has not been yet linked to a clear diagnosis classification and the indications for CBCT acquisition have not been defined yet. Further research is needed in the interpretation of orthodontic information from CBCT data. Second, some available tools have not been validated yet, and studies to assess accuracy and precision are mandatory before these applications become standard. This type of research needs close collaboration between universities and companies.

A comparison of landmarks position in two modalities of cephalograms: digital cephalogram and cone-beam generated cephalogram showed no systematic error between average homologous landmarks' coordinates in digital cephalograms and CBCT-generated cephalograms. In other words, when distances are measured on cephalograms created with different modalities the average difference is centered around zero. That is not the case when these distances are measured on serial cephalograms acquired by different modalities on the same patient. When both modalities are used in the same individual, which is happening now as patients who had standard cephalograms initially are followed over time, the error of the method could produce clinically significant differences. While the scientific community is waiting for normative data to be generated in 3D, caution should be employed when comparisons are made with current 2D normative databases. A method of calculating the amount of variability that should be added to measurements while comparing across modalities was presented. Further research is necessary to

establish consistent records gathering protocols and information sharing. An idea presented in numerous meeting is the creation of a joint multi-center database (cross-sectional) of CBCT records. Multimodal images – where different modalities of records are combined in the same space – could help bridge the gap between 2D and 3D records.

In order to develop a method of measuring tooth position discrepancies, validation studies needed to be performed. The data presented in chapter 5 showed that based on repeated measures of maximum surface distance between positional replicates, it is possible to register independently scanned models to a scanned surface of the models in occlusion with little or no error. Further research would be needed to determine the accuracy of the occlusal position in both dental casts and digital orthodontic models. Reliability assessment of the registration of setup models on the final models, by means of repeated measures of the standard deviation of the surface distances, showed that surface to surface registration of final orthodontic digital models to planned setup models is reproducible. While this type of registration allows for quantification of tooth position discrepancies, the absolute tooth displacement – between initial and final time points – is not considered. In order to measure tooth movements between initial and final time points, a stable structure within (palatal rugae) or external (cranial base) to the digital models should be used as registration surface. CBCT images can also be registered on known stable structures to validate (or refute) rugae registration to assess tooth movement.

Finally a method to compute accuracy in post-treatment orthodontic tooth position was presented in chapter 6. Differences between the planned and achieved

tooth position were expressed in terms of six degrees of freedom. Based on a prospective sample of 94 patients treated with CAD/CAM lingual technique, the difference between the planned tooth position and the achieved tooth position was calculated. On average, Incognito lingual technique was extremely accurate in positioning the teeth within a small discrepancy of their planned positions. Most differences were seen in the labio-lingual position of upper molars and angulation of lower molars.

Further research is needed in order to determine the ideal description of tooth movement in three-dimensions, and the biological limits of tooth movement. The fact that a specific tooth displacement can be produced does not necessarily mean that it has to be produced. This method could be used for assessment of orthodontic treatment outcomes instead of the current methods, for instance ABO-OGS, which are based on 2D measurements and influenced by tooth anatomy. Validation of other CAD/CAM orthodontic technique should be conducted and compared with the current one. Given that This fully customized lingual technique is in constant evolution, it would be interesting to compare the present study on cases debonded between January 2008 and January 2009 with a study on cases debonded between January 2010 and January 2011.

The use of technology in orthodontics should have two main goals: shorter and better orthodontic treatments. Shorter treatments have the potential to decrease those secondary effects that are related to the length of treatment: for instance root resorption, white spot lesions and periodontal damage. The use of cone-beam CT has the potential to improve our diagnosis classification and generate more

knowledge on bone remodeling, tooth movement and soft-tissue adaptation.

CAD/CAM orthodontic techniques potentially can shorten the treatment time by increasing the accuracy of tooth positioning and reducing the amount of corrections performed by the orthodontist. New materials and bracket manufacturing techniques have the potential to make orthodontic treatment more comfortable. Hopefully in the future more patients will undergo orthodontic treatment and improve their oral health and smile esthetics. Smile esthetics has shown to have a big impact on quality of life. After all, “A smile is the shortest distance between two people”

## APPENDIX A

### DETAILED STATISTICAL METHOD FOR CHAPTER 4

To estimate the bias and variability of the measurement errors obtained from the use of the two modalities at each landmark we employed a two-step process.

First, at the  $l$ -th landmark, we assume that

$m_i^{(1)}(l) = \mu_i(l) + \varepsilon_i^{(1)}(l)$ ,  $m_i^{(2)}(l) = \mu_i(l) + \varepsilon_i^{(2)}(l)$ , where  $\mu_i(l)$  denotes the true location of the  $l$ -th landmark and  $m_i^{(1)}(l)$  and  $m_i^{(2)}(l)$  represent the measurements obtained

from the two modalities, respectively. Assume that measurement errors  $\varepsilon_i^{(1)}(l)$  and  $\varepsilon_i^{(2)}(l)$  are independent Gaussian random vectors with mean zero and covariance

$\Sigma(l)$ , we can estimate  $\Sigma(l)$  as follows: (1) calculate the difference vectors

$m_i^{(1)}(l) - m_i^{(2)}(l)$  for all subjects and then compute the sample covariance matrix

$S_i^{(1,2)}(l)$  of these difference vectors; (2) use  $S_i^{(1,2)}(l)/2$  as a consistent estimate of

$\Sigma(l)$ . Finally, we can use Gaussian random vector with mean zero and covariance

$S_i^{(1,2)}(l)/2$  to characterize measurement errors from both modalities.

Second, we estimated the bias and variability of the distance between any two landmarks obtained from the use of the two modalities. Specifically, we

assume that 
$$\begin{aligned} m_i^{(1)}(l_1) - m_i^{(1)}(l_2) &= \mu_i(l_1) - \mu_i(l_2) + \varepsilon_i^{(1)}(l_1) - \varepsilon_i^{(1)}(l_2), \\ m_i^{(2)}(l_1) - m_i^{(2)}(l_2) &= \mu_i(l_1) - \mu_i(l_2) + \varepsilon_i^{(2)}(l_1) - \varepsilon_i^{(2)}(l_2), \end{aligned}$$

where  $\mu_i(l_1) - \mu_i(l_2)$  denotes the true location difference between the  $l_1$ -th and  $l_2$ -th

landmarks and where  $m_i^{(k)}(l_1) - m_i^{(k)}(l_2)$  for  $k = 1, 2$  represent the measured location

difference vector obtained from the two modalities. Assume that measurement error difference vectors  $\varepsilon_i^{(1)}(l_1) - \varepsilon_i^{(1)}(l_2)$  and  $\varepsilon_i^{(2)}(l_1) - \varepsilon_i^{(2)}(l_2)$  are independent Gaussian random vectors with mean zero and covariance  $\Sigma(l_1, l_2)$ . Similar to estimating  $\Sigma(l)$ , we can use the half of the sample covariance matrix of  $m_i^{(1)}(l_1) - m_i^{(1)}(l_2) - m_i^{(2)}(l_1) + m_i^{(2)}(l_2)$ , denoted by  $S_i^{(1,2)}(l_1, l_2)/2$ , to consistently estimate  $\Sigma(l_1, l_2)$ . Then, we can use the Gaussian random vector with mean zero and covariance  $S_i^{(1,2)}(l_1, l_2)/2$  to characterize measurement errors of location difference vectors between any two landmarks from both modalities. Finally, we can estimate the bias and variability of the measurement error of the distance between any two landmarks from both modalities.

APPENDIX B

DETAILED STATISTICAL METHOD FOR CHAPTER 6

TABLE B.1

Table B.1: Between and within subject variables

Between-Subject Variables		
- Variables	Levels	Values
- Age (X1)	Continuous – Centered at 26.27 prior to modeling	
- Gender (X2)	M	X2=0
	F	X2=1
- Crowding upper (X3)	Continuous	
- Crowding lower (X4)	Continuous	
- Overbite (X5)	Continuous	
- Overjet (X6)	Continuous	
- ANB (X7)	Continuous	
- Treatment days (X8)	Continuous – Centered at 601.44 and divided by 120 prior to modeling	
- Upper slot filling wire (X9, X10)	No slot-finishing wire	X9=X10=0
	1-180 days	X9=1
	181- days	X10=1
- Lower slot filling wire (X11, X12)	No slot-finishing wire	X11=X12=0
	1-180 days	X11=1
	181- days	X12=1
- Class II elastics (X13, X14)	no elastics	X13=X14=0
	2-3 months	X13=1
	4- months	X14=1
- Vertical elastics (X15)	no elastics	X15=0
	2- months	X15=1
- Stripping (X16)	No	X16=0
	L, U, UL	X16=1
- Rebonding (X17)	Continuous	
Within-Subject Variables		
- Jaw (X18)	Maxilla	X18=0
	Mandible	X18=1
- Tooth type X19 - X24)	CI	X19=X20=X21=X22=X23=X24=X24=0

	2M	X19=1
	1M	X20=1
	2PM	X21=1
	1PM	X22=1
	C	X23=1
	LI	X24=1

From Table B.1, the equation (1) can be expressed as:

$$\begin{aligned}
Y_{ijkl} = & \beta_0 + b_i + b_{ij} + \beta_1 X_{1i} + \beta_2 X_{2i} + \beta_3 X_{3i} + \beta_4 X_{4i} + \beta_5 X_{5i} + \beta_6 X_{6i} + \beta_7 X_{7i} \\
& + \beta_8 X_{8i} + \beta_9 X_{9i} + \beta_{10} X_{10i} + \beta_{11} X_{11i} + \beta_{12} X_{12i} + \beta_{13} X_{13i} + \beta_{14} X_{14i} + \\
& \beta_{15} X_{15i} + \beta_{16} X_{16i} + \beta_{17} X_{17i} + \beta_{18} X_{18ij} + \beta_{19} X_{19ijk} + \beta_{20} X_{20ijk} + \\
& \beta_{21} X_{21ijk} + \beta_{22} X_{22ijk} + \beta_{23} X_{23ijk} + \beta_{24} X_{24ijk} + e_{ijkl}
\end{aligned}$$

where  $Y_{ijkl}$  is the discrepancies for the  $l$ th tooth level of the  $k$ th tooth type of the  $j$ th jaw from the  $i$ th patient.  $\beta_0$  is an intercept term,  $b_i$  is a random subject-specific effect,  $b_{ij}$  is the random effect for the jaw within a patient, and  $e_{ijkl}$  is a random error at the tooth level. The model assumes that  $b_i \sim N(0, \sigma^2)$ ,  $b_{ij} \sim N(0, \sigma_j^2)$ , and  $e_{ijkl} \sim N(0, \sigma_{e2})$ , and thus, the total error is  $u_{ijkl} = b_i + b_{ij} + e_{ijkl}$ . REML (restricted maximum likelihood) in Proc Mixed of SAS 9.1 was used to estimate the parameters.

TABLE B.2

Table B.2. Interpretations for the parameters in the model

Parameter		Interpretation
Intercept	$\beta_0$	The expected discrepancies for the discrepancies with centered age and treatment days
Age	$\beta_1$	The difference in the expected discrepancies due to a 1-year increase in age
Gender	$\beta_2$	The difference in the expected discrepancies between females and males
Crowding upper	$\beta_3$	The difference in the expected discrepancies due to a 1mm increase in crowding upper
Crowding down	$\beta_4$	The difference in the expected discrepancies due to a 1mm increase in crowding down
Overbite	$\beta_5$	The difference in the expected discrepancies due to a 1mm increase in overbite
Overjet	$\beta_6$	The difference in the expected discrepancies due to a 1mm increase in overjet
ANB	$\beta_7$	The difference in the expected discrepancies due to a 1 degree in ANB
Treatment days	$\beta_8$	The difference in the expected discrepancies due to a 120 days increase in treatment
Upper slot filling wire	$\beta_9$	The difference in the expected discrepancies between 1-180 days and no slot-finishing wire in upper
	$\beta_{10}$	The difference in the expected discrepancies between more than 180 days and no slot-finishing wire in upper
Upper slot filling wire	$\beta_{11}$	The difference in the expected discrepancies between 1-180 days and no slot-finishing wire in lower
	$\beta_{12}$	The difference in the expected discrepancies between more than 180 days and no slot-finishing wire in lower
Class II elastics	$\beta_{13}$	The difference in the expected discrepancies between 2-3 months and no class II elastics
	$\beta_{14}$	The difference in the expected discrepancies between more than 4 months and no class II elastics
Vertical elastics	$\beta_{15}$	The difference in the expected discrepancies between more than 2 months and no vertical elastics
Stripping	$\beta_{16}$	The difference in the expected discrepancies between more than (L, U, UL) and no

Rebonding	$\beta_{17}$	The difference in the expected discrepancies due to a 1 increase in rebonding
Jaw	$\beta_{18}$	The difference in the expected discrepancies between maxilla and mandible
Tooth type	$\beta_{19}$	The difference in the expected discrepancies between 2M and CI
	$\beta_{20}$	The difference in the expected discrepancies between 1M and CI
	$\beta_{21}$	The difference in the expected discrepancies between 2PM and CI
	$\beta_{22}$	The difference in the expected discrepancies between 1PM and CI
	$\beta_{23}$	The difference in the expected discrepancies between C and CI
	$\beta_{24}$	The difference in the expected discrepancies between LI and CI

TABLE B.3

TABLE B.3 Parameter estimates and significance for all translational discrepancies.

Effect	Level	Mesio-distal		Labio-lingual		Vertical	
		Estimate	p-value	Estimate	p-value	Estimate	p-value
Intercept		0.18	0.06	0.08	0.62	0.01	0.92
Age		0.00	0.06	0.01	0.02	0.00	0.05
Gender	F	0.00	0.98	0.00	0.99	0.04	0.31
	M	0.00	.	0.00	.	0.00	.
Crowding_UP		-0.02	0.02	0.01	0.39	-0.01	0.24
Crowding_LO		0.00	0.81	0.03	0.06	0.01	0.45
Overbite		0.00	1.00	-0.02	0.27	0.00	0.82
Overjet		0.02	0.09	0.02	0.23	0.00	0.82
ANB		0.00	1.00	-0.01	0.69	0.01	0.08
Days_in_tx1		-0.03	0.06	0.06	0.02	0.00	0.95
Days_in_U18	1	-0.08	0.44	0.22	0.14	0.01	0.86
	2	-0.07	0.39	0.08	0.39	0.03	0.43
	0	0.00	.	0.00	.	0.00	.
Days_in_L18	1	0.07	0.45	-0.01	0.97	-0.04	0.51
	2	-0.07	0.39	-0.02	0.84	-0.04	0.36
	0	0.00	.	0.00	.	0.00	.
Class_II_Elastics	1	0.05	0.64	-0.12	0.46	0.13	0.02
	2	-0.05	0.48	-0.05	0.63	-0.07	0.08
	0	0.00	.	0.00	.	0.00	.
Vertical_elastics	1	-0.07	0.38	0.22	0.04	0.09	0.07
	0	0.00	.	0.00	.	0.00	.
IPR	1	-0.19	0.01	-0.12	0.25	-0.02	0.61
	0	0.00	.	0.00	.	0.00	.
Re_bondings		0.03	0.03	0.01	0.70	0.02	0.02
jaw	md	-0.37	<.0001	0.49	<.0001	0.27	<.0001
	mx	0.00	.	0.00	.	0.00	.
Tooth_type	1M	-0.14	0.03	-1.15	<.0001	-0.23	<.0001
	1PM	0.14	0.00	-0.62	<.0001	-0.18	<.0001
	2M	-0.15	0.03	-1.41	<.0001	-0.14	0.04
	2PM	-0.02	0.56	-0.87	<.0001	-0.16	<.0001
	C	0.27	<.0001	-0.49	<.0001	-0.22	<.0001
	LI	0.25	<.0001	-0.27	<.0001	-0.10	<.0001
	CI	0.00	.	0.00	.	0.00	.

TABLE B.4

TABLE B.4 Parameter estimates and significance for all rotational discrepancies.

Effect	Level	Inclination		Angulation		Rotation	
		Estimate	p-value	Estimate	p-value	Estimate	p-value
Intercept		1.35	0.25	-0.42	0.38	-0.30	0.62
Age		-0.04	0.06	0.02	0.11	-0.01	0.53
Gender	F	0.42	0.45	-0.02	0.95	0.02	0.95
	M	0.00	.	0.00	.	0.00	.
Crowding_UP		0.01	0.85	0.11	0.00	0.12	0.02
Crowding_LO		-0.40	0.00	-0.06	0.27	-0.13	0.02
Overbite		-0.02	0.86	-0.08	0.06	-0.05	0.35
Overjet		-0.04	0.73	-0.04	0.41	0.02	0.76
ANB		-0.11	0.33	0.07	0.16	-0.13	0.02
Days_in_tx1		-0.25	0.10	0.13	0.06	0.10	0.33
Days_in_U18	1	-1.14	0.24	0.22	0.53	-0.39	0.52
	2	-0.57	0.40	-0.08	0.76	-0.78	0.06
	0	0.00	.	0.00	.	0.00	.
Days_in_L18	1	-0.68	0.50	-0.17	0.66	0.48	0.40
	2	-0.03	0.96	0.47	0.12	1.01	0.02
	0	0.00	.	0.00	.	0.00	.
Class_II_Elastics	1	0.97	0.28	-0.47	0.19	-0.12	0.76
	2	0.34	0.54	-0.24	0.37	0.31	0.31
	0	0.00	.	0.00	.	0.00	.
Vertical_elastics	1	-1.06	0.07	-0.71	0.03	0.25	0.52
	0	0.00	.	0.00	.	0.00	.
IPR	1	1.03	0.12	-0.36	0.15	0.01	0.98
	0	0.00	.	0.00	.	0.00	.
Re_bondings		0.13	0.33	-0.03	0.63	0.00	0.98
jaw	md	-2.93	<.0001	2.01	<.0001	0.14	0.45
	mx	0.00	.	0.00	.	0.00	.
Tooth_type	1M	-0.50	0.12	0.55	0.05	-2.36	<.0001
	1PM	0.21	0.52	-1.12	<.0001	-1.35	<.0001
	2M	-1.19	0.00	0.93	0.02	-0.33	0.45
	2PM	0.01	0.97	-0.26	0.34	-0.45	0.15
	C	0.54	0.04	-0.87	0.00	-2.61	<.0001
	LI	0.61	0.00	-0.89	<.0001	-1.64	<.0001
	CI	0.00	.	0.00	.	0.00	.